



University of Kentucky
UKnowledge

Theses and Dissertations--Plant and Soil
Sciences

Plant and Soil Sciences

2012

ENANTIOSELECTIVE DEMETHYLATION: THE KEY TO THE NORNICOTINE ENANTIOMERIC COMPOSITION IN TOBACCO LEAF

Bin Cai

University of Kentucky, bcai2@uky.edu

[Right click to open a feedback form in a new tab to let us know how this document benefits you.](#)

Recommended Citation

Cai, Bin, "ENANTIOSELECTIVE DEMETHYLATION: THE KEY TO THE NORNICOTINE ENANTIOMERIC COMPOSITION IN TOBACCO LEAF" (2012). *Theses and Dissertations--Plant and Soil Sciences*. 5.
https://uknowledge.uky.edu/pss_etds/5

This Doctoral Dissertation is brought to you for free and open access by the Plant and Soil Sciences at UKnowledge. It has been accepted for inclusion in Theses and Dissertations--Plant and Soil Sciences by an authorized administrator of UKnowledge. For more information, please contact UKnowledge@lsv.uky.edu.

STUDENT AGREEMENT:

I represent that my thesis or dissertation and abstract are my original work. Proper attribution has been given to all outside sources. I understand that I am solely responsible for obtaining any needed copyright permissions. I have obtained and attached hereto needed written permission statements(s) from the owner(s) of each third-party copyrighted matter to be included in my work, allowing electronic distribution (if such use is not permitted by the fair use doctrine).

I hereby grant to The University of Kentucky and its agents the non-exclusive license to archive and make accessible my work in whole or in part in all forms of media, now or hereafter known. I agree that the document mentioned above may be made available immediately for worldwide access unless a preapproved embargo applies.

I retain all other ownership rights to the copyright of my work. I also retain the right to use in future works (such as articles or books) all or part of my work. I understand that I am free to register the copyright to my work.

REVIEW, APPROVAL AND ACCEPTANCE

The document mentioned above has been reviewed and accepted by the student's advisor, on behalf of the advisory committee, and by the Director of Graduate Studies (DGS), on behalf of the program; we verify that this is the final, approved version of the student's dissertation including all changes required by the advisory committee. The undersigned agree to abide by the statements above.

Bin Cai, Student

Dr. Lowell Bush, Major Professor

Dr. Arthur G Hunt, Director of Graduate Studies

ENANTIOSELECTIVE DEMETHYLATION:
THE KEY TO THE NORNICOTINE ENANTIOMERIC
COMPOSITION IN TOBACCO LEAF

DISSERTATION

A dissertation submitted in partial fulfillment of the
requirements for the degree of Doctor of Philosophy in the
College of Agriculture
at the University of Kentucky

By
Bin Cai

Lexington, Kentucky

Director: Dr. Lowell Bush, Professor of Plant Physiology

Lexington, Kentucky

2012

Copyright © Bin Cai 2012

ABSTRACT OF DISSERTATION

ENANTIOSELECTIVE DEMETHYLATION: THE KEY TO THE NORNICOTINE ENANTIOMERIC COMPOSITION IN TOBACCO LEAF

Nicotine and nornicotine are the two main alkaloids that accumulate in *Nicotiana tabacum* L. (tobacco), and nornicotine is the *N*-demethylation metabolite of nicotine. Nicotine is synthesized in the root, and probably primarily in the root tip. Both nicotine and nornicotine exist as two isomers that differ from each other by the orientation of H atom at the C-2' position on the pyrrolidine ring. (*S*)-nicotine is the dominant form in tobacco leaf and the enantiomer fraction of nicotine (EF_{nic}), the fraction of (*R*)-enantiomer over the total nicotine, is approximately 0.002. Despite considerable efforts to elucidate nicotine and nornicotine related metabolism, a comprehensive understanding of the factors responsible for regulating the variable EF for nornicotine (0.04 to 0.75) relative to nicotine has been lacking. The objectives of these investigations were to understand the mechanisms behind the discrepancy. There are three nicotine demethylases reported to be active in tobacco. *In vitro* recombinant CYP82E4, CYP82E5v2 and CYP82E10 demethylated (*R*)-nicotine three, ten and ten-fold faster than (*S*)-nicotine, respectively, and no racemization was observed in either nicotine or nornicotine during demethylation. To confirm these *in vitro* results, the accumulation and demethylation of nicotine enantiomers throughout the growth cycle and curing process were investigated. Scion stock grafts were used to separate the contributions of roots (source) from leaves (sink) to the final accumulation of nicotine and nornicotine in leaf. The results indicate that nicotine consists of 4% of the R enantiomer (0.04 EF_{nic}) when synthesized. However, (*R*)-nicotine is selectively demethylated by CYP82E4, CYP82E5 and CYP82E10, resulting in an approximate 0.01 EF_{nic} and 0.60 EF_{nic} in the root. After most of (*R*)-nicotine is demethylated in root, nicotine and nornicotine are translocated to leaf, where nicotine is further demethylated. Depending on the CYP82E4 activity, an EF_{nic} of 0.04 to 0.60 is produced and only 0.2% of the remaining nicotine in the leaf is (*R*)-configuration.

Keywords: (*R*)-nicotine, nornicotine, cytochrome P450, enantioselectivity, tobacco

Bin Cai
Student's Signature

July 13, 2012
Date

ENANTIOSELECTIVE DEMETHYLATION:
THE KEY TO THE NORNICOTINE ENANTIOMERIC
COMPOSITION IN TOBACCO LEAF

By
Bin Cai

Lowell Bush

Director of Dissertation

Arthur G Hunt

Director of Graduate Studies

July 13, 2012

ACKNOWLEDGMENTS

While an individual work, the following dissertation benefited from the insights and direction of many people.

Name	Comments
Lowell Bush	Dissertation chair, mentor, inspiration and guidance throughout my graduate study
Bob Pearce	Committee member, valuable suggestions
Hongyan Zhu	Committee member, valuable suggestions
Joe Chappell	Committee member, valuable suggestions, provided tools and ideas critical for the experiments in Chapter 3
Sharyn Perry	Committee member, valuable suggestions
Neil Fannin	Lab member, technical support
Huihua Ji	Lab member, technical support
Wenbin Yang	Lab member, technical support
Anne Jack	Lab member, help me design and execute experiments in the field
Colin Fisher	Lab member, help me design and execute experiments in the field
Balazs Siminszky	Provided yeast line overexpressing CYP82E4 and CYP82E5v2 enzyme
Ralph Dewey	Professor at North Carolina State University, provided yeast line overexpressing CYP82E10 enzyme
Ramsey Lewis	Associate professor at North Carolina State University, provided nicotine demethylase mutant seeds

List of Contents

TITLE.....	1
ABSTRACT OF DISSERTATION.....	III
ACKNOWLEDGMENTS	iii
List of Contents.....	iv
List of Tables	viii
List of Figures.....	ix
Chapter 1. Literature review	1
1.1. Tobacco pyridine alkaloids and derivatives.....	1
1.2. Biosynthesis of the four main alkaloids in tobacco.....	3
1.2.1. Pyridine, pyrrolidine and piperidine ring formation.....	3
1.2.2. Nicotine, nornicotine, anabasine and anatabine formation.....	4
1.3. Nicotine demethylation in tobacco.....	7
1.3.1. Nicotine demethylation mechanism.....	7
1.3.2. Structure and function studies of tobacco nicotine demethylase enzymes.....	8
1.3.3. Nicotine demethylase specificity	10
1.3.4. Evolution of nicotine demethylases in <i>N. tabacum</i> L.....	12
1.4. Theoretical studies of enzymes responsible for nicotine metabolism.....	13
1.4.1. Cytochrome P450.....	13
1.4.2. Model studies of CYP-catalyzed nicotine demethylation.....	15
1.5. Compartmentation and trafficking of nicotine.....	20
1.5.1. Long distance translocation from roots to leaves	20
1.5.2. Cell type.....	23
1.6. Pharmacological effects of enantiomers of nicotine and TSNAs	23
1.6.1. Pharmacological effects of nicotine and TSNAs	24

1.6.2. Pharmacological effects of the enantiomers of nicotine and TSNA	24
1.7. Experimental aim of this dissertation	27
Chapter 2. Variable nornicotine enantiomeric composition caused by nicotine demethylase CYP82E4 in tobacco leaf	29
2.1. Introduction	29
2.1.1. Highly variable nornicotine enantiomeric composition in tobacco	29
2.1.2. Putative reasons for wide range of EF _{nic}	31
2.2. Results	33
2.2.1. EF _{nic} in among different lines and tissues	33
2.2.2. Ethephon-induced CYP82E4 expression associated with decreased EF _{nic}	35
2.2.3. Nicotine demethylase CYP82E4 mutant results in increased EF _{nic}	37
2.2.4. Selectivity of other nicotine demethylases for (R)-nicotine	38
2.3. Discussion	39
2.4. Conclusions	40
2.5. MATERIALS AND METHODS	40
2.5.1. Plant materials	40
2.5.2. Alkaloids quantification and separation of enantiomers of nicotine and nornicotine	41
Chapter 3 Enantioselective demethylation of nicotine as a mechanism for variable nornicotine composition in tobacco leaf	43
3.1. Introduction	43
3.2. Results	45
3.2.1. Optimization of <i>in vitro</i> enzyme assay of nicotine enantiomers	45
3.2.2. Enantioselectivity of CYP82E4, CYP82E5v2 and CYP82E10	47
3.2.3. Combination of the three demethylases to generate leaf nornicotine composition <i>in vitro</i>	49

3.2.4. Substrate specificity of CYP82E4, CYP82E5v2 and CYP82E10	51
3.3. Discussion	53
3.4. Conclusion.....	56
3.5. MATERIALS AND METHODS	56
3.5.1. Expression of nicotine demethylases CYP82E4, CYP82E5v2 and CYP82E10 in yeast	56
3.5.2. Yeast microsomes preparation	57
3.5.3. <i>In vitro</i> enzyme assay.....	57
Chapter 4. (R)-nicotine biosynthesis, metabolism and translocation as determined in nicotine demethylase mutants.....	60
4.1. Introduction	60
4.2. Results	62
4.2.1. Effects of nicotine demethylases on enantiomeric composition of nicotine, nornicotine, and TSNA level in air-cured leaf lamina	62
4.2.2. Accumulation of alkaloids in mutants leaf lamina during the growth and curing	64
4.2.3. Accumulation of nicotine and nornicotine enantiomers in mutant leaf lamina during growth and curing.....	67
4.2.4. Contributions of three nicotine demethylases in root and leaf to the leaf nicotine and nornicotine composition.....	70
4.3. Discussion	74
4.4. Conclusion.....	78
4.5. MATERIALS AND METHODS	78
4.5.1. Plant materials.....	78
4.5.2. Mutants grown in the field.....	79
4.5.3. Graft study	79

4.5.4. Alkaloids quantification and separation of enantiomers of nicotine and nornicotine	80
Chapter 5 Concluding remarks	82
5.1. Combining the activities of CYP82E4, CYP82E5v2 and CYP82E10 is enough to explain the enantiomeric discrepancy between nicotine and nornicotine	82
5.2. Lessons from enantioselective demethylation study	82
5.2.1 Nicotine composition	82
5.2.2. Demethylation location of nicotine enantiomers	83
5.2.3. Lack of additive effects for CYP82E5v2 and CYP82E10.....	83
5.2.4. Prediction of future changes of nicotine and nornicotine composition	83
Appendix.....	84
Literature Cited	117
Vita.....	129

List of Tables

Table 1.1. Predominant alkaloid found in the <i>Nicotiana</i> species in greenhouse-grown plants.	1
Table 1.2. Plants, other than <i>Nicotiana</i> , in which nicotine has been reported (Davis et al., 1991; Leete, 1992)	3
Table 1.3. Functionality of tobacco nicotine demethylases possessing mutations.	9
Table 1.4. Specificity of demethylation process.	11
Table 1.5. Origin of nicotine demethylases found in <i>N. tabacum L.</i> genome.	12
Table 1.6. Species differences in nicotine metabolism.	16
Table 1.7. Spatial expression patterns of genes encoding nicotine biosynthesis pathway enzymes in tissues.	21
Table 2.1. Enantiomer fraction, EF, of nicotine and nornicotine in tobacco (<i>Nicotiana tabacum L.</i>)	30

List of Figures

Figure 1.1. Alkaloid biosynthesis in tobacco plant (<i>Nicotiana</i> species).....	6
Figure 1.2. Two possible mechanisms in <i>N'</i> -demethylation of nicotine catalyzed by cytochrome P450 enzymes	8
Figure 1.3. The catalytic cycle of cytochrome P450	15
Figure 1.4. Human CYP2A6-catalyzed demethylation of (S)-nicotine	17
Figure 1.5. CYP2A6-catalyzed 5'-hydroxylation of (S)-nicotine.	18
Figure 1.6. Oxidative degradation of nicotine in <i>Arthrobacter nicotinovorans</i>	19
Figure 1.7. Hydroxylation of nicotine by P450 _{cam} , based on crystallographic data	20
Figure 1.8. Nicotine and nornicotine distribution in leaf (Burton et al., 1992)	21
Figure 1.9. A simplified diagram of nicotine synthesis in <i>Nicotiana</i>	22
Figure 1.10. A model of nicotine translocation and accumulation in leaf cells from root cells	23
Figure 1.11. Structures and biological effects of tobacco alkaloids and tobacco-specific nitrosamines	26
Figure 1.12. Possible mechanisms for high and variable (R)-nornicotine percentage in tobacco leaf	27
Figure 2.1. Structures of R and S enantiomers of nicotine, nornicotine and <i>N'</i> -nitrosanornicotine	30
Figure 2.2. Possible mechanisms to account for the high and variable EF _{nic} in tobacco leaf.....	33
Figure 2.3. There is wide range of EF _{nic} in different tobacco lines	34
Figure 2.4. (R)-nornicotine (A) and (S)-nornicotine (B) accumulate to different levels in different tissues of four tobacco lines	35
Figure 2.5. EF _{nic} decreases after the induction of nicotine demethylation	36
Figure 2.6. (R)-nornicotine (A) and (S)-nornicotine (B) increase differently after ethephon induction of nicotine demethylase.....	36
Figure 2.7. Changes of EF _{nic} and demethylation due to the mutation of nicotine demethylase CYP82E4	37
Figure 2.8. EF _{nic} and demethylation in different RNAi lines	39

Figure 3.1. Biosynthesis and enantiomeric composition of the four main alkaloids in <i>Nicotiana tabacum</i> L.....	44
Figure 3.2. Dependence of CYP82E4-catalyzed demethylation of (R)-nicotine or (S)-nicotine on the amount of protein (A), pH (B) and reaction time (C)	46
Figure 3.3. Substrate preferences of CYP82E4 (A), CYP82E5v2 (B) and CYP82E10 (C) for (R)-nicotine and (S)-nicotine.	48
Figure 3.4. Generation of leaf nornicotine enantiomeric composition using CYP82E4 (E4), CYP82E5v2 (E5) and CYP82E10 (E10) <i>in vitro</i>	50
Figure 3.5. Nicotine and nicotine analogues used by tobacco through <i>N</i> -dealkylation reaction.....	52
Figure 3.6. Proposed nicotine and nornicotine enantiomeric composition affected by three nicotine demethylases in tobacco leaf.....	53
Figure 4.1. The puzzle of the discrepancy between nicotine and nornicotine enantiomeric composition.....	61
Figure 4.2. Effects of nicotine demethylases on nicotine, nornicotine and NNN in air-cured leaf lamina in 2010 and 2011.	64
Figure 4.3. Leaf lamina alkaloids profile of different nicotine demethylase mutants during growth and curing	66
Figure 4.4. Accumulation of nicotine and nornicotine enantiomers in leaf lamina of different nicotine demethylase mutants during growth and curing	68
Figure 4.5. Nicotine and nornicotine enantiomeric composition of different nicotine demethylase mutant leaf lamina during growth and curing.....	69
Figure 4.6. Relationships between nicotine demethylation and nornicotine enantiomeric composition from leaf lamina of demethylase mutants during growth and curing.	70
Figure 4.7. Demethylation, nicotine and nornicotine enantiomeric composition in self-grafted mutant tissues	72
Figure 4.8. Nicotine and nornicotine composition in tomato/tobacco grafts.....	73
Figure 4.9. Nicotine and nornicotine enantiomeric composition in tobacco/ <i>e4e5e10</i> grafts	73
Figure 4.10. Effects of three nicotine demethylases on the enantiomeric composition of nicotine and nornicotine in high demethylation tobacco (<i>Nicotiana tabacum</i> L.)	75

Figure 4.11. Evolution of nicotine and nornicotine enantiomeric composition in tobacco leaf, driven by human selections..... 77

Chapter 1. Literature review

1.1. Tobacco pyridine alkaloids and derivatives

Alkaloids are a group of basic substances which contain a cyclic nitrogenous nucleus. In *Nicotiana* plants most alkaloids are 3-pyridyl derivatives. Pyridine alkaloids in tobacco are listed in Figure S1.1. The genus *Nicotiana*, commonly referred to as tobacco plants, contains 3 subgenera, 14 sections and 66 species. The alkaloid composition has been reported by different independent investigations (Saitoh et al., 1985; Sisson and Severson, 1990). Among the many alkaloids found in *Nicotiana*, nicotine is the principal alkaloid in commercial tobaccos. In leaves of 60 species of *Nicotiana*, nicotine is the predominant alkaloid in 33 species, nornicotine is the principal alkaloid in 24 species, anabasine is the principal alkaloid in 2 species, and anatabine is the principal alkaloid in 1 specie (Table 1.1) (Saitoh et al., 1985). For the roots of 60 species of *Nicotiana*, Saitoh found 51 species accumulated nicotine, 2 species accumulated nornicotine and 7 species accumulated anabasine.

Table 1.1. Predominant alkaloid found in the *Nicotiana* species in greenhouse-grown plants (Saitoh et al., 1985). The two most abundant alkaloids are listed for each species. Results in parenthesis are from (Sisson and Severson, 1990).

SUBGENUS Section species	Leaf		Root		SUBGENUS Section species	Leaf		Root	
	1 st	2 rd	1 st	2 rd		1 st	2 rd	1 st	2 rd
RUSTICA					PETUNIOIDES (cont'd.)				
Paniculatae					Noctiflorae				
<i>glauca</i>	ab	n	ab	n	<i>noctiflora</i>	nn(ab)	n(nn)	n	ab
<i>paniculata</i>	n	nn	n	nn	<i>petunioides</i>	(ab)	(nn)		
<i>knightiana</i>	n	nn	n	nn	<i>acaulis</i>	(ab)	(nn)		
<i>solanifolia</i>	nn	ab	ab	n	<i>ameghinoi</i>				
<i>benavidesii</i>	n	ab	ab	n	Acuminatae				
<i>cordifolia</i>	n	ab	ab	n	<i>acuminata</i>	n	nn	n	nn
<i>raimondii</i>	n	ab	n	ab	<i>pauciflora</i>	n	nn	n	nn
Thyrsiflorae					<i>attenuata</i>	n	nn	n	nn
<i>thyrsiflora</i>	(nn)	(n)			<i>longibracteata</i>				
Rusticae					<i>miersii</i>	nn	n	n	nn
<i>rustica</i>	n	at	n	at	<i>corymbosa</i>	n	nn	n	nn
TABACUM					<i>linearis</i>	(n)	(nn)		
					<i>spegazzinii</i>	nn(n)	at(nn)	n	at

Table 1.1 (continued)

SUBGENUS Section species	Leaf		Root		SUBGENUS Section species	Leaf		Root	
	1 st	2 rd	1 st	2 rd		1 st	2 rd	1 st	2 rd
<i>Tomentosae</i>					<i>Bigelovinae</i>				
<i>tomentosa</i>	nn	n(at)	n	nn	<i>bigelovii</i>	n	nn(at)	n	nn
<i>tomentosiformis</i>	nn	n(at)	n	at	<i>clevelandii</i>	n	at	n	at
<i>otophora</i>	at(nn)	nn(at)	n	nn	<i>Nudicaules</i>				
<i>setchellii</i>	nn	anab	n	nn	<i>nudicaulis</i>	nn	at(ab)	n	nn
<i>gultinosa</i>	nn	n	n	at	<i>Suaveolentes</i>				
<i>kawakamii</i>	nn	at(n)	n	nn	<i>benthamiana</i>	n	ab	n	ab
<i>Genuinae</i>					<i>umbratica</i>	n(nn)	nn(n)	n	ab
<i>tabacum</i>	n	nn(at)	n	at	<i>cavicola</i>	nn	n	n	ab
PETUNIOIDES					<i>debneyi</i>	ab	n	ab	n
<i>Undulatae</i>					<i>gossei</i>	n	at	n	ab
<i>undulata</i>	n	nn	n	nn	<i>amplexicaulis</i>	n	at	n	at
<i>arentsii</i>	n	ab	n	ab	<i>maritima</i>	nn	ab	ab	nn
<i>wigandioides</i>	n	ab	n	ab	<i>velutina</i>	nn	ab	n	ab
<i>Trigonophyllae</i>					<i>hesperis</i>	n	ab(nn)	ab	n
<i>trigonophylla</i>	nn	at	n	nn	<i>occidentalis</i>	nn	ab	n	ab
<i>Alatae</i>					<i>simulans</i>	nn	ab(n)	n	ab
<i>sylvestris</i>	n	nn	n	nn	<i>megalosiphon</i>	nn	ab	n	ab
<i>langsдорffii</i>	n	at	n	at	<i>rotundifolia</i>	n	ab	n	ab
<i>alata</i>	n	(ab)	nn	n	<i>excelsior</i>	n	at	n	ab
<i>forgetiana</i>	n	(nn)	n	at	<i>suaveolens</i>	n	nn	n	ab
<i>bonariensis</i>	n	(nn)	n	nn	<i>ingulba</i>	nn(n)	ab(nn)	n	ab
<i>longiflora</i>	n(nn)	(n)	n	nn	<i>exigua</i>	n	nn	n	ab
<i>plumbaginifolia</i>	nn	n	n	nn	<i>goodspeedii</i>	nn	ab	n	ab
<i>Repandae</i>					<i>rosulata</i>	nn	n	n	ab
<i>repanda</i>	nn	ab	n	nn	<i>fragrans</i>	n	at	n	at
<i>stocktonii</i>	n	nn	n	at	<i>africana</i>	nn	n	nn	n
<i>nesophila</i>	nn	n	n	at					

Note: n: nicotine; nn: nornicotine; ab: anabasine; at: anatabine

Besides *Nicotiana*, nicotine has also been found in other species (Table 1.2). Edible Solanaceae plants (tomato, potato, eggplant and peppers) contain 15-240 ng g⁻¹ dry weight nicotine (Davis et al., 1991; Siegmund et al., 1999). Based on average quantities

of foods consumed, the daily intake of nicotine would be 1.4 μg (Siegmund et al., 1999), or 8.8 μg (Davis et al., 1991).

Table 1.2. Plants, other than *Nicotiana*, in which nicotine has been reported (Davis et al., 1991; Leete, 1992).

Scientific name	Common name	Scientific name	Common name
<i>Asclepias syriacus</i>	Milk weed	<i>Erythroxylum coca</i>	Coca
<i>Acacia concinna</i>	Acacia	<i>Lycopersicon esculentum</i>	Tomato
<i>Atropa belladonna</i>	Deadly nightshade	<i>Lycopodium clavatum</i>	Club moss
<i>Cannabis sativa</i>	Marijuana	<i>Mucuna</i>	Velvet-ban
<i>Carica papaya</i>	Papaya	<i>Petunia violacea</i>	Petunia
<i>Capsicum annuum</i>	Green peppers	<i>Sedum acre</i>	Mossy stonecrop
<i>Datura stramonium</i>	Jimson weed	<i>Sempervivum arachnoideum</i>	Hens and chicks
<i>Duboisia hopwoodii</i>	Pituri	<i>Solanum melagena</i>	Egg-plant
<i>Duboisia myoporoides</i>	Corkwood	<i>Solanum tuberosum</i>	Potato
<i>Equisetum palustre</i>	Horsetail	<i>Zinnia elegans</i>	Garden zinnia

1.2. Biosynthesis of the four main alkaloids in tobacco

1.2.1. Pyridine, pyrrolidine and piperidine ring formation

The pyridine ring is synthesized from nicotinic acid or its derivatives. Nicotinic acid is an intermediate of the nicotinamide adenine dinucleotide (NAD) pathway (Kato and Hashimoto, 2004). In nicotinic acid biosynthesis, aspartate is oxidized by aspartate oxidase (AO) to form α -iminosuccinic acid (Figure 1.1). Then α -iminosuccinic acid is condensed and cyclized with glyceraldehyde-3-phosphate (GAP) by quinolinic acid

synthase (QS), yielding quinolinic acid. Finally nicotinic acid with its pyridine ring is formed from quinolinic acid in the NAD cyclic steps.

The pyrrolidine ring is derived mostly from ornithine and possibly some from arginine via the symmetric diamine putrescine (Leete, 1992). First, ornithine is converted to putrescine by ornithine decarboxylase (ODC). Additionally, arginine is converted to putrescine, via agmatine and N-carbamoylputrescine, with arginine decarboxylase (ADC) and agmatine deiminase (AIH). Next, putrescine is converted to N-methylputrescine through S-adenosylmethionine-dependent N-methylation catalyzed by putrescine N-methyltransferase (PMT), which is the first committed step in the formation of pyrrolidine. N-methylputrescine is oxidatively deaminated by N-methylputrescine oxidase (MPO) to 4-methylaminobutanal, which spontaneously cyclizes to N-methyl- Δ^1 -pyrrolinium cation.

The piperidine ring is derived from lysine (Leete, 1992). Lysine is converted to cadaverine through decarboxylation by lysine decarboxylase (LDC). Cadaverine is then oxidatively deaminated by diamine oxidase (DAO) to 5-aminopentanal, which spontaneously cyclizes to piperidine.

1.2.2. Nicotine, nornicotine, anabasine and anatabine formation

The synthases responsible for nicotine, anabasine and anatabine have not been identified. There are two genes, *A622* and *BBL* involved in coupling of pyridine, pyrrolidine and piperidine rings. Reductase gene *A622* is a member of the PIP family of NADPH-dependent reductases. In *A622* suppressed cells, nicotinic acid *N*-glycoside and N-methyl pyrrolinium cation accumulate at the expense of all tobacco pyridine alkaloids (DeBoer et al., 2009). *BBLs* encode flavin-containing oxidases of berberine bridge enzyme family. When expression of the *BBL* genes was suppressed in tobacco hairy roots or in tobacco plants, nicotine production was highly reduced, with a gradual accumulation of dihydrometanicotine. Inhibition of *BBL* expression in cultured tobacco cells inhibited the formation of all pyridine alkaloids (Kajikawa et al., 2011).

Nicotine is composed of two heterocyclic rings, pyridine and pyrrolidine rings. 3, 6-dihydronicotinic acid and 3, 6-dihydronicotine are postulated as potential intermediates during the condensation between nicotinic acid and N-methylpyrrolinium. These putative intermediates are proposed based on the observation that N-methylpyrrolidine is attached to the C-3 position of the pyridine ring, and the hydrogen at C-6 of nicotinic acid is lost during nicotine formation.

Nornicotine is mainly, if not exclusively, synthesized through *N'*-demethylation of nicotine by nicotine demethylases, which belong to the CYP82E subfamily of cytochrome P450 monooxygenases. Cytochrome P450 enzymes are reviewed in section 1.4.1 of this chapter. In tobacco, functional nicotine demethylases are encoded by *CYP82E4* (Siminszky et al., 2005), *CYP82E5v2* (Gavilano and Siminszky, 2007) and *CYP82E10* (Lewis et al., 2010). *CYP82E2* and *CYP82E3* are present in the tobacco genome, but they encode for inactive enzymes and hence can be classified as pseudogenes. Besides nicotine demethylation, direct synthesis of nornicotine is implied by the existence of nornicotine in tobacco when all three demethylases are silenced (Lewis et al., 2010). In addition to its preferred *N*-methylputrescine substrate, the recombinant MPO1 enzyme can, to a lesser degree, utilize putrescine, resulting in an unmethylated pyrrolinium salt (Kato et al., 2007). If the nicotine synthase can use this unmethylated pyrrolinium salt, nornicotine could be directly produced, bypassing nicotine.

Anabasine is composed of pyridine and piperidine rings. As in nicotine and anatabine, nicotinic acid is incorporated into anabasine with elimination of a hydrogen at C-6 and loss of a carboxyl group. The formation of anatabine is quite different from that of anabasine, although they differ only by two hydrogens. The piperidine ring of anatabine is derived from nicotinic acid, not lysine. During the coupling of two molecules of nicotinic acid, one hydrogen atom at the C-6 position and both carboxyl groups are eliminated.

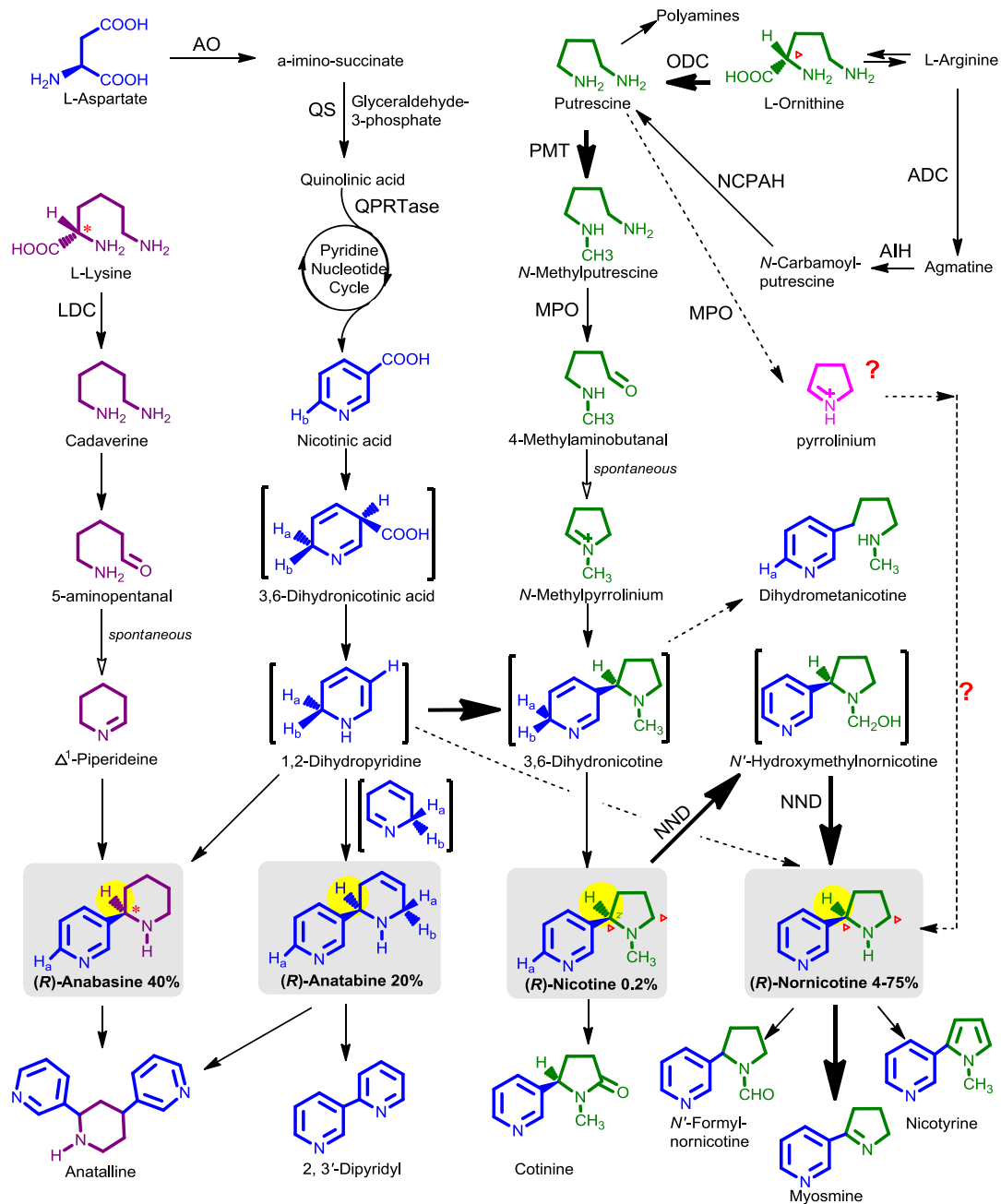


Figure 1.1. Alkaloid biosynthesis in tobacco plant (*Nicotiana* species) (Leete, 1992; Hakkinen et al., 2007; Kajikawa et al., 2011; Shoji and Hashimoto, 2011). The C-2 carbons of ornithine and lysine, and the hydrogen at C-6 of nicotinic acid are indicated using symbols to show their fates. Enzymes listed: ADC: arginine decarboxylase; AIH: agmatine deiminase; AO: aspartate oxidase; AP: aspartate oxidase; AS: arginase; LDC: lysine decarboxylase; MPO: methylputrescine oxidase; NCPAH: N-carbamoylputrescine amidohydrolase; ODC: ornithine decarboxylase; PMT: putrescine N-methyltransferase; QS: quinolinate synthase; QPRTase: quinolinate phosphoribosyltransferase; NND: nicotine N-demethylase. Hollow arrows mean that the reaction is spontaneous. Hypothetical intermediates are included in brackets.

1.3. Nicotine demethylation in tobacco

1.3.1. Nicotine demethylation mechanism

To study the mechanism of the nicotine demethylation in tobacco, nicotine with different positions labeled were incubated with tobacco plants and cultured cells. Results from [2'-¹⁴C, 2'-³H]nicotine feeding to *N. glauca* excluded the oxidation at C- 2' (Figure 1.2) (Leete and Chedekel, 1974). [4',4',5',5'-²H₄]nicotine incubation in *N. alata* root cultures ruled out the possibility of oxidation at C-5' (Botte et al., 1997). *N'*-formylnornicotine is not the intermediate of demethylation supported by the observation of [¹³C, ²H₃-methyl]nicotine and [1'-¹⁵N]nornicotine feeding (Bartholomeusz et al., 2005a) and is probably produced by the condensation of nornicotine and formaldehyde. CO₂ formation during demethylation implies the involvement of tetrahydrofolate-mediated pathways of one-carbon metabolism and *N'*-hydroxymethylnornicotine (Mesnard et al., 2002). Based on these feeding results, two possible mechanisms were proposed for nicotine demethylation in *N. tabacum*. The hydrogen atom transfer pathway is the more probable one, according to CYP2A6 catalyzed nicotine demethylation in humans.

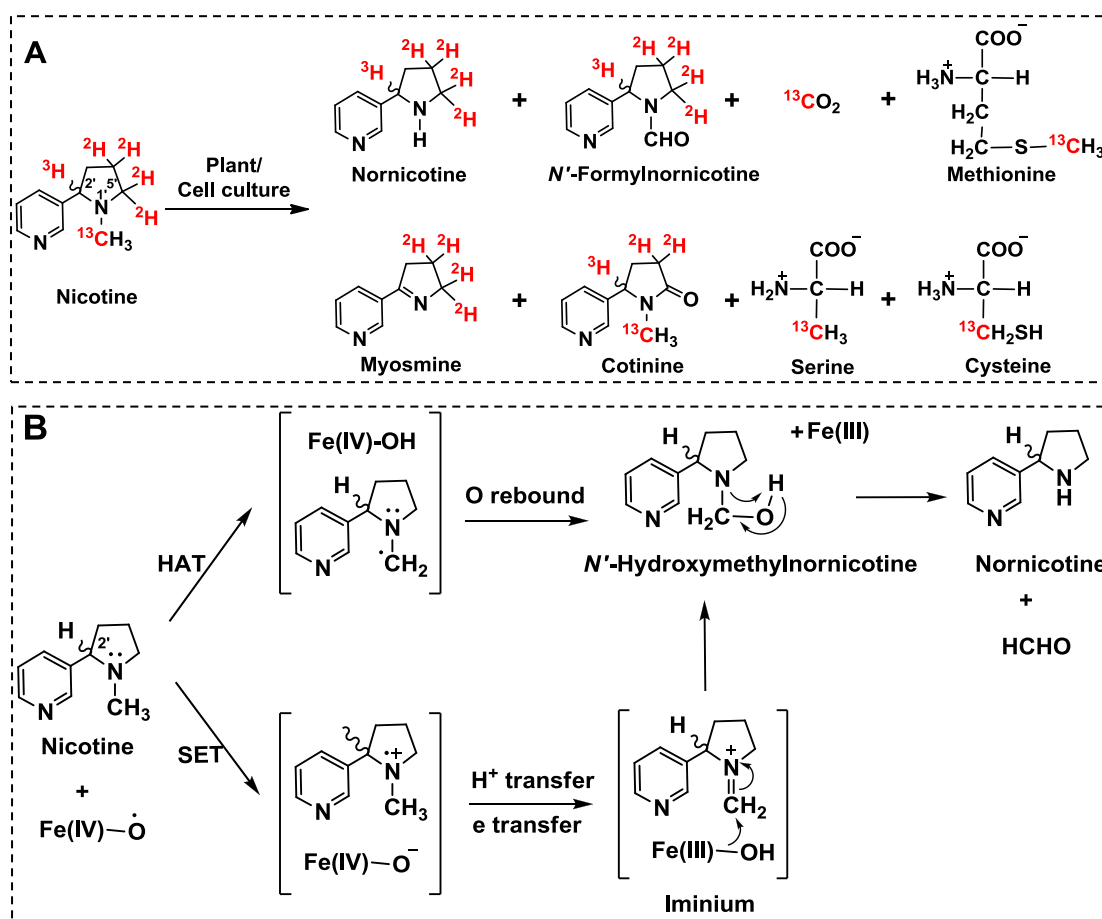


Figure 1.2. Two possible mechanisms in *N'*-demethylation of nicotine catalyzed by cytochrome P450 enzymes. (A) Metabolites profiles of nicotine feeding assays (Leete and Chedekel, 1974; Botte et al., 1997; Mesnard et al., 2002; Bartholomeusz et al., 2005a). Nicotine demethylation is a direct oxidation of *N'*-methyl group. Label patterns of amino acids suggest that methyl group is transferred into one-carbon pathway. (B) Two possible mechanisms of nicotine demethylation based on general cytochrome P450 catalyzed *N*-dealkylation reaction (Meunier et al., 2004): hydrogen atom transfer (HAT) versus single electron transfer (SET). HAT is a more probable mechanism based on the nicotine demethylation in humans. Note the hydrogen atom at the C-2' position is not involved in either mechanism. Presumably (R)-nicotine is demethylated into (R)-nornicotine, and (S)-nicotine is converted into (S)-nornicotine.

1.3.2. Structure and function studies of tobacco nicotine demethylase enzymes

During the process of screening nicotine demethylase mutants plants, a number of plants containing mutation(s) in demethylase genes were identified by sequencing, and the functionality of the demethylases was accessed by alkaloid analysis or in vitro enzyme

assays (Table 1.3). The sequence alignment of CYP82E4, CYP82E5v2 and CYP82E10 is shown in Figure S1.3. In tobacco, CYP82E3 is an ortholog of CYP82E4, with 95% sequence identity at the amino acid level, but it lacks nicotine *N'*-demethylase activity. The same amino acid substitution causes the functional turnover of CYP82E3 and CYP82E4 (Table 1.3) (Gavilano et al., 2007). Homologous model and molecular dynamics analysis of CYP82E4 and CYP82E3 and their mutants show the single amino acid mutation outside the active site region may have indirectly mediated the flexibility of the F-G and B-C loops through helix I, causing a functional turnover of the P450 monooxygenase (Wang et al., 2011).

Table 1.3. Functionality of tobacco nicotine demethylases possessing mutations (Gavilano et al., 2007; Xu et al., 2007b; Lewis et al., 2010). The functionalities of CYP82E3 and CYP82E10 variants were confirmed by *in vitro* enzyme assays. Except G900C mutation, the functionality of all CYP82E4 variants was accessed based on the nicotine and nornicotine ratio in tobacco plants. CYP82E5v2 with G1266A mutation lack the heme-binding domain which is essential for all P450 enzyme activity.

Enzyme	Mutation	Amino acid	Enzyme functionality
CYP82E3	C900G	C330W	Functional
CYP82E4	C113T	P38L	Wild type
	C320T	P107L	Nonfunctional
	G511A	D171N	Wild type
	G601A	E201K	Wild type
	G886A	E296K	Wild type
	G900C	W330C	Nonfunctional
	G986A	W329Stop	Nonfunctional
	G1026A	T342T	Reduced conversion
	G1092T	K364N	Nonfunctional
	G1126A	V376M	Half of wild type
	G1293A	E431E	Reduced conversion
	C1372T	P458S	Nonfunctional
	G1375A	G459R	Nonfunctional
CYP82E5v2	G1266A	W422Stop	Nonfunctional

Table 1.3 (continued)

Enzyme	Mutation	Amino acid	Enzyme functionality
CYP82E10	G235A	G79S	Nonfunctional
	C319T	P107S	Nonfunctional
	G1030A	A344T	Wild type
	C1141T	P381S	Nonfunctional
	G1228A	A410T	Wild type
	G1250A	R417H	Wild type
	C1255T	P419S	A quarter of wild type

1.3.3. Nicotine demethylase specificity

Many nicotine demethylation investigations in tobacco used a series of nicotine analogs incubated with excised tobacco leaves and cultured tobacco cells (Table 1.4) (Dawson, 1951; Kisaki et al., 1978; Mesnard et al., 2001; Bartholomeusz et al., 2005b; Molinié et al., 2007). The feeding assays demonstrated that the tobacco could use a broad spectrum of compounds for the *N*-dealkylation reactions. Plant materials used in these feeding assays were all high demethylating tissues, implying that it could be the nicotine demethylases that catalyzed these reactions. It is interesting to note that many of the cytochrome P450s have a broad spectrum of possible substrates. In humans, some CYPs (e.g., CYP2D6 and CYP2C9) are promiscuous and are responsible for the oxidation of approximately 70% of all therapeutic drugs. Instead of “lock and key” concept, they seem to represent the “induced fit” model in which the enzyme may accommodate very different substrates in the active center by virtue of relatively high flexibility (Pylypenko and Schlichting, 2004; Wade et al., 2004) and ability to undergo appropriate conformational changes (Denisov et al., 2005).

Table 1.4. Specificity of demethylation process. Nicotine analogues were fed to tobacco leaves or cells. The compounds are classified based on whether the *N*-dealkylation product is isolated. Details of the feeding assays are given in Table S1.2.

Compound structures	
N-dealkylation	
Non-N-dealkylation	

Note: Compounds with dashed border are found in tobacco. The compound with solid border has inconsistent reports of the detection of *N*-dealkylation production.

1.3.4. Evolution of nicotine demethylases in *N. tabacum* L.

Nornicotine is typically a minor alkaloid in tobacco, accounting for about 3-5% of the total alkaloid content. In some tobacco populations, especially burley tobacco, individual plants known as “converters” can demethylate as much as 97% of the nicotine to nornicotine during leaf senescence and curing. Cultivated tobacco (*N. tabacum*) is an allotetraploid species derived from the hybridization of ancestral *N. tomentosiformis* and *N. sylvestris* (Clarkson et al., 2005). Interestingly, the alkaloid profile of *N. tabacum* is different from that of either of its two progenitors. To explain such discrepancies, nicotine demethylase genes from tobacco and the two parents were isolated and functionally characterized. In tobacco, functional nicotine demethylases are encoded by *CYP82E4* (Siminszky et al., 2005; Xu et al., 2007a), *CYP82E5* (Gavilano and Siminszky, 2007) and *CYP82E10* (Lewis et al., 2010). *CYP82E4* is silenced in nonconverters (Table 1.5). Additionally, *CYP82E2* and *CYP82E3* are present in the tobacco genome, but they do not encode for active or functional enzymes. *CYP82E3*, *CYP82E4* and *CYP82E5* are derived from *N. tomentosiformis*, while *CYP82E2* and *CYP82E10* are from *N. sylvestris*. Although being inactive in tobacco, all ancestral orthologues of *CYP82E2*, *CYP82E3* and *CYP82E4* encode active nicotine demethylases. *CYP82E* genes in modern tobacco have gained stable mutations in *CYP82E2* and *CYP82E3* and an unstable mutation in *CYP82E4*, after the hybridization of the two parental species (Chakrabarti et al., 2007).

Table 1.5. Origin of nicotine demethylases found in *N. tabacum* L. genome.

Demethylase genes	Originality	Function	References
<i>CYP82E2</i>	<i>N. sylvestris</i>	Inactive, E375K and W422 mutations	(Chakrabarti et al., 2007)
<i>CYP82E3</i>	<i>N. tomentosiformis</i>	Inactive, W330C	(Gavilano et al., 2007)
<i>CYP82E4</i>	<i>N. tomentosiformis</i>	Active, Unstable mutation	(Gavilano et al., 2007)
<i>CYP82E5</i>	<i>N. tomentosiformis</i>	Active	(Gavilano and Siminszky, 2007)
<i>CYP82E10</i>	<i>N. sylvestris</i>	Active	(Lewis et al., 2010)

1.4. Theoretical studies of enzymes responsible for nicotine metabolism

1.4.1. Cytochrome P450

1.4.1.1. Primary sequence motif, nomenclature

Cytochrome P450s are heme monooxygenases that catalyze diverse oxidation reactions and are biologically important for their roles in the oxidative transformation of both exogenous and endogenous small molecules. Broadly, cytochrome P450 enzymes biosynthesize endogenous molecules, inactivate/activate compounds with biological activities, and increase the hydrophilicity of compounds which facilitates their excretion and prevents toxic accumulation. They are able to catalyze the hydroxylation of saturated carbon-hydrogen bonds, the epoxidation of double bonds, the oxidation of heteroatoms, dealkylation reactions, oxidations of aromatics and many other reactions (Meunier et al., 2004). Plant P450s participate in many biochemical pathways, including those devoted to the synthesis of plant products such as phenylpropanoids, alkaloids, terpenoids, lipids, cyanogenic glycosides, glucosinolates and plant growth regulators such as gibberellins, jasmonic acid and brassinosteroids (Chapple, 1998).

There are three conservative P450 primary sequence motifs (Chapple, 1998): 1) consensus (P/I)PGPx(G/P)xP, proline-rich region immediately after the N-terminal hydrophobic helix. This region acts as a “hinge” that is required for optimal orientation of the enzyme with regard to the membrane; 2) consensus (A/G)Gx(D/E)T(T/S), a threonine-containing binding pocket for the oxygen molecule; 3) FxxGx(H/R)xCxG, “P450 signature” motif and heme-binding domain. A cysteine is the proximal or “fifth” ligand to the heme iron.

All P450 systematic gene names include the designation CYP for cytochrome P450. The nomenclature for CYP isoforms is derived from amino acid sequence similarity determined through gene sequencing (Brown et al., 2008). Usually, amino acid sequences with more than 40% similarity are placed in the same family, designated by a number (e.g., CYP1), while those with greater than 55% similarity are grouped in the same subfamily, designated by a letter (e.g., CYP1A), and those with more than 97% identity comprise alleles, designated again with a number (e.g., CYP1A1). The numbering of

plant P450 gene families begins with CYP71 through CYP99. These family designations have now been exhausted and continue from CYP701.

1.5.1.2. Enzymatic reaction cycle of cytochrome P450

Because of the vast variety of reactions catalyzed by CYPs, the activities and properties of the many CYPs differ in many aspects. In general, the P450 catalytic cycle proceeds (mainly based on P450_{cam}, a microbial cytochrome P450) as follows (Figure 1.3C): 1) The substrate enters into the active site of the enzyme and the bound substrate induces a change in the conformation of the active site, often displacing a water molecule from the distal axial coordination position of the heme iron (Figure 1.3A); 2) The change in the electronic state of the active site makes the heme a better electron sink and triggers an electron transfer of an electron from NAD(P)H via cytochrome P450 reductase or another associated reductase, which reduces the ferric heme iron to the ferrous state; 3) Molecular oxygen binds covalently to the distal axial coordination position of the heme iron. One electron from the iron(II) center and one from the triplet oxygen pair create an iron(III)-oxygen bond; 4) A second electron is transferred via the electron-transport system, reducing the dioxygen adduct to a negatively charged peroxy group. This generates a negatively charged iron(III)-peroxy complex, which is a short-lived intermediate state. Electrons from NADPH are transferred one by one to P450s via cytochrome P450 reductases (CPR). Both plant P450s and their reductases are usually bound via their N-terminus to the cytoplasmic surface of the endoplasmic reticulum (Werck-Reichhart et al., 2000); 5) The peroxy group formed in step 4 is rapidly protonated twice by local transfer from water or from surrounding amino acid side chains, releasing one water molecule, and forming a highly reactive species commonly referred to as P450 Compound 1 (Cpd I). P450 Compound 1 is most likely an iron(IV)oxo with additional oxidizing equivalent delocalized over the porphyrin and thiolate ligands (Por⁺Fe(IV)-oxo); 6) Depending on the substrate and enzyme involved, P450 enzymes catalyze a wide variety of reactions. Figure 1.3C is an illustration of a hypothetical hydroxylation. After the product has been released from the active site, the enzyme returns to its original state, with a water molecule returning to occupy the distal coordination position of the iron nucleus.

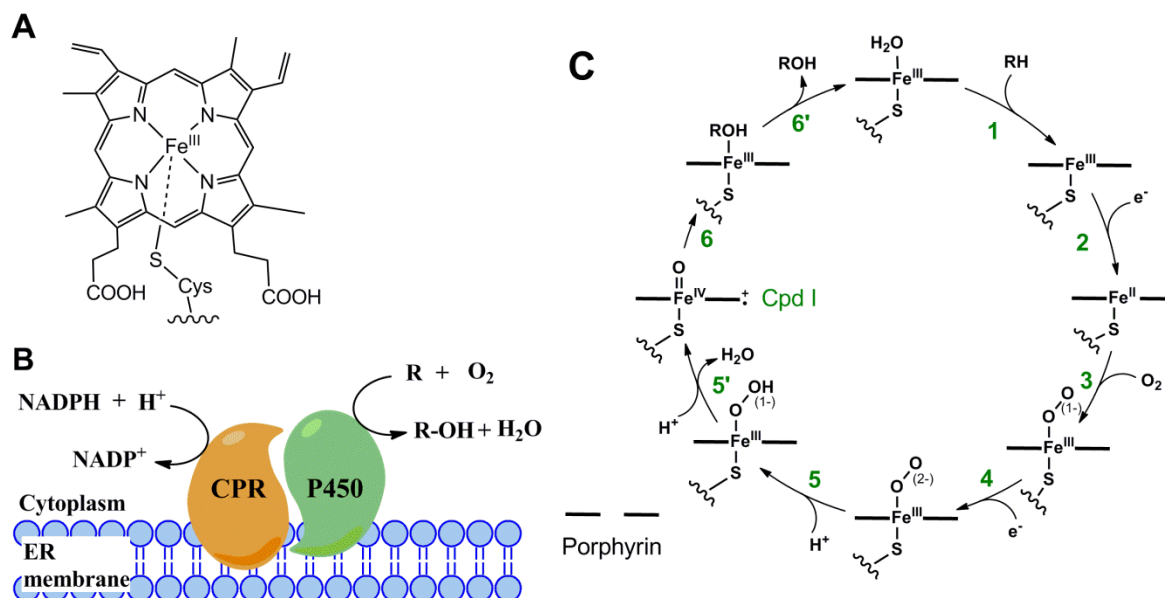


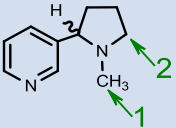
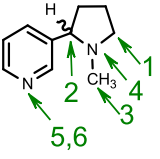
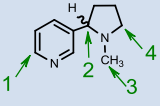
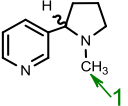
Figure 1.3. The catalytic cycle of cytochrome P450. (A) Prosthetic of cysteinato-heme enzymes: an iron(III) protoporphyrin-IX linked with a proximal cysteine ligand (Meunier et al., 2004). (B) Schematic organization of plant cytochrome P450 systems (Werck-Reichhart et al., 2000; Bernhardt, 2006). CPR: cytochrome P450 reductase. (C) Schematic representation of the different intermediates generated during the catalytic cycle of cytochrome P450 (Denisov et al., 2005).

1.4.2. Model studies of CYP-catalyzed nicotine demethylation

In humans, nicotine is degraded principally by CYP2A6 through 5'-hydroxylation and *N'*-demethylation is only a minor pathway (Table 1.6 and Figure 1.4). The preponderance of 5'-hydroxylation over the *N'*-demethylation is by a factor of 19:1 (Murphy et al., 2005), confirmed by computational calculation (Li et al., 2010). Li et al. (2010) performed a series of first-principle electronic structure calculations to examine the fundamental reaction pathways for 5'-hydroxylation and *N'*-demethylation of nicotine catalyzed by the active species of P450 enzyme, Cpd I. *N'*-demethylation of nicotine involves a *N'*-methylhydroxylation followed by the decomposition of *N'*-(hydroxymethyl)nornicotine. The *N'*-methylhydroxylation of nicotine occurs through a stepwise process, that is, a bond activation hydrogen transfer step and a rebound step. The hydrogen transfer step is rate-determining. After the *N'*-methylhydroxylation process, *N'*-(hydroxymethyl)nornicotine decomposes to nornicotine and formaldehyde with a very low energy barrier. This

decomposition process occurs on the deprotonated *N'*-(hydroxymethyl)nornicotine species and is assisted by a water molecule.

Table 1.6. Species differences in nicotine metabolism. Details of how nicotine is metabolized by microbes and humans are provided in Supplement S1.1 and S1.2.

Species	Substrate	Enzymes	Metabolites	Reference
Tobacco (<i>Nicotiana L.</i>)		1. CYP82E4(major), CYP82E5, CYP82E10 [1] 2. Unknown	1. Nornicotine [1] 2. Cotinine [2]	[1] (Lewis et al., 2010); [2] (Botte et al., 1997)
Human (<i>Homo sapiens</i>)		1. CYP2A6(major), CYP2B6, CYP2A13 [1] 2. CYP2A6 [2] 3. CYP2A6, CYP2B6, CYP2A13 [3] 4. FMO3 [4] 5. Amine N- methyltransferase 6. UGT1A3, UGT1A4 (major), UGT1A9 [6]	1. 5'-Hydroxynicotine [1] 2. 2'-Hydroxynicotine [2] 3. Nornicotine [3] 4. <i>Trans</i> -nicotine <i>N</i> -1'- oxide 5. Nicotine isomethonium ion [5] 6. Nicotine glucuronide [6]	[1] (Flammang et al., 1992); [2] (Hecht et al., 2000); [3] (Yamanaka et al., 2005); [4] (Park et al., 1993) [5] (Crooks and Godin, 1988); [6] (Kuehl and Murphy, 2003)
Bacterial		1. Nicotine dehydrogenase [1] 2. nicA [2] 3. Unknown 4. Unknown	1. 6-Hydroxynicotine [1] 2. N-Methylmyosmine 3. Myosmine [3] 4. 5'-Hydroxylation [3]	[1] (Freudenberg et al., 1988); [2] (Tang et al., 2009); [3] (Wang et al., 2012)
Fungi (<i>Aspergillus oryzae</i> 112822)		1. Unknown	1. Nornicotine [1]	[1] (Meng et al., 2010)

Note: FMO3: Flavin-Containing Monooxygenase 3; UGT1A3: UDP-glucuronosyltransferase 1A3.

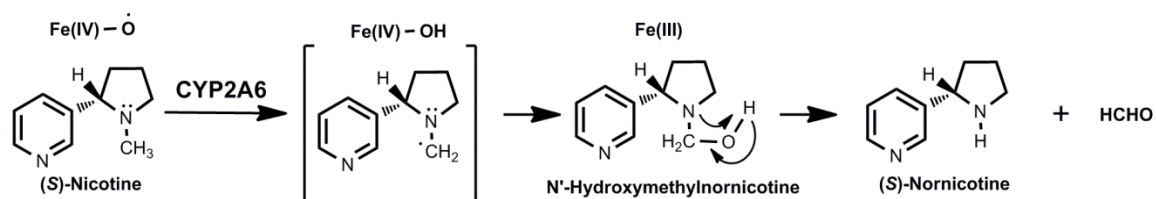


Figure 1.4. Human CYP2A6-catalyzed demethylation of (S)-nicotine (Li et al., 2010).

The CYP2A6-catalyzed 5'-hydroxylation of nicotine has been studied by quantum mechanics (Li et al., 2010), molecular docking, molecular dynamics simulations, and binding free energy calculations, in combination with first-principles electronic structure calculations accounting for solvent effects (Li et al., 2011a). The 5'-hydroxylation process is similar to the *N*-methylhydroxylation, namely, that a rate-determining hydrogen transfer step in a two-state reactivity mechanism is followed by a rebound step. (S)-nicotine in the active site of the enzyme exists in the neutral state, in contrast with the protonated state in aqueous solution. CYP2A6-catalyzed (S)-nicotine 5'-hydroxylation proceeds mainly with the stereoselective loss of the *trans*-5'-hydrogen. The calculated overall stereoselectivity is 97% favoring the *trans*-5'-hydroxylation. The stereoselectivity of the reaction originates from the different binding affinity of two conformations of (S)-nicotine free base with CYP2A6 (Figure 1.5).

Recently, the CYP2A6 and CYP2A13 crystal structures were solved with nicotine soaked into the CYP crystals (DeVore and Scott, 2012). Both CYP2A6 and CYP2A13 oxidize nicotine at various locations on the methylpyrrolidine ring (Table 1.6). Although the CYP2A6 and CYP2A13 enzymes are 94% identical, the catalytic efficiency of CYP2A13 with nicotine is over 20-fold higher than CYP2A6 (Bao et al., 2005). DeVore and Scott (2012) investigated the structural differences in nicotine binding between CYP2A6 and CYP2A13 by determining the structures of both complexes. In CYP2A13 the methylpyrrolidine ring is oriented more parallel to the heme plane, while in CYP2A6 the orientation is closer to perpendicular. Another difference is that in CYP2A6 the N297 side chain is rotated, slightly farther away from nicotine, compared to CYP2A13

structure. N297 is important for the orientation of several ligands in the CYP2A6 active site (Schlicht et al., 2009).

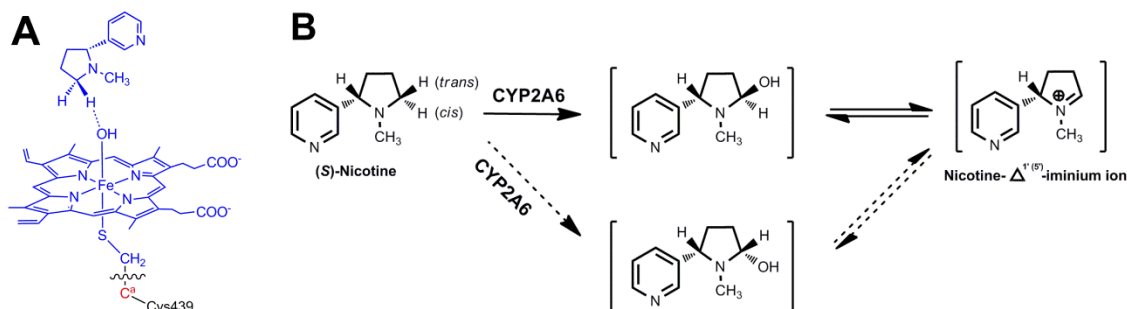


Figure 1.5. CYP2A6-catalyzed 5'-hydroxylation of (S)-nicotine. (A) Representative binding structure of Compound I of CYP2A6 with *trans*-5'-hydrogen of (S)-nicotine. Atoms in blue are subjected to the quantum mechanical calculation. The boundary carbon atom (red) is treated with improved pseudobond parameters. All other atoms are treated with the molecular mechanical method. (B) CYP2A6-catalyzed 5'-hydroxylation of (S)-nicotine. CYP2A6 catalyzes hydroxylation of nicotine at prochiral 5'-position to form the $\Delta^{1',(5')}$ -iminium ion. *Trans*-5'-hydrogen is stereoselectively used by CYP2A6.

Several bacterial species are able to grow on nicotine. The pathway for oxidative degradation of nicotine in *Arthrobacter nicotinovorans* includes two genetically and structurally unrelated flavoenzymes, 6-hydroxy-L-nicotine oxidase (6HLNO) and 6-hydroxy-D-nicotine oxidase (6HDNO), which act with absolute stereospecificity on the L- (S) and D- (R) forms, respectively, of 6-hydroxy-nicotine (Figure 1.6). Crystal structures of 6HLNO and 6HDNO have been solved and stereoselectivity of these two enzymes has been studied (Koetter and Schulz, 2005; Kachalova et al., 2010). The orientation of the chiral center atom C-2' of 6-hydroxy-L-nicotine with respect to the flavin N-5 atom is suitable for dehydrogenation by abstraction of a hydrogen from C-2' to the flavin. The absolute stereospecificity of the enzymatic reaction is suggested to be the difference in the orientation of the L- and D-substrates with respect to the flavin.

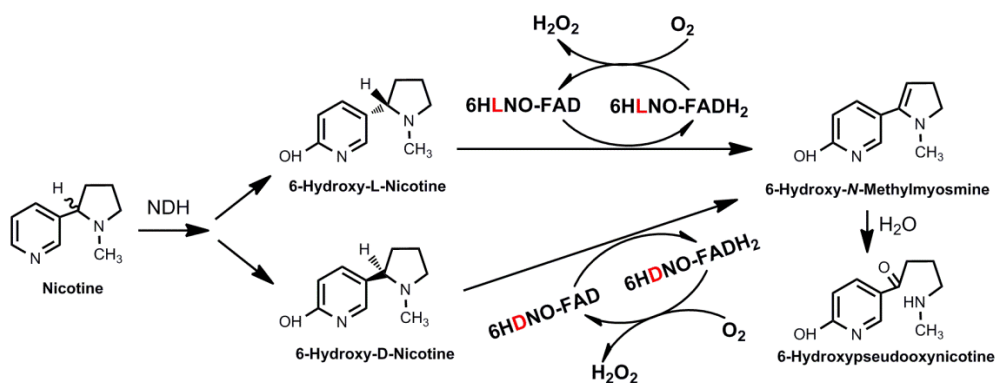


Figure 1.6. Oxidative degradation of nicotine in *Arthrobacter nicotinovorans*. NDH: nicotine dehydrogenase; 6HLNO: 6-hydroxy-L-nicotine oxidases; 6HDNO: 6-hydroxy-D-nicotine oxidases

Bacterial cytochrome P450 101 (P450_{cam}) is a well studied enzyme and used as model for structure and function relationship investigation. Nicotine is a non-native substrate of P450_{cam}, and used to probe the active site of P450_{cam}. P450_{cam} comes from *Pseudomonas putida*, which has been used to prepare (R)-nicotine (Edwards and McCuen, 1983). Based on P450_{cam} crystal structure, molecular dynamics calculations of nicotine and P450_{cam} complex predicate that P450_{cam} binds (R)-nicotine 1.4-fold faster than (S)-nicotine, and the product formation occurs at a faster rate at the 5' methylene group than at the N'-methyl group of the pyrrolidine ring for both enantiomers, which were confirmed by a parallel experimental study (Jones et al., 1993). In vitro incubation of P450_{cam} and (S)-nicotine shows that P450_{cam}, like human CYP2A6, catalyzes the stereoselective, energetically less favorable loss of the trans-5'-hydrogen (Carlson et al., 1995). Despite the existence of a theoretical model that is consistent with the observed distribution of monooxygenation products, it is interesting to note that the primary binding mode of nicotine is unproductive (Figure 1.7) (Strickler et al., 2003). Crystallographic and spectroscopic data indicate direct coordination of nicotine pyridine nitrogen with the heme iron. Reduction of the heme from Fe(III) to Fe(II) and introduction of carbon monoxide into crystals of the nicotine-P450_{cam} complex, to simulate molecular oxygen binding, produces reorientation of the nicotine. So P450_{cam}-nicotine interactions

exhibited complicated behavior, questioning the value of a single crystal structure for binding mode study of a given substrate-enzyme complex.

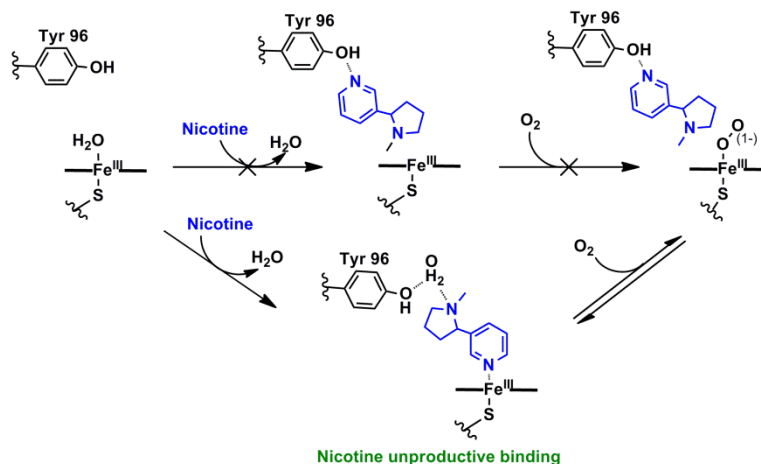


Figure 1.7. Hydroxylation of nicotine by P450_{cam}, based on crystallographic data (Strickler et al., 2003).

1.5. Compartmentation and trafficking of nicotine

1.5.1. Long distance translocation from roots to leaves

Nicotine is produced in tobacco roots (Dawson, 1942), probably only in root tips (Solt, 1957), then translocated to leaf via xylem (Guthrie et al., 1962) and finally deposited in leaf vacuole. As much as 60 mM of nicotine accumulates in the vacuoles of the leaf epidermal cells at the leaf tip (Lochmann et al., 2001). Nicotine demethylation can occur in both root (Mizusaki et al., 1965) and leaf (Dawson, 1945), mainly in aging leaves (Wernsman and Matzinger, 1968). The accumulation patterns of nicotine and nornicotine in leaf have been investigated (Burton et al., 1992)(Figure 1.8). The four main alkaloids are found in tobacco stem sap (Wada et al., 1959), suggesting all four alkaloids can be translocated from root to leaf. About 0.1 mM nicotine is present in the xylem fluid (Baldwin, 1989). Results from metabolite studies are confirmed by the expressions of genes encoding enzymes important for nicotine biosynthesis. The important genes *MPO*, *QPRTase*, *A622* and *BBL* in *N. tabacum* are all expressed in root, not in leaf (Table 1.7 and Figure 1.9). The putative alkaloid biosynthetic gene *A622* expresses in the first 10mm of root tips, which is consistent with the results obtained from excised root culture

study (Solt, 1957). The expression patterns of nicotine demethylase genes are also consistent with where nornicotine formation and accumulation occur.

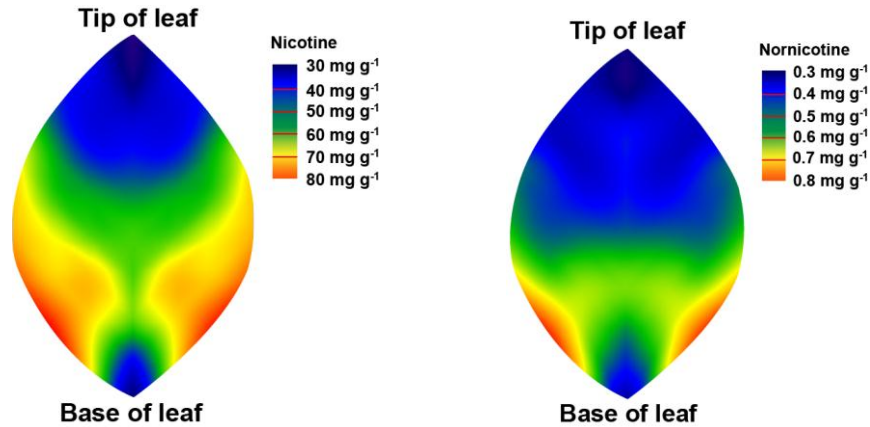


Figure 1.8. Nicotine and nornicotine distribution in leaf (Burton et al., 1992). The air-cured leaf of dark tobacco Ky171 was cut into 7cm long X 4cm wide segments along the length of the leaf. The mirror image segments of the lamina were combined and analyzed.

Table 1.7. Spatial expression patterns of genes encoding nicotine biosynthesis pathway enzymes in tissues.

Genes	Expression location			Material	Method	Reference		
	Leaf	Stem	Root					
<i>PMT</i>	+	*	-	+	**	<i>N. tabacum</i>	RNA gel blot[1]; RT-PCR and immunoblot [2]	[1] (Hibi et al., 1994; Katoh et al., 2007); [2] (Sachan and Falcone, 2002)
<i>MPO</i>	-	-	-	+		<i>N. tabacum</i>	RNA gel blot	(Katoh et al., 2007)
<i>QPRTase</i>	-	ND	+	+		<i>N. tabacum</i>	RNA gel blot	(Sinclair et al., 2000)
	+	ND	+	+		<i>N. glauca</i>	RNA gel blot	(Sinclair et al., 2000)
<i>A622</i>	-	-	-	+	**	<i>N. tabacum</i>	RT-PCR[1]; RNA gel blot[2, 3]; immunoblot[3]	[1] (Kajikawa et al., 2009); [2] (Hibi et al., 1994); [3] (Shoji et al., 2002)
	-	ND	+	+		<i>N. sylvestris</i>	Northern analysis	(Sinclair et al., 2004)
	+	*	ND	+		<i>N. glauca</i>	Northern analysis	(Sinclair et al., 2004)
<i>BBL</i>	-	-	-	+		<i>N. tabacum</i>	qRT-PCR	(Kajikawa et al., 2011)
<i>CYP82E4</i>	+	*	+	+		<i>N. tabacum</i>	Promoter fused with GUS[1]; qRT-PCR[2]	[1] (Chakrabarti et al., 2008); [2] (Gavilano and Siminszky,

Table 1.7 (continued)

Genes	Expression location			Material	Method	Reference
	Leaf	Stem	Root			
						2007; Xu et al., 2007a)
<i>CYP82E5</i>	+	ND	ND	<i>N. tabacum</i>	qRT-PCR	(Gavilano and Siminszky, 2007)
<i>CYP82E10</i>	ND	ND	+	<i>N. tabacum</i>	Root specific cDNA library	(Lewis et al., 2010)

Note: ND: not determined; * low level before induction; ** first 10mm root tip.

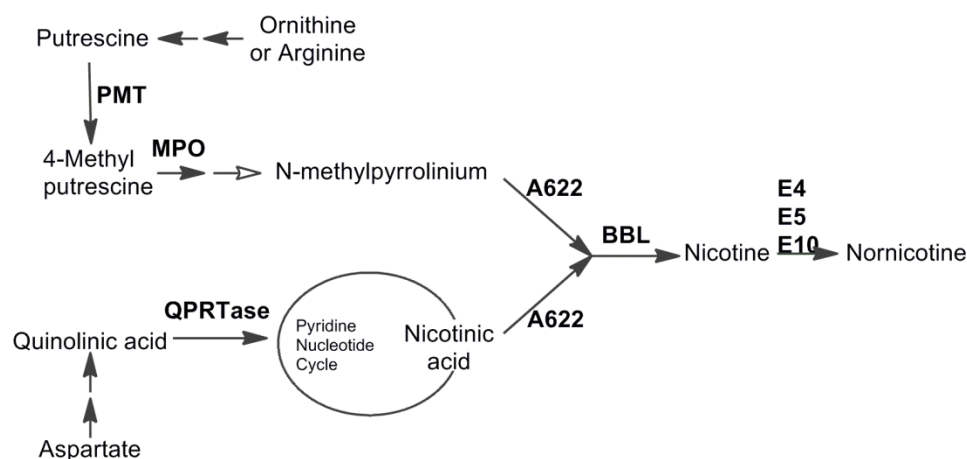


Figure 1.9. A simplified diagram of nicotine synthesis in *Nicotiana*. Enzymes listed: BBL: berberine bridge enzyme-like protein; E4/ E5/ E10: nicotine N-demethylase CYP82E4/ CYP82E5/ CYP82E10; MPO: methylputrescine oxidase; PMT: putrescine N-methyltransferase; QPRTase: quinolinate phosphoribosyltransferase. Hollow arrow means the reaction is spontaneous.

Jasmonate-inducible Alkaloid Transporter 1 (NtJAT1) and a pair of homologous proteins NtMATE1 and NtMATE2 have been identified as tonoplast-localized nicotine transporters in tobacco (Figure 1.10) (Morita et al., 2009; Shoji et al., 2009). NtJAT1 and NtMATEs are Multidrug And Toxic compound Extrusion (MATE)-type transporters, which have been shown to efflux low-molecular weight compounds as drug/H⁺ or drug/Na⁺ antiport systems. *NtJAT1* is expressed in leaves, stems and roots, and localized to the tonoplast in leaves. Biochemical analysis demonstrated that NtJAT1 functioned as a H⁺-antiporter, transporting nicotine and anabasine (Morita et al., 2009). In contrast to

NtJAT1, *NtMATE* genes are specifically expressed in nicotine-producing root cells and localized to the tonoplast (Shoji et al., 2009).

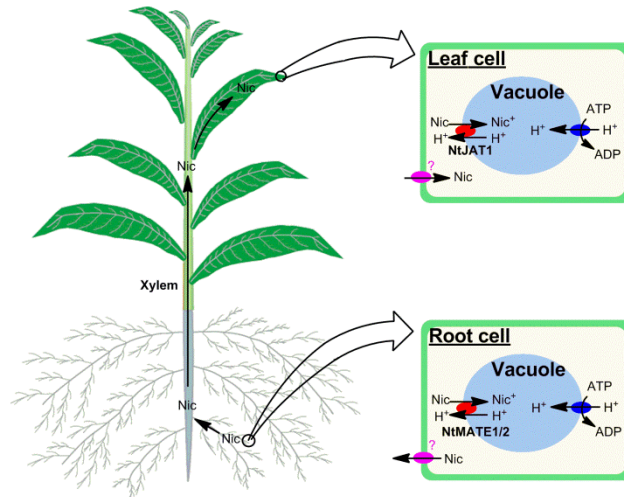


Figure 1.10. A model of nicotine translocation and accumulation in leaf cells from root cells (Morita et al., 2009; Shoji et al., 2009; Shoji and Hashimoto, 2011).

1.5.2. Cell type

Alkaloids generally accumulate in specific cell types owing to their cytotoxicity and probable role in plant defense responses (Ziegler and Facchini, 2008). The early NAD biosynthetic pathway for tobacco alkaloids biosynthesis consists of aspartate oxidase (EC 1.4.3.16), quinolinate synthase, and quinolinic acid phosphoribosyl transferase (EC 2.4.2.19), all of which are localized in the plastid and are coordinately regulated with nicotine biosynthesis (Figure 1.1) (Sato et al., 2007). *PMT* and *A622* are expressed strongly in epidermis and cortex cells of the tobacco root tip, and moderately in the outermost layer of the cortex, and in parenchyma cells surrounding the xylem of the differentiated region of the root (Sato et al., 2007). *CYP82E4* promoter fused *GUS* is expressed in epidermis, palisade parenchyma, spongy mesophyll, trichome, and petiole of leaf (Chakrabarti et al., 2008). Promoter regulated gene expression is directed to pith and cortex region of the stem constitutively.

1.6. Pharmacological effects of enantiomers of nicotine and TSNAs

1.6.1. Pharmacological effects of nicotine and TSNAs

Nicotine is not carcinogenic, but is pharmacologically active in animals. Nicotinic cholinergic receptors are ligand-gated ion channels. When nicotine binds to the outside of the channel, the channel opens allowing the entry of cations, including sodium and calcium. Nicotinic receptor facilitates the release of neurotransmitters, such as dopamine, norepinephrine, acetylcholine, serotonin, GABA, glutamate, and endorphins. These neurotransmitters mediate various behaviors associated with nicotine (Benowitz, 2008).

In contrast to nicotine some tobacco-specific nitrosamines (TSNAs) are carcinogenic and seven TSNAs have been identified in tobacco products: *N'*-nitrosonornicotine (NNN), 4-(methylnitrosamino)-1-(3-pyridyl)-1-butanone (NNK), 4-(methylnitrosamino)-1-(3-pyridyl)-1-butanol (NNAL), *N'*-nitrosoanatabine (NAT), *N'*-nitrosoanabasine (NAB), 4-(methylnitrosamino)-4-(3-pyridyl)-1-butanol (*iso*-NNAL), and 4-(methylnitrosamino)-4-(3-pyridyl)butanoic acid (*iso*-NNAC) (Figure 1.11) (Hecht, 1998). They are nitrosated products of four main alkaloids formed during the tobacco curing process. NNN, NNK, and NAT generally occur in greater quantities than the others, and NNK, NNAL, and NNN are the most carcinogenic. NAB, NAT, *iso*-NNAL and *iso*-NNAC have shown weak or no carcinogenic activity. NNK is the strongest carcinogen among the TSNAs in rodents. The TSNAs are procarcinogens, agents that require metabolic activation. The carcinogenicity of NNK and NNN is dependent on its metabolic activation. The primary mechanism of NNK/NNN-mediated carcinogenesis is metabolic activation by cytochrome P450 enzymes and generation of unstable metabolites (electrophiles) that react with DNA and result in appreciable genotoxicity (Hecht, 2008).

1.6.2. Pharmacological effects of the enantiomers of nicotine and TSNAs

The two nicotine enantiomers behave differently in human. The LD_{50S} for intravenous administration of (R)-nicotine in several animal species have been approximately 18 times higher than that of (S)-nicotine (Pogocki et al., 2007). Also a significantly lower level of toxic and carcinogenic metabolites is produced from (R)-nicotine. Based on the overall cytotoxicity of the compound and its metabolites, it appears that (R)-nicotine is

approximately 80-times less cytotoxic than (S)-nicotine (Yildiz et al., 1998). Interestingly, behavioral studies have shown that the subjective hedonic effects among the smokers caused by (R)-nicotine are of an intensity comparable to that caused by the (S)-enantiomer (Thurauf et al., 2000). Therefore, the R form of nicotine is suggested to be used as a smoke cessation agent.

(S)-NNN undergoes significantly more 2-hydroxylation than (R)-NNN in cultured rat esophagus and in vivo in rats. In rats treated with racemic NNN, 66% of 2-hydroxylation metabolites are from (S)-NNN, while 74% of the 5-hydroxylation products are produced from (R)-NNN (McIntee and Hecht, 2000). 2-hydroxylation of NNN is the major metabolic activation pathway, suggesting carcinogenicity of (S)-NNN may be greater than that of (R)-NNN.

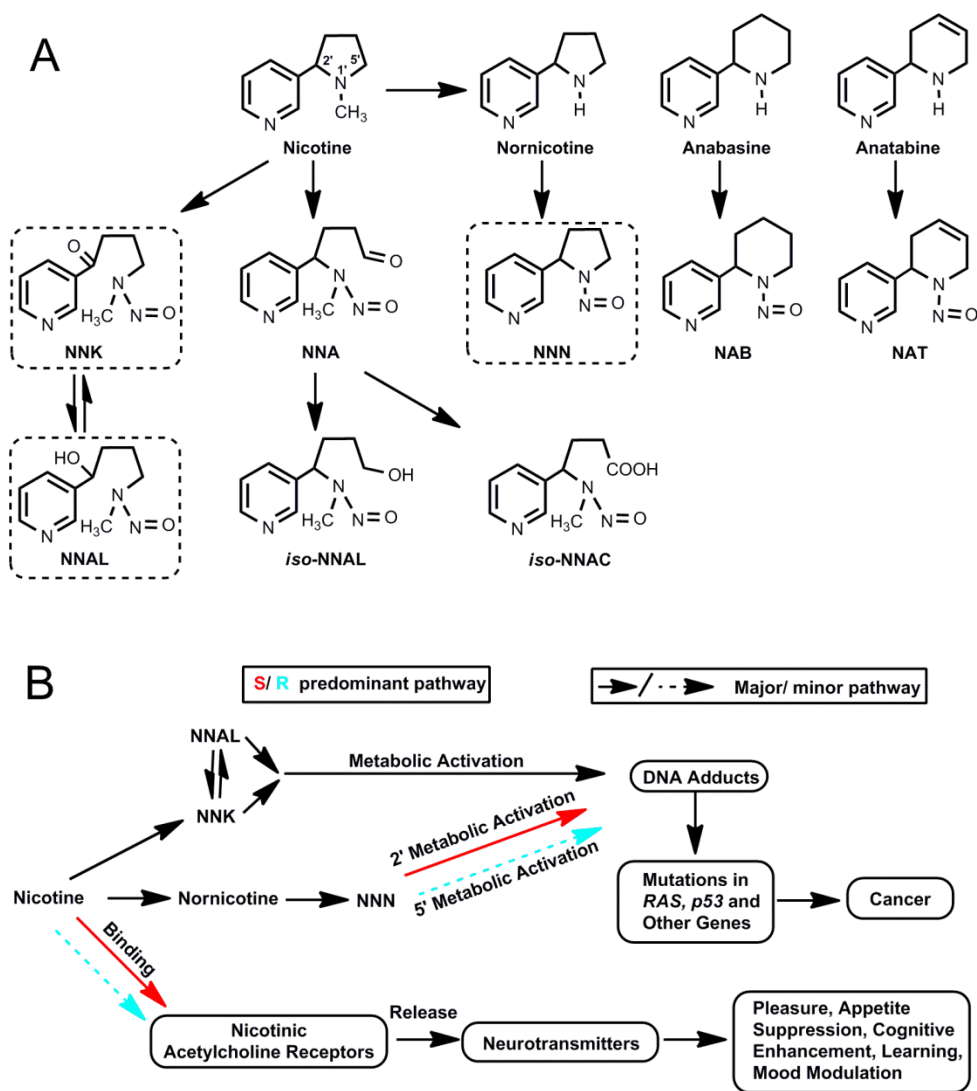


Figure 1.11. Structures and biological effects of tobacco alkaloids and tobacco-specific nitrosamines. (A) Structures of tobacco-specific nitrosamines and tobacco alkaloid precursors (Hecht, 1998; Carmella et al., 2000). With the exception of NNA, all have been detected in tobacco products. NNK, NNAL, and NNN are the most carcinogenic of the tobacco-specific nitrosamines that have been identified in tobacco products. (B) Schematic representation of pathways associated with the biological role of nicotine demethylation (McIntee and Hecht, 2000; Pogoeki et al., 2007; Benowitz, 2008; Hecht, 2008). Green/cyan arrow represents *S/R* isomer predominant pathway, respectively. Dotted arrow means minor pathway. *iso*-NNAL: 4-(methylnitrosamino)-4-(3-pyridyl)-1-butanol; *iso*-NNAC: 4-(methylnitrosamino)-4-(3-pyridyl)butanoic acid; NAB: *N'*-nitrosoanabasine; NNAL: 4-(methylnitrosamino)-1-(3-pyridyl)-1-butanol; NAT: *N'*-nitrosoanatabine; NNA: 4-(methylnitrosamino)-4-(3-pyridyl)butanal; NNK: 4-(methylnitrosamino)-1-(3-pyridyl)-1-butanone; NNN: *N'*-nitrosornicotine.

1.7. Experimental aim of this dissertation

Despite extensive studies, the nornicotine enantiomeric composition in tobacco leaf cannot be explained by current data. In tobacco about 0.2 % of the nicotine is the (R)-enantiomer (Armstrong et al., 1998), whereas nornicotine displays considerably high and variable (R)-enantiomer composition (4 to 75 % of total nornicotine) in leaf (Fannin et al., 1996; Armstrong et al., 1999; Liu et al., 2008). Different alkaloid enantiomers have different pharmacological activities as previously reviewed in section 1.6.2.

Understanding the mechanisms behind the discrepancies of the enantiomeric composition between substrate and product will not only help to better understand the accumulation of enantiomers of nicotine and nornicotine in tobacco leaves, but to provide a basis for future manipulation of the enantiomeric composition of nicotine, nornicotine and their metabolites. The goal of this dissertation is to explore possible reasons and to identify the most probable mechanism behind the variable nornicotine composition (Figure 1.12).

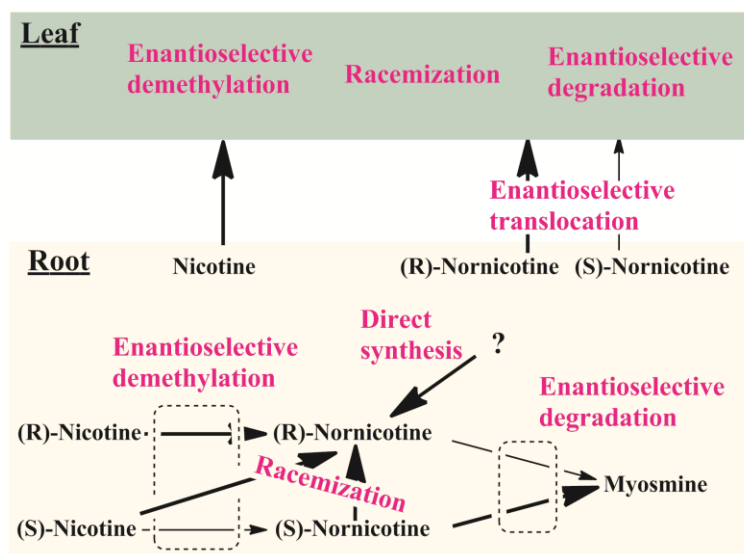


Figure 1.12. Possible mechanisms for high and variable (R)-nornicotine percentage in tobacco leaf.

Supplemental materials:

Table S1.1. Pyridine alkaloids and its derivatives in tobacco plants (*Nicotiana L.*).

Table S1.2. *N'*-dealkylation in *Nicotiana* species, based on feeding assays.

Table S1.3. Compounds not *N'*-demethylated by excised leaves of *N. tabacum* (Kisaki et al., 1978).

Figure S1.1. Nicotine degradation in bacteria and fungi.

Figure S1.2. Nicotine degradation in human based on urinary metabolites (Hukkanen et al., 2005).

Figure S1.3. Alignment of the CYP82E4, CYP82E5 and CYP82E10 predicted protein sequences.

Chapter 2. Variable nornicotine enantiomeric composition caused by nicotine demethylase CYP82E4 in tobacco leaf

2.1. Introduction

2.1.1. Highly variable nornicotine enantiomeric composition in tobacco

Nornicotine is one of the four major alkaloids in *Nicotiana tabacum* L. Nornicotine is, at least mainly, synthesized by demethylation of nicotine which is produced in roots and transported to leaves and accumulates in the vacuole (Shitan and Yazaki, 2007). However, the details of nornicotine biosynthesis and translocation are not clear and recently published results of nicotine and nornicotine enantiomeric composition cannot be explained based on current knowledge. The enantiomeric fraction of nornicotine (EF_{nornic}) (0.05-0.70) is much higher than what is expected from enantiomeric fraction of nicotine (EF_{nic}) (0.001-0.004) (Table 2.1). Enantiomer fraction (EF_x) is used to represent the proportion of R enantiomer compared to the S enantiomer of compound x (Harner et al., 2000).

Investigating nornicotine biosynthesis has both fundamental metabolic and practical applications. Nornicotine has received much attention due to its relationship to tobacco-specific nitrosamine *N'*-nitrosonornicotine (NNN) which is carcinogenic in many bioassays. Understanding nornicotine biosynthesis and accumulation will greatly facilitate the interpretation of the enantiomeric components of nicotine and NNN (Figure 2.1.). Chiral compounds with identical physical and chemical properties in achiral environments, generally exhibit different biological and toxicological activities, because each enantiomer can enantioselectively interact with enzymes and biological receptors in organisms (Seifert and Dove, 2009). For example, NNN is present in unburned tobacco as well as cigarette smoke, and the carcinogenicity of (S)-NNN is suggested to be greater than (R)-NNN in rat esophagus (McIntee and Hecht, 2000; Lao et al., 2007). Nicotine also exhibit different biological activity. (R)-nicotine has many of the same physicochemical properties as (S)-nicotine, but (S)-nicotine has a greater level of toxicity. LD_{50s} for intravenous administration of (R)-nicotine in several species of animals have been approximately 18 times higher than that of (S)-nicotine, which means (R)-nicotine is less potent. This suggests a potential application for (R)-nicotine as a therapeutic agent

(Pogocki et al., 2007). Since nornicotine is the major metabolite of nicotine and precursor of NNN, we may minimize the harmful effects of cigarettes through adjusting the enantiomeric ratio of nicotine and NNN.

Table 2.1. Enantiomer fraction, EF, of nicotine and nornicotine in tobacco (*Nicotiana tabacum* L.).

	EF	Material	References
Nicotine	0.001-0.004	Leaves	(Armstrong et al., 1998)
	<0.025	Leaves	(Perfetti and Coleman, 1998)
Nornicotine	Predominantly R	Roots	(Kisaki and Tamaki, 1960)
	0.14-0.25	Leaves	(Armstrong et al., 1999)
	0.10-0.40	Leaves	(Liu et al., 2008)
	0.30-0.70	Leaves	(Fannin et al., 1996)
	0.05-0.43	Leaves	(Perfetti and Coleman, 1998)

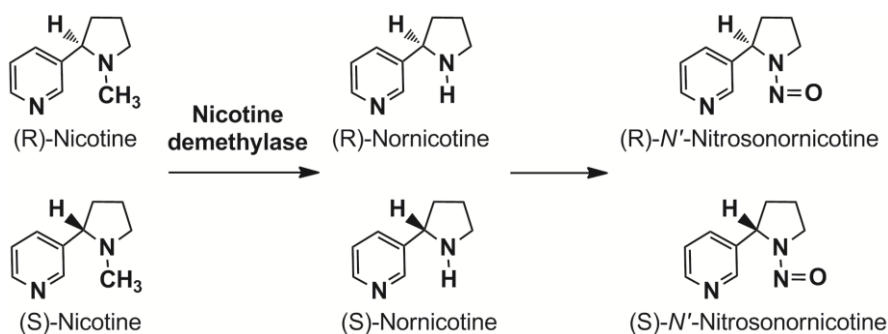


Figure 2.1. Structures of R and S enantiomers of nicotine, nornicotine and N'-nitrosoneurine.

2.1.2. Putative reasons for wide range of EF_{nic}

There are several reasons potentially responsible for the large and variable EF_{nic} (Figure 2.2.). Among these putative reasons, enantioselective demethylation likely plays a major role. Stereoselective translocation, enantioselective metabolism and direct synthesis may contribute along with enantioselective demethylation. Racemization is unlikely a reason for variable nornicotine composition, but we cannot exclude the possibility.

The most plausible explanation for variable composition of nornicotine is enantioselective demethylation of nicotine. Demethylation rates of (R)- and (S)- nicotine have been reported to be different (Mesnard et al., 2001; Bush et al., 2003). Exogenous nicotine feeding assays in cell culture (Mesnard et al., 2001) and plant tissue (Bush et al., 2003) demonstrate the rate of (R)-nicotine demethylation is higher than (S)-nicotine. There are three functional nicotine demethylases in tobacco (Siminszky et al., 2005; Gavilano and Siminszky, 2007; Xu et al., 2007a; Lewis et al., 2010). Each demethylase may have its own preference for nicotine enantiomers. Throughout the life cycle of a tobacco plant, different expressions and activities of nicotine demethylases can contribute to the variable values of nornicotine enantiomeric composition.

Also, stereoselective degradation of (S)-nornicotine may contribute to the variable EF_{nic} . Kisaki and Tamaki (1966) found that (R)-nornicotine was recovered more when feeding (R) and (S)-nornicotine to excised leaves of *N. tabacum*, respectively. This result implied the enantioselective degradation of (S)-nornicotine. Cell culture feeding assay supported Kisaki and Tamaki's work, but myosmine level, the main product of nornicotine degradation, was the same (Mesnard et al., 2001). This could be due to the possibility that myosmine is degraded as fast as it is formed, or that other intermediates are involved.

Stereoselective translocation may play a minor role. Transporters which are strictly stereoselective are found in plants (Bandell and Lolkema, 1999) and animals (Luurtsema et al., 2004). ABC transporter is a common transporter for plant secondary metabolites, and is a potential candidate for nicotine and nornicotine transportation. However, the first discovered transporter for vacuolar transport of nicotine in *Nicotiana tabacum* L. is a

multidrug and toxic compound extrusion-type (MATE) transporters (Morita et al., 2009; Shoji et al., 2009). There is still no report of a nornicotine transporter and stereoselectivity of the transporter.

Nornicotine may be directly synthesized which would be a possible explanation of the varying EF_{nic} . In the biosynthetic pathway of nicotine, putrescine is first *N*-methylated by putrescine *N*-methyltransferase. The product *N*-methylputrescine is then deaminated oxidatively to 4-methylaminobutanal, which spontaneously cyclizes to give the *N*-methylpyrrolinium. This oxidative deamination reaction is catalyzed by *N*-methylputrescine oxidase (MPO). The *N*-methylpyrrolinium condense with nicotinic acid-derived metabolite 1,2-dihydropyridine to give nicotine in tobacco (Leete, 1992). In addition to its preferred *N*-methylputrescine substrate, recombinant MPO1 enzyme could to a lesser degree utilize putrescine, probably resulting in an unmethylated pyrrolinium salt (Kato et al., 2007). If the nicotine synthase can use this unmethylated pyrrolinium salt, nornicotine could be directly produced, bypassing nicotine. Mutant plants with knockouts of all three demethylases still contain some nornicotine, implying the existence of the direct synthesis of nornicotine (Lewis et al., 2010).

Racemization during (Kisaki and Tamaki, 1961a) or after demethylation (Leete, 1992) was proposed for (R)-nornicotine production. (R)-nornicotine may come from the racemization of (S)-nornicotine (Leete, 1992). Chemically nornicotine may be racemized in the presence of pyridoxal (Jacob, 1996), which is present in green plants as natural forms of vitamin B₆. Nornicotine derived from pure (S)-nicotine was partially racemized in *N. tabacum* during demethylation, and feeding (S)-nornicotine only (S)-nornicotine was recovered, implying that the racemization occurs during demethylation (Kisaki and Tamaki, 1961b). However, feeding one form of nicotine to cell cultures (Mesnard et al., 2001) and tobacco leaves (Fannin et al., 1996) only resulted in the corresponding form of nornicotine being recovered which makes racemization the unlikely explanation for (R)-nornicotine production.

In this paper, EF_{nic} in different tobacco lines and tissues were investigated to validate the variable results in the literature. Induction and suppression of nicotine demethylase CYP82E4 demonstrate that CYP82E4 reduces EF_{nic} in tobacco and produces a variable EF_{nic} .

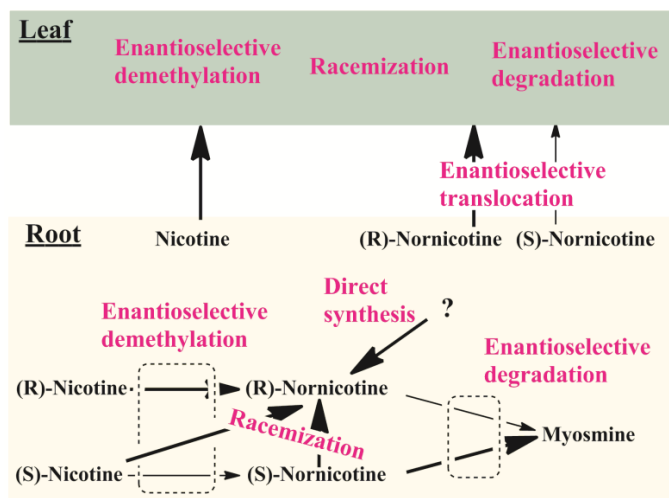


Figure 2.2. Possible mechanisms to account for the high and variable EF_{nic} in tobacco leaf.

2.2. Results

2.2.1. EF_{nic} in among different lines and tissues

To verify the literature reports, tobacco varieties with different nicotine demethylation capability were chosen. Nornicotine composition of different tissues from burley tobacco lines TN90LC, L8, RM52 and RNAi were analyzed. TN90LC is a widely used commercial variety. L8 is a breeding line for root disease resistance. RM52 is a high nicotine tobacco line. The RNAi line had nicotine demethylases silenced. A wide range of EF_{nic} was measured (Figure 2.3), which confirms the earlier literature reports. Considering the 0.002 EF_{nic} (Armstrong et al., 1998), one may wonder what is the source of the additional (R)-nornicotine, resulting in the elevated EF_{nic} .

Further investigations of each enantiomer of nornicotine found different patterns among TN90LC, L8, RM52 and RNAi plants (Figure 2.4). There was no correlation between

demethylation and EF_{nic} . The R or S form of nornicotine changes individually not proportionally with the other form. Lamina from lower leaves (referred to bottom lamina) from RNAi and RM52 plants have lower EF_{nic} than L8 and TN90LC. Reasons for these results are different. RNAi plants had a lower (R)-nornicotine level than L8 and TN90LC, while RM52 had a much higher (S)-nornicotine level.

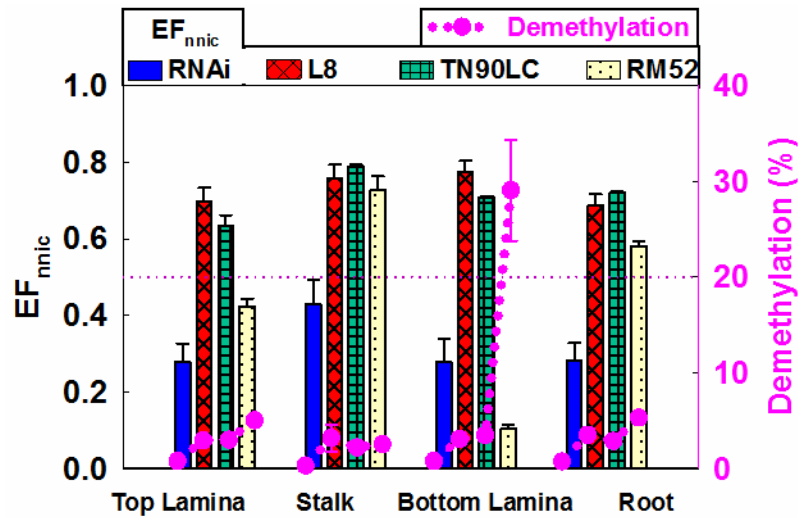


Figure 2.3. There is wide range of EF_{nic} in different tobacco lines. Four tobacco lines have different nicotine demethylation abilities. All samples were from mature stage of plant growth and were analyzed for alkaloid levels and nornicotine composition. Demethylation is calculated based on nicotine and nornicotine levels and EF_{nic} is calculated based on (R)-nornicotine and (S)-nornicotine levels. L8 is a tobacco breeding line for disease resistance. TN90LC is a commercial tobacco cultivar. RM52 is a tobacco line with high nicotine demethylation ability. Nicotine demethylases in RNAi plants are silenced by RNAi technique (Gavilano et al., 2006). Each bar is an average of four plants. Error bar represents the standard deviation.

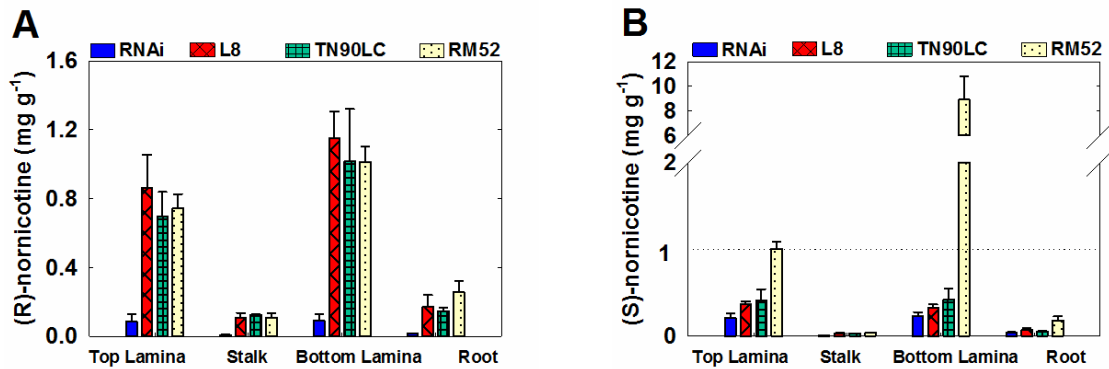


Figure 2.4. (R)-nornicotine (A) and (S)-nornicotine (B) accumulate to different levels in different tissues of four tobacco lines. Four tobacco lines have different nicotine demethylation abilities. All samples were from mature stage of plant growth and were analyzed for alkaloid levels and nornicotine composition. L8 is a tobacco breeding line for disease resistance. TN90LC is a commercial tobacco cultivar. RM52 is a tobacco line with high nicotine demethylation ability. Nicotine demethylases in RNAi plants are silenced by RNAi technique (Gavilano et al., 2006). Each bar is an average of four plants. Error bar represents the standard deviation.

2.2.2. Ethephon-induced *CYP82E4* expression associated with decreased EF_{nic}

As mentioned above, several reasons can account for the high and variable EF_{nic} . To investigate how demethylation affects EF_{nic} , tobaccos with different nicotine demethylating capability were chosen and treated with ethephon. Ethephon promotes leaf senescence and stimulates nicotine demethylation (Jack and Bush, 2007) and *CYP82E4* expression (Chakrabarti et al., 2008). Compared to freeze-dried leaves, ethephon treated converter leaves had increased nicotine demethylation (dotted line in Figure 2.5.), and decreased EF_{nic} . For individual nornicotine isomer levels (Figure 2.6.), both (R)- and (S)- nornicotine amounts increased after ethephon induction. But (S)-nornicotine increased much more than (R)-nornicotine, which makes the relative (R)-nornicotine level decrease. Since *CYP82E4* expression is dramatically induced by ethephon and E4 is the major demethylase in converter plants (Gavilano et al., 2006), we can infer that at mature growth stage when E4 expression will be induced, (S)-nornicotine is produced more than (R)-nornicotine which results in increased demethylation and decreased EF_{nic} . Why does (R)-nornicotine increase less? It is probably due to the limitation of (R)-nicotine substrate. It is also noteworthy that freeze-dried leaf and roots have similar, if not equivalent, EF_{nic} and demethylation (Figure 2.5.).

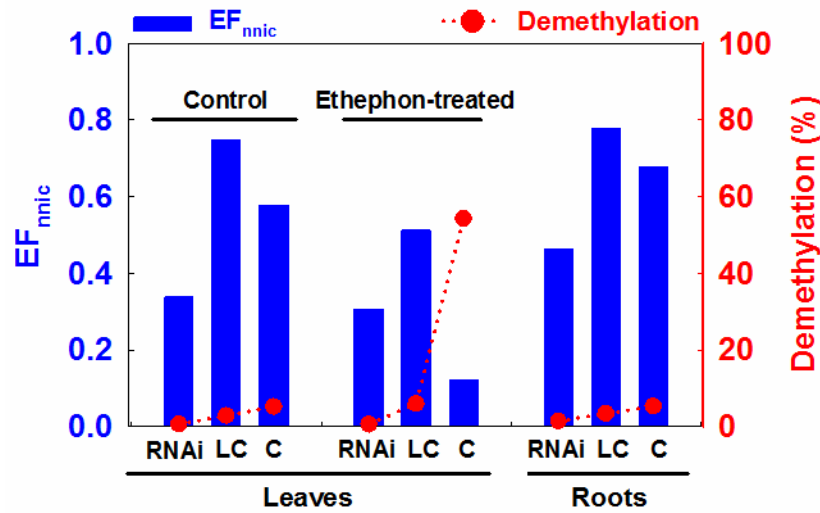


Figure 2.5. EF_{nnic} decreases after the induction of nicotine demethylation. All tobacco lines were grown in greenhouse. Two top leaves and roots from each line were sampled at two weeks after topping. One leaf was freeze-dried used as control, and the other one was sprayed 0.1% ethephon and air-dried. All dried samples were analyzed for alkaloid levels and nornicotine composition. Demethylation is calculated based on nicotine and nornicotine levels and EF_{nnic} is calculated based on (R)-nornicotine and (S)-nornicotine levels. RNAi: RNAi plant DH98-325-6 RNAi #2-8; LC: low converter DH98-325-5; C: converter DH98-325-6.

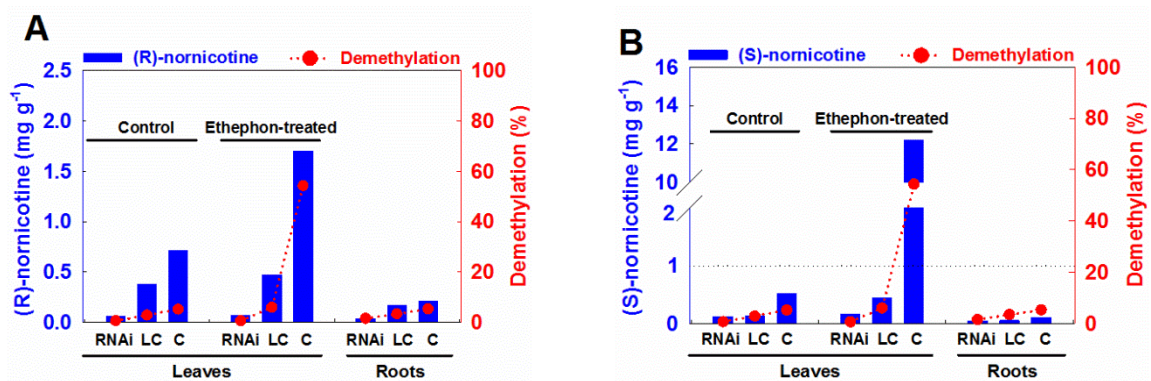


Figure 2.6. (R)-nornicotine (A) and (S)-nornicotine (B) increase differently after ethephon induction of nicotine demethylase. All tobacco lines were grown in greenhouse. Two top leaves and roots from each line were sampled at two weeks after topping. One leaf was freeze-dried used as control, and the other one was sprayed 0.1% ethephon and air-dried. All dried samples were analyzed for alkaloid levels and nornicotine composition. RNAi: RNAi plant DH98-325-6 RNAi #2-8; LC: low converter DH98-325-5; C: converter DH98-325-6.

2.2.3. Nicotine demethylase CYP82E4 mutant results in increased EF_{nic}

To further confirm CYP82E4 effects, *e4* mutants (Lewis et al., 2010) were analyzed for nornicotine enantiomeric composition. Tobacco line DH98-325-6 was chosen as parent for EMS mutation (“P” in Figure 2.7). Mutants with homologous mutation in *CYP82E4* gene and their backcross with parental line were grown in the field, and cured leaves were analyzed for alkaloid levels and nornicotine composition. Demethylation is used to confirm that the CYP82E4 is effectively silenced.

Four *e4* mutants, *e4* #1-4, have much lower demethylation than the parent line (P), which means they are effective mutant lines (Figure 2.7.). All these effective mutant lines have high EF_{nic} , like control TN90LC. Four effective mutants were backcrossed with converter parent to produce four heterozygous lines (F1 plants). These four backcross lines have increased nicotine demethylation and decreased EF_{nic} . The profile of four effective *e4* mutants and their backcross lines clearly demonstrate that CYP82E4 can increase demethylation and decrease EF_{nic} .

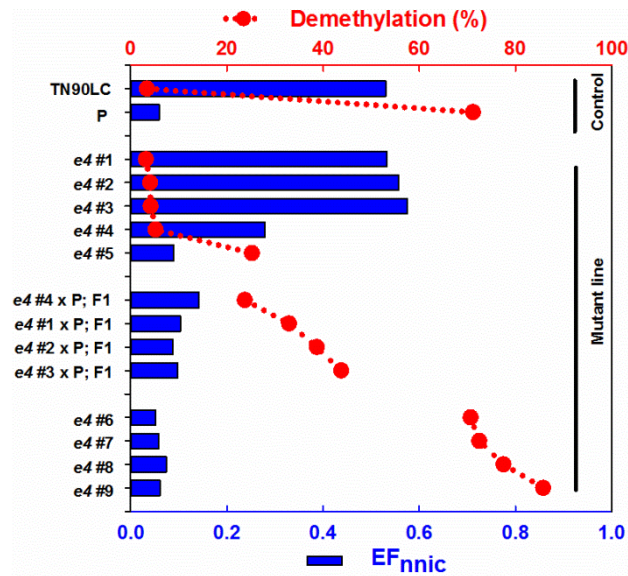


Figure 2.7. Changes of EF_{nic} and demethylation due to the mutation of nicotine demethylase CYP82E4. Tobacco lines were grown in the field and top leaves were sampled from air-cured plants. All dried samples were analyzed for alkaloid levels and nornicotine composition. Demethylation is calculated based on nicotine and nornicotine levels and EF_{nic} is calculated based on (R)-nornicotine and (S)-nornicotine levels.

Controls were the parent DH98-325-6 (P) and the commercial line TN90LC. Details of how the mutant lines were created are described by Lewis et al. (2010).

2.2.4. Selectivity of other nicotine demethylases for (R)-nicotine

Nicotine demethylation was also measured in individual tobacco plants with *CYP82E4* silenced by RNAi (Figure 2.8.). Being different from mutants, RNAi not only inhibits the enzyme activity of *CYP82E4*, but its related family members as well. Therefore, we would expect to see complex effects in RNAi plants. Two parent lines were chosen for RNAi knockdown: one has low demethylating ability (P1 L) and the other has high demethylating ability (P2 H). The two parents are full-sib doubled haploid burley lines. They share the same parents and have similar genetic background. RNAi plants were grown in the field in 2006, and sampled after being air-cured. Most RNAi lines from the low converter parent had lower demethylation and EF_{nic} than their parent. This demonstrates that in these lines demethylation is further inhibited (lower demethylation), and (R)-nicotine demethylation is inhibited more than (S)-nicotine demethylation (lower EF_{nic}). RNAi lines have similar demethylation but lower EF_{nic} than effective *e4* mutants, suggesting that other demethylases can use (R)-nicotine more readily than (S)-nicotine. This could be *CYP82E5*, *CYP82E10* or other unidentified demethylases. RNAi lines from the converter parent had striking differences in demethylation and EF_{nic} . Line P2 RNAi #1-1 behaved like a converter, which has high demethylation and low EF_{nic} . Line P2 RNAi #1-2 behaves like a RNAi plant from the low converter parent, which had low demethylation and low EF_{nic} . Line P2 RNAi #3-2 behaved like a low converter with low demethylation and high EF_{nic} .

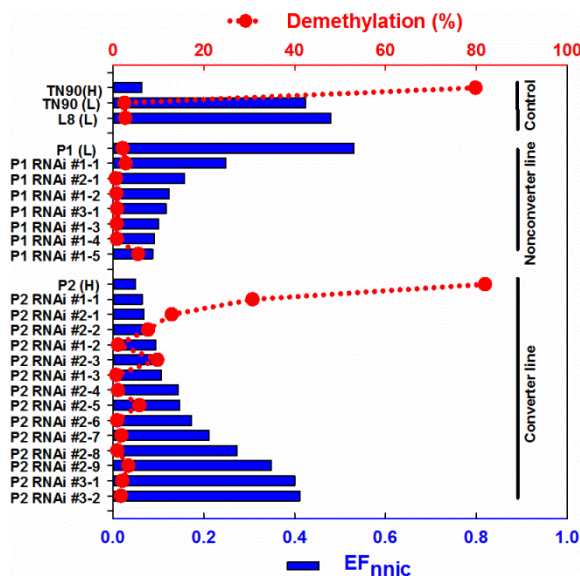


Figure 2.8. EF_{nic} and demethylation in different RNAi lines. All tobacco lines were grown and air-cured in Blackstone, VA. All dried samples were analyzed for alkaloid levels and nornicotine composition. Demethylation is calculated based on nicotine and nornicotine levels and EF_{nic} is calculated based on (R)-nornicotine and (S)-nornicotine levels. TN90 is a commercial cultivar. DH98-325-5 (P1) and DH98-325-6 (P2) are full-sib doubled haploid burley lines, which are the parents of all other RNAi lines. Details of how RNAi plants were created are described by Lewis et al. (2008).

2.3. Discussion

The discrepancy between nicotine and nornicotine composition has puzzled researchers for a long time. It has been reported that there is a wide range of EF_{nic}. In this study, we found that 60-80% of nornicotine in root of conventional tobacco was the R form, and 5-80% of nornicotine in leaf was the R form (Figure 2.3). These results are consistent with previous reports (Table1). CYP82E4 expression induction by ethephon treatment is correlated with elevated demethylation. Both (R)- and (S)- nornicotine accumulation is increased but (S)-nornicotine accumulated much more than (R)-nornicotine, which results in reduced EF_{nic}. The effects of CYP82E4 on nornicotine composition were confirmed by CYP82E4 mutants and their backcross to parent. There are two other functional nicotine demethylases in tobacco, CYP82E5v2 and CYP82E10, besides CYP82E4. RNAi plants which have all nicotine demethylases silenced have lower EF_{nic} than only the *e4* mutants, suggesting that combination of CYP82E5v2 and CYP82E10, or other

unidentified demethylases, have a high selectivity for (R)-nicotine. Based on the results reported above, a model to explain the nornicotine composition is proposed. CYP82E5v2 and CYP82E10 have high selectivity for (R)-nicotine, and can produce 0.80 EF_{nic} from low EF_{nic}. CYP82E4 produced more (S)-nornicotine than (R)-nornicotine at the mature growth stage, resulting in a reduced EF_{nic}.

Potentially there are several reasons responsible for the high and variable EF_{nic}. We show in this study three demethylases have significant impacts on the nornicotine composition, suggesting that the enantioselectivity of nicotine demethylases play a pivotal role in nornicotine enantiomer accumulations. These three demethylases have been biochemically studied. In the future, the selectivity of these three demethylases for nicotine enantiomers should be characterized.

2.4. Conclusions

High and variable EF_{nic} is found in tissues of tobacco with different demethylating capabilities. Experiments of induction and inhibition of CYP82E4 activity in tobacco demonstrate that CYP82E4 decreases EF_{nic} in tobacco leaf. Results from RNAi silenced demethylation plants suggest that enantioselective demethylation has an important role in the high and variable EF_{nic}.

2.5. MATERIALS AND METHODS

2.5.1. Plant materials

TN90LC represents low nicotine demethylation (low converter) plants. For several RNAi plants, burley tobacco breeding lines DH98-325-5 and DH98-325-6 were transformed with 298-bp of *CYP82E4* cDNA to silence *CYP82E4* and its closely related homologues. Based on PCR and ultra-low demethylation phenotype, R2 families of stable expressing the *CYP82E4*-silenced condition were used in this study. Details of generation and growth conditions of low converter and RNAi plant have been described in a previous paper (Lewis et al., 2008). Details of development of mutants is described in a previous paper (Lewis et al., 2010). Both low converter and RNAi plants were grown at Spindletop farm in Lexington (KY) in 2006, and were topped and sampled at mature

growth stage. RM52 represents high nicotine demethylation (converter) plants which have high nornicotine accumulation. Converter plants were grown at Spindletop farm in Lexington (KY) in 2007 and were sampled at flowering stage. All the samples were freeze-dried and ground for further individual alkaloids content and nornicotine enantiomers analysis.

2.5.2. Alkaloids quantification and separation of enantiomers of nicotine and nornicotine

Nicotine, nornicotine, anabasine and anatabine were quantitatively analyzed by gas chromatography (GC) (Perkin-Elmer Autosystem XL with PreventTM) according to the 'LC-Protocol' (Jack and Bush, 2007). Alkaloids of ground tobacco samples were extracted by methyl *tert*-butyl alcohol (MTBE) and aqueous sodium hydroxide. The MTBE extracts was injected into GC, and quantification of alkaloids was against chemical standards.

Nornicotine enantiomer analysis was done by extracting ground tobacco samples with MTBE and aqueous sodium hydroxide. Nornicotine in MTBE extract was purified by thin layer chromatography (TLC). TLC plates were TLC Silica Gel 60 F254 (EMD Chemicals Inc.). Developing solvent for TLC was chloroform: methanol: ammonia hydroxide (85:15:2, v/v/v). Nornicotine band was scraped from TLC plates and the TLC powder was directly derivatized by camphanic acid chloride solution for 30 min. The reaction was stopped by addition of saturated sodium carbonate solution, and the solution was extracted by MTBE. MTBE extracts were dried with anhydrous sodium sulfate and then were injected into GC (6890 Agilent GC, Agilent Technologies) for R/S nornicotine analysis. Samples were injected in splitless mode at 250 °C. The oven temperature program was initially 120 °C, increased 30 °C min⁻¹ to 215 °C, then 0.2 °C min⁻¹ to 220 °C held for 10 min, then 3 °C min⁻¹ to a final temperature 300 °C, and held for 20 min. Temperature of flame ionization detector (FID) was 320 °C. GC column was DB1 (60 m (L) × 320 µm (D) × 0.25 µm (FT)) (J&W Scientific). The carrier gas was helium, and the flow was 1.7 ml min⁻¹. R/S ratio of nornicotine was calculated based on peak area of each

isomer. Nornicotine isomer amount was calculated based on total nornicotine amount and R/S ratio.

Enantiomer fraction (EF) (Harner et al., 2000): $EF = R \text{ enantiomer} / (R \text{ enantiomer} + S \text{ enantiomer})$

Supplemental Material

Table S2.1. Alkaloids concentrations in different tissues of four tobacco lines.

Table S2.2. Alkaloids concentrations in ethephon-treated tobacco.

Table S2.3. Alkaloids concentrations in *e4* mutants.

Table S2.4. Alkaloids concentrations in RNAi plants.

Chapter 3 Enantioselective demethylation of nicotine as a mechanism for variable nornicotine composition in tobacco leaf

3.1. Introduction

Nicotine, nornicotine, anabasine and anatabine are the four main alkaloids in tobacco (*Nicotiana tabacum* L.). Nornicotine is the product of nicotine demethylation in tobacco leaves. There are three functional P450 nicotine demethylases of *Nicotiana tabacum* L. reported in the literature: CYP82E4 (Siminszky et al., 2005), CYP82E5v2 (Gavilano and Siminszky, 2007) and CYP82E10 (Lewis et al., 2010). CYP82E4 is the major nicotine demethylase, and loss of function of CYP82E4 can cause up to a 95 % reduction of nicotine demethylation to nornicotine (Lewis et al., 2010). During maturation and curing, nornicotine in the leaf may be *N'*-nitrosated to *N'*-nitrosornicotine (NNN), one of the major tobacco-specific *N*-nitrosamines (TSNAs) which has received much research attention because of its carcinogenicity.

Different alkaloid enantiomers have different pharmacological activities. It has been reported that (S)-nicotine is more physiologically potent (Pogocki et al., 2007) and (S)-NNN is more carcinogenic than the (R)- form (McIntee and Hecht, 2000). Due to the importance of the enantiomer composition, the enantiomers of all the four main alkaloids have been investigated. Of the four alkaloids, nornicotine is the only one that has a wide range of enantiomer fraction (EF) (Figure 3.1). Despite extensive studies, the nornicotine enantiomeric composition in tobacco leaf cannot be explained by current data. In tobacco about 0.2 % of the nicotine is the (R)-enantiomer (0.002 EF) (Armstrong et al., 1998), whereas nornicotine displays considerably high and variable EF_{nic} (0.04 to 0.75) in leaf (Fannin et al., 1996; Armstrong et al., 1999; Liu et al., 2008). Understanding the mechanisms behind the discrepancies of the enantiomeric composition between substrate and product will not only help to better understand the accumulation of enantiomers of nicotine and nornicotine in tobacco leaves, but could also provide a basis for future manipulation of the enantiomeric composition of nicotine, nornicotine and their metabolites.

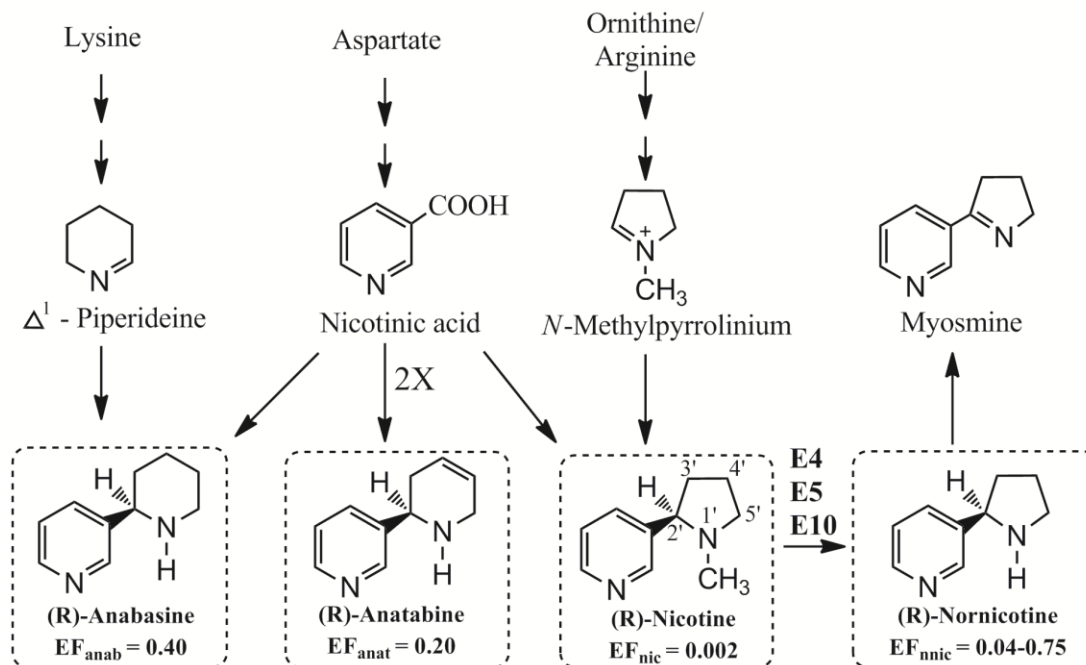


Figure 3.1. Biosynthesis and enantiomeric composition of the four main alkaloids in *Nicotiana tabacum* L. Four major alkaloids in tobacco are boxed and only (R) form structure is drawn. The percentage value in the figure is from leaf samples. Enzyme E4: CYP82E4; E5 CYP82E5v2; E10: CYP82E10.

The large differences between the enantiomeric composition of the precursor, nicotine, and the product nornicotine have puzzled researchers for half a century (Kisaki and Tamaki, 1961b). Racemization of nornicotine was proposed to explain the high (R)-nornicotine accumulation (Leete, 1992), supported by the claim that (R)-nornicotine was observed in leaf when feeding (S)-nicotine (Kisaki and Tamaki, 1961b). However, the racemization was not confirmed in cell culture assay (Hao and Yeoman, 1996; Mesnard et al., 2001).

Besides racemization, the significant differences in R/S nornicotine ratios could be caused by enantioselective demethylation of (R)-nicotine suggested in the assays of excised leaf (Kisaki and Tamaki, 1961b; Kisaki and Tamaki, 1964), whole plant (Bush et al., 2003) and the tobacco cell cultures (Mesnard et al., 2001). Although Leete and Chedekel (1974) claimed that demethylation rates of (R)- and (S)-nicotine were the same in a whole plant feeding assay, there was a slightly higher amount of (R)-nornicotine

recovered. All three demethylases have been biochemically characterized *in vitro* (Gavilano and Siminszky, 2007; Xu et al., 2007a; Lewis et al., 2010), but their enantioselectivity are not known.

In this study, we confirmed the enantioselective demethylation and found no racemization during demethylation by using recombinant CYP82E4, CYP82E5v2 and CYP82E10 *in vitro*. We also showed *in vitro* that the cooperation of three demethylases could generate the enantiomeric composition of nornicotine accumulated in tobacco leaf.

3.2. Results

3.2.1. Optimization of *in vitro* enzyme assay of nicotine enantiomers

Effects of protein concentration, pH and reaction time on recombinant CYP82E4 were studied to optimize the *in vitro* enzyme assay. Protein concentration did not affect enzyme reaction rate until it exceeded 1.0 mg ml⁻¹ (Figure 3.2A). Enzyme demethylation had the highest activity at pH 7.5 (Figure 3.2B), which is consistent with a previous report using a partially purified protein extract (Chelvarajan et al., 1993). Rate of nornicotine formation increased linearly for 30 min incubation at which time 95 % of (R)-nicotine had been demethylated to (R)-nornicotine (Figure 3.2C). Therefore, 0.5 mg ml⁻¹ protein concentration, pH 7.5 reaction buffer and 10 min reaction time were used in following enzyme assays. Under conditions other than the optimum, the differences between (R) and (S)- nicotine demethylation were reduced.

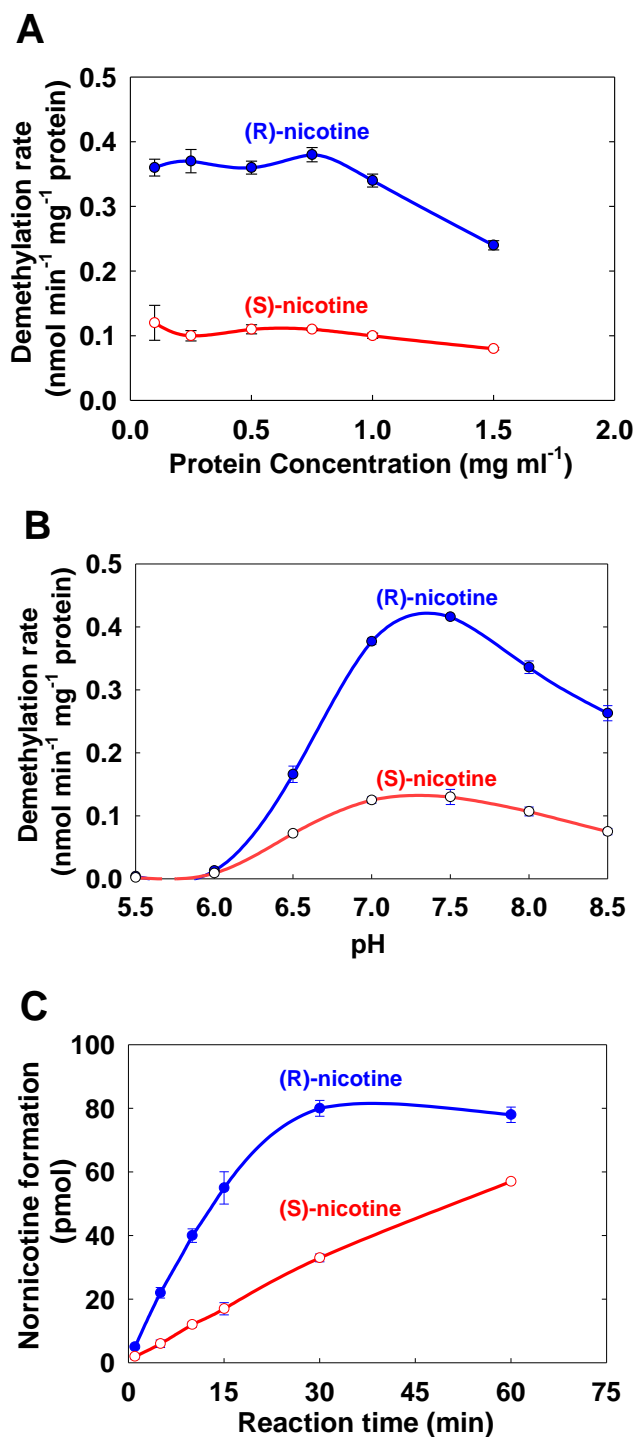


Figure 3.2. Dependence of CYP82E4-catalyzed demethylation of (R)-nicotine or (S)-nicotine on the amount of protein (A), pH (B) and reaction time (C). Microsomes from yeast over-expressing the *CYP82E4* gene were incubated with 5 μ M nicotine, followed by extraction and quantification of (R)-nornicotine and (S)-nornicotine. Nicotine substrate in panel B was mainly monoprotonated at the low pH and at pH 8.0 about 1:1 monoprotonated: free base. Each data point is the average of three replicates and the error bar represents the standard deviation.

3.2.2. Enantioselectivity of CYP82E4, CYP82E5v2 and CYP82E10

To test the enantioselectivity of CYP82E4 for nicotine, different amounts of (R)- or (S)-[2'-¹⁴C]nicotine were incubated with the enzyme preparation. V_{\max} for (R)-nicotine (0.55 nmol min⁻¹ mg⁻¹ protein) was three-fold higher than V_{\max} for (S)-nicotine (0.17 nmol min⁻¹ mg⁻¹ protein), and there was no significant difference between K_m of (R)-nicotine and (S)-nicotine (Figure 3.3A). V_{\max} of (R)-nicotine was close to the previously reported V_{\max} using racemic nicotine as substrate (0.54 nmol min⁻¹ mg⁻¹ protein) (Xu et al., 2007a). Results from inhibition assays illustrate the competitive inhibition between the two nicotine enantiomers (Figure S3.1).

CYP82E5v2 and CYP82E10 account for less than 5% of nicotine demethylation in plants accumulating high nornicotine (Lewis et al., 2010). Besides CYP82E4, enantioselectivity of CYP82E5v2 and CYP82E10 was also determined (Figure 3.3B and Figure 3.3C). Enzyme kinetics show CYP82E5v2 and CYP82E10 almost exclusively used (R)-nicotine over (S)-nicotine, and in both cases $V_{\max,R}$ was over 10 fold higher than $V_{\max,S}$. Compared with Michaelis-Menten constants in the literature (Table S3.1), $K_{m,R}$ in this study were always about half of the K_m in previous reports using racemic nicotine.

After demethylation of either (R)- or (S)-nicotine, only the corresponding form of nornicotine enantiomer was detected in these assays. There was no racemization found during the CYP82E4-, CYP82E5v2- and CYP82E10- catalyzed demethylation.

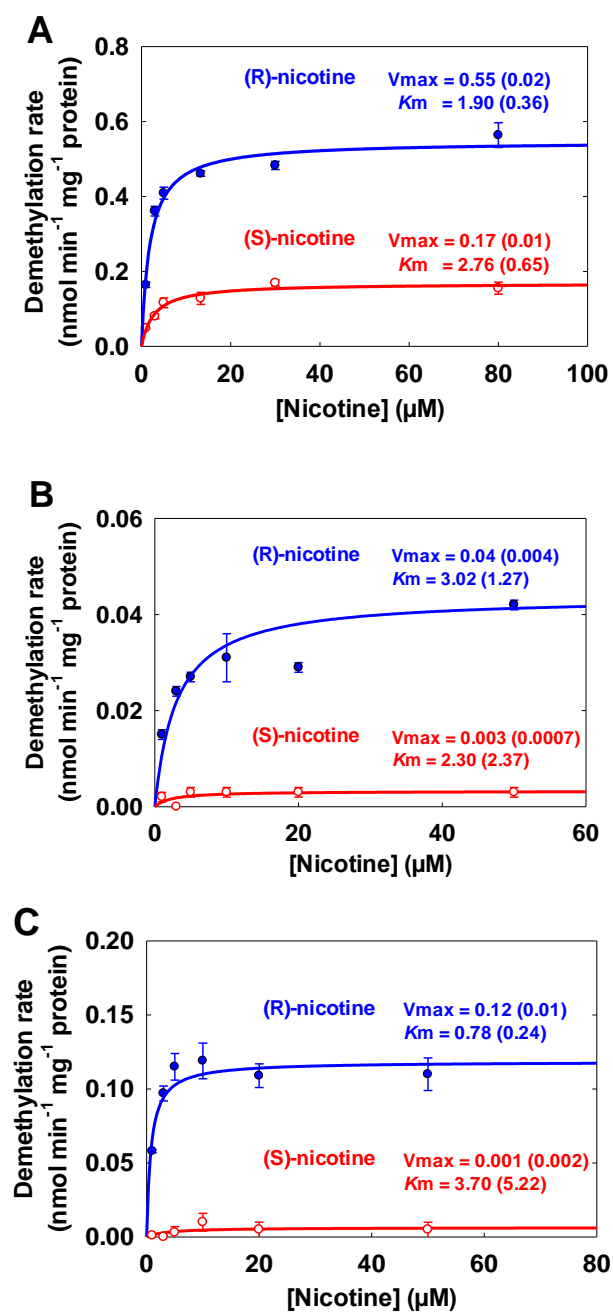


Figure 3.3. Substrate preferences of CYP82E4 (A), CYP82E5v2 (B) and CYP82E10 (C) for (R)-nicotine and (S)-nicotine. 0.5 mg ml⁻¹ microsomes from yeast over-expressing the CYP82E4, CYP82E5v2 or CYP82E10 were incubated with varying amount of nicotine for 10 min, followed by extraction and quantification of (R)-nornicotine and (S)-nornicotine. Values in the parenthesis represent the standard error for V_{max} and K_m . Each data point is the average of three replicates. The error bars and data in the parenthesis represent the standard deviation.

3.2.3. Combination of the three demethylases to generate leaf nornicotine composition *in vitro*

After demonstrating the enantioselectivity of three demethylases, the next question would be, can they convert a low R percentage of nicotine into the high R percentages of nornicotine reported in the literature. RNAi plants with all three demethylases silenced accumulate about 3 % (R)-nicotine of total nicotine (unpublished data). Therefore, 3% (R)-nicotine could be the nicotine composition at the time of synthesis and was used in the following assays.

In tobacco plants, nicotine is stored in cell vacuoles and the P450 demethylases are integrated into the endoplasmic reticulum membrane facing the cytosol. Although the concentration of endogenous nicotine is 60 mM in the vacuoles in the leaf tip (Lochmann et al., 2001) and is much higher than the concentration needed for the maximum rate of nicotine demethylation, the actual concentration of available nicotine in cytosol for the demethylase enzyme is not known. Therefore, a large range of total nicotine was tested *in vitro*, and no concentration effect on nornicotine composition was measured (Figure S3.2A). Nicotine substrates with different R/S ratios were used in *in vitro* assays to determine the relationship between (R)-nicotine substrate and (R)-nornicotine produced in the presence of (S)-nicotine (Figure S3.2B). Since there was no concentration effect on product profile (Figure S3.2A), (R)-nicotine mixtures with variable concentrations were used to cover a wide range of (R/S)-nicotine ratios as substrate. Based on the results presented in Figure S3.2B, it would require a EF_{nic} from 0.008 to 0.27 to obtain the 0.04 to 0.75 of EF_{nic} . These values of (R)-nicotine are much higher than generally found in the plant and also the nicotine composition in RNAi plants, which implies the involvement of other demethylases.

Each of the three demethylases was incubated with 3% (R)-nicotine for a time course study, and product compositions at different reaction time were observed for each demethylase (Figure 3.4 and Figure S3.3). During the 3 h reaction, less than 5% of total

nicotine substrate was demethylated by CYP82E5v2 and CYP82E10, and the nornicotine formed consisted of over 70% of (R) form, which reaches the upper limit of EF_{nic} found in tobacco plants. In contrast to CYP82E5v2 and CYP82E10, CYP82E4 demethylated over 30% of nicotine in 3 h reaction, and the nornicotine product consisted of 5-20% of (R) form, which is close to the lower limit of EF_{nic} found in tobacco plants. So it is logical to speculate that the mixture of three nicotine demethylases could potentially produce nornicotine with 0.04 to 0.75 EF_{nic} from nicotine with 0.03 EF_{nic} . To test the combination effects of three demethylases on nornicotine composition, a mixture of equal protein amount of CYP82E5v2 and CYP82E10 was first incubated with 0.03 EF_{nic} of nicotine for 30 min, and then the same protein amount of CYP82E4 was added to the mixture for another 2.5 h (Figure 3.4 insert). The EF of the nornicotine product continuously decreased, as the duration of the incubation time increased.

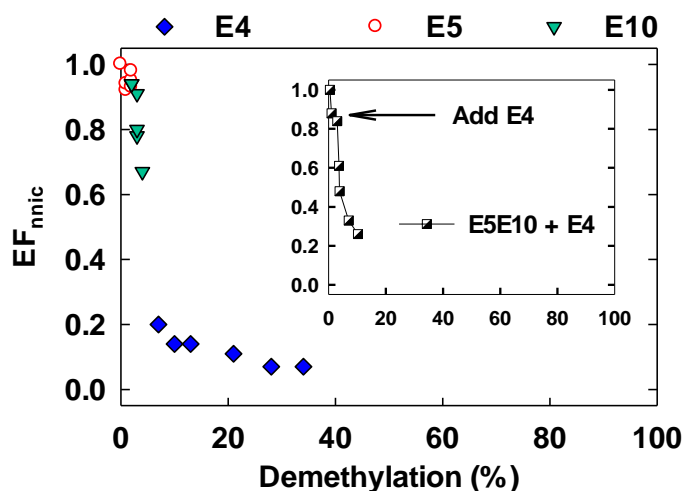


Figure 3.4. Generation of leaf nornicotine enantiomeric composition using CYP82E4 (E4), CYP82E5v2 (E5) and CYP82E10 (E10) *in vitro*. Nicotine solutions (0.03 EF_{nic}) were incubated with each of three demethylases separately or collectively (see insert), and the nornicotine enantiomeric composition was analyzed after varying time of incubation. This figure is a rearrangement of figure S3.3. For collective incubation, same amount of CYP82E5v2 and CYP82E10 were mixed and incubated with substrate, and at 30 min equal amount of CYP82E4 was added into mixture for incubation. Total protein in single and collective enzyme incubation are same. Each data are average of two independent assays.

3.2.4. Substrate specificity of CYP82E4, CYP82E5v2 and CYP82E10

A series of nicotine analogues have been shown to be used by tobacco through *N*-dealkylation (Dawson, 1951; Kisaki and Tamaki, 1964; Kisaki et al., 1978; Bartholomeusz et al., 2005b; Robins et al., 2007) (Figure 3.5). The tobacco used in these reports all have high ability to demethylate nicotine. The question would be whether nicotine and nicotine analogues were used by the same enzymes. Methylanabasine and *N'*-ethylnornicotine, two compounds from the list (highlighted in red in Figure 3.5), were chosen to test substrate specificity of the three nicotine demethylases. Very low concentration of methylanabasine could be found tobacco leaf (Matsush et al., 1983), and methylanabasine can be formed in *N. tabacum* and *N. glauca* by aberrant biosynthesis feeding *N'*-methyl- Δ^1 -piperideinium choride (Leete and Chedekel, 1972). *N'*-ethylnornicotine has been found in burley tobacco (Braumann et al., 1990). Anabasine was formed from methylanabasine by CYP82E4, CYP82E5v2 and CYP82E10 (Figure S3.4), and product identity was confirmed by GC-MS. Methylanabasine and ethylnornicotine inhibit nicotine demethylation catalyzed by CYP82E4, CYP82E5v2 and CYP82E10 (Figure S3.5). So these three nicotine demethylases could potentially use a broad range of substrates.

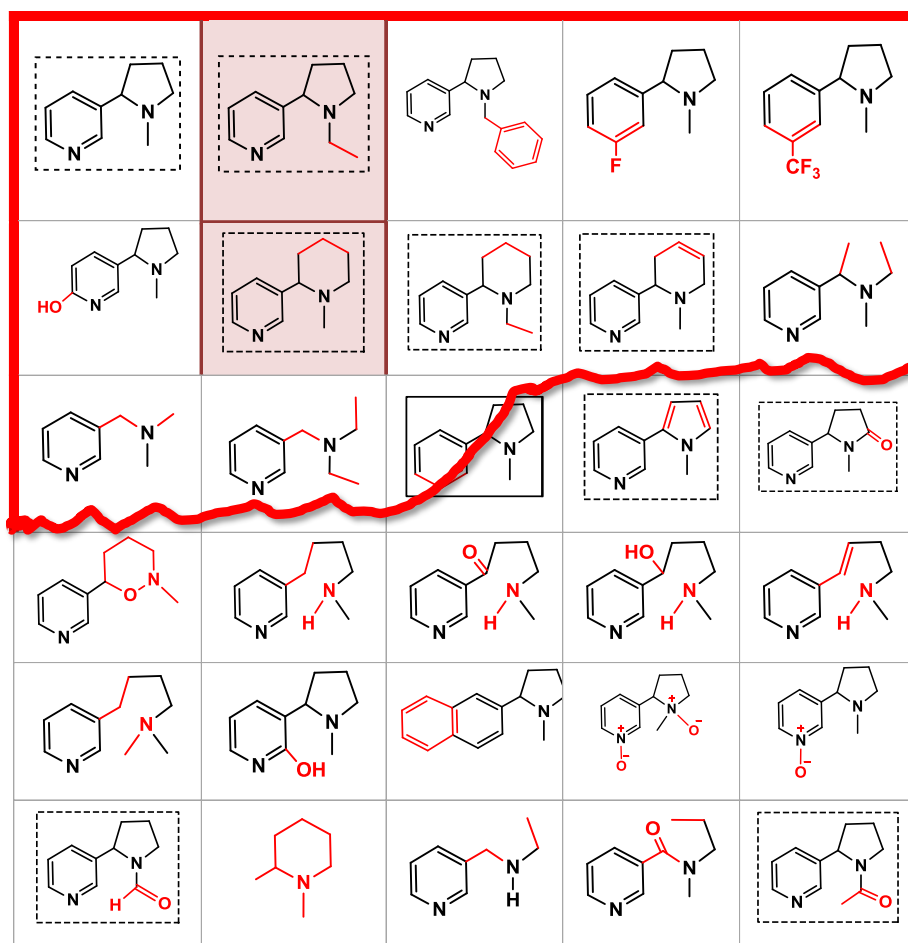


Figure 3.5. Nicotine and nicotine analogues used by tobacco through *N*-dealkylation reaction (Dawson, 1951; Kisaki and Tamaki, 1964; Kisaki et al., 1978; Bartholomeusz et al., 2005b; Robins et al., 2007). Nicotine analogues were fed to tobacco leaves or cells, followed by the identification of *N*-dealkylation products. The compounds used by tobacco through *N*-dealkylation reaction are circled by red lines. (R, S)-1-methyl-2-phenylpyrrolidine (solid borders; cut into half by the line in the table) has inconsistent reports. In this study, methylanabasine and ethylnornicotine were incubated with microsomes over-expressing three demethylase genes *in vitro*, highlighted by red. Details of the feeding assays are given in Table S1.2. Compounds with dashed border are found in tobacco.

3.3. Discussion

The hypothesis of enantioselective demethylation was proposed to explain that the high and wide range of EF_{nic} in tobacco leaf could result from a low EF_{nic} . *In vitro* all three nicotine demethylases CYP82E4, CYP82E5v2 and CYP82E10 demethylate (R)-nicotine faster than (S)-nicotine, but they exhibit different product accumulation patterns. Although being minor demethylases in tobacco, CYP82E5v2 and CYP82E10 have very strong, if not exclusively, selectivity for (R)-nicotine, and can produce 0.75 EF_{nnic} from 0.03 EF_{nic} . CYP82E4 can demethylate both (R)- and (S)- nicotine, and the highest EF_{nnic} produced by CYP82E4 *in vitro* from 0.03 EF_{nic} of nicotine substrate is 0.20. The EF_{nnic} will decrease as the CYP82E4 catalyzed demethylation proceeds. Based on the *in vitro* results, a model is proposed to explain the variable nornicotine enantiomeric composition (Figure 3.6). In tobacco, expression of CYP82E5v2 is constitutive, and CYP82E4 expression is induced during senescence. So newly synthesized nicotine with a higher EF_{nic} , could have the (R)-nicotine demethylated by CYP82E5v2 and CYP82E10 prior to activation of CYP82E4 and thus yield the higher EF_{nnic} . Then during senescence, CYP82E4 demethylates both (R) and (S)- nicotine and reduces EF_{nnic} . Therefore, the high and variable EF_{nnic} relative to EF_{nic} can be putatively explained by the combined action of CYP82E4, CYP82E5v2 and CYP82E10.

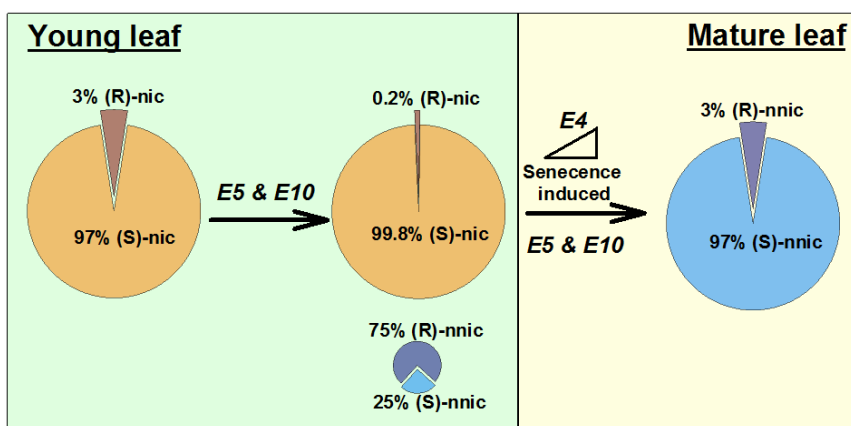


Figure 3.6. Proposed nicotine and nornicotine enantiomeric composition affected by three nicotine demethylases in tobacco leaf. The pie charts represent the relative abundance of (R)- and (S)- nicotine and nornicotine.

In tobacco, *CYP82E5v2* and *CYP82E10* are dominant, but not additive (Lewis et al., 2010). This could be explained by the observation of the enantioselectivity of *CYP82E5v2* and *CYP82E10*. Since *CYP82E5v2* and *CYP82E10* almost exclusively use (R)-nicotine, and the (R) isomer only accounts for 3% of total nicotine, presence of either of them is enough to use that amount of (R)-nicotine. The promiscuity of *CYP82E4* could explain the results that addition of *CYP82E5v2* and *CYP82E10* to plant with *CYP82E4* do not cause an increase in nicotine demethylation. The selectivity of *CYP82E4*, *CYP82E5v2* and *CYP82E10* can also explain the choice of 3 % conversion in the “LC” protocol (Jack and Bush, 2007). “LC” protocol is a standard practice used by tobacco breeders to remove high demethylation plants during seed production to reduce demethylation in the progeny. Of the three nicotine demethylases, *CYP82E4* is responsible for over 90% of the demethylation and plants with high expression of *CYP82E4* should be excluded from seed production. Since *CYP82E5v2* and *CYP82E10* can only use no more than 3% of nicotine, any plant with more than 3% demethylation must contain *CYP82E4* expressed gene and should be excluded.

In planta there may be other factors contributing to the nornicotine enantiomeric composition. Although nornicotine is mainly synthesized in leaf (Dawson, 1945), some nornicotine can also be produced in the root (Mizusaki et al., 1965) and be translocated to the leaf like nicotine. Translocation of nornicotine from root to leaf could influence the nornicotine composition in leaf. Mutant plants with all three demethylases knockout still contain some nornicotine, which suggests the possibility of direct synthesis of nornicotine other than by demethylation (Lewis et al., 2010). The report that (S)-nornicotine is degraded faster than (R)-nornicotine could account for some of the increased (R/S)-nornicotine ratios and introduces another level of complexity *in planta* (Kisaki and Tamaki, 1966; Mesnard et al., 2001).

Recombinant human CYP2A6, CYP2B6 and CYP2A13 expressed in baculovirus-infected insect cells, can catalyze the demethylation of nicotine, and they all use a broad range of substrates (Yamanaka et al., 2005). It has been shown in tobacco cell cultures

and leaf feeding assays that a wide range of nicotine analogues can be used as substrate, through the *N*-dealkylation process. Methylanabasine and ethylnornicotine, two of the analogues used by tobacco, were shown to be the substrate of nicotine demethylase. Therefore, demethylation of nicotine could be one of a specific case of the general *N*-dealkylation reaction catalyzed by these nicotine demethylases.

(S)-nicotine is more physiologically potent than the (R)-enantiomer (Pogocki et al., 2007) and it is often speculated that from an evolutionary point of view nicotine is accumulated in tobacco to deter herbivores (Steppuhn et al., 2004). Therefore, an evolutionary selection could be operative for plants that produced the more potent form, (S)-nicotine with lower demethylation of the (S) than (R)- enantiomer.

Racemization has been proposed to explain the high R/S ratios of nornicotine but racemization would unlikely occur during the demethylation in *planta*. Nicotine demethylation in tobacco is catalyzed by cytochrome P450 (Siminszky et al., 2005), and the demethylation proceeds by oxidation of *N*-methyl group (Mesnard et al., 2002). Based on *N*-dealkylation catalyzed by P450s (Meunier et al., 2004), it has been hypothesized that demethylation of (S)-nicotine yields (S)-nornicotine and that demethylation of (R)-nicotine yields (R)-nornicotine (Figure S3.6). The *in vitro* experimental results in this study also indicate that racemization during demethylation is not a mechanism of altering the enantiomeric composition of nornicotine.

Nicotine synthase has not been genetically or biochemically characterized. Until now only a putative enzyme mixture (Friesen and Leete, 1990) and candidate genes (A622 gene (DeBoer et al., 2009; Kajikawa et al., 2009); berberine bridge enzyme-like gene (Kajikawa et al., 2011)) were identified. It is general belief that nicotine biosynthesis is an enantiospecific process. However, selective demethylation of (R)-nicotine *in vitro* and the presence of 0.03 EF_{nic} in RNAi silenced demethylation plants suggest that the originally synthesized (R)-nicotine may account for more than the reported 0.2 % of total nicotine.

Nicotiana tabacum L. (tobacco) is an allotetraploid derived from ancestors of the modern diploids, *N. sylvestris* and *N. tomentosiformis*. Five nicotine demethylase have been identified, and the functional nicotine demethylases CYP82E4 and CYP82E5v2 originate from *N. tomentosiformis*, and CYP82E10 comes from *N. sylvestris* (Table S3.2). CYP82E5v2 and CYP82E10 have higher amino acid sequence similarity and similar selectivity compared to CYP82E4. Therefore, CYP82E4 could be the duplication and mutation of CYP82E5v2.

3.4. Conclusion

There is high and variable enantiomer fraction of nornicotine in conventional tobacco, while the EF_{nic} is always low. All three nicotine demethylases were used to test the hypothesis of enantioselective demethylation. *In vitro* recombinant demethylase CYP82E4, CYP82E5v2 and CYP82E10 all had a preference for (R)-nicotine substrate, and combined activity of these three demethylases could be the reason that cause the differences between nicotine and nornicotine composition in *planta*. No racemization was found during demethylation. The demethylation of nicotine could be a specific case of a general *N*-dealkylation catalyzed by CYP82E4, CYP82E5v2 and CYP82E10. In summary, our enzymatic studies reveal a possible role for enantioselective demethylation in nornicotine enantiomeric composition, by which preference of (R)-nicotine as substrate over (S)-enantiomer form a high enantiomer fraction of nornicotine.

3.5. MATERIALS AND METHODS

3.5.1. Expression of nicotine demethylases CYP82E4, CYP82E5v2 and CYP82E10 in yeast

CYP82E4v1, *CYP82E5v2* and *CYP82E10* cDNA were cloned into the yeast expression vector pYeDP60 and transformed into yeast strain WAT11 (Siminszky et al., 2005; Gavilano and Siminszky, 2007; Xu et al., 2007a; Lewis et al., 2010). WAT11 is a yeast line engineered to enhance the expression of plant P450s through the coexpression of *Arabidopsis* P450 reductase gene (Pompon et al., 1996). Transformed WAT11 yeast cells were spread on synthetic galactose induction (SGI) plates. A single colony was used to

inoculate 10 ml SGI media and was grown with shaking at 30 °C for 24 h. An aliquot of this culture was diluted 1:50 into 250 ml of YPGE medium (10 g L⁻¹ yeast extract, 20 g L⁻¹ bacto peptone, 5 g L⁻¹ glucose and 30 g L⁻¹ ethanol). The culture was grown until the glucose was completely consumed as indicated by the Diastix urinalysis reagent strip. DL-galactose was added to a final concentration of 2 % (W/V) to induce production of the cloned gene. Cells in the culture were grown for an additional 20 h prior to the microsome preparations.

3.5.2. Yeast microsome preparation

Induced yeast cells were collected and used for microsome preparation (Xu et al., 2007a). The collected cells were washed twice with TES buffer and TES-M buffer. Then the cells were resuspended in extraction buffer and broken with glass beads. The cell extracts were centrifuged for 20 min at 20 000 g, and the supernatant was ultracentrifuged at 100 000 g for 90 min. The pellets containing the microsomal protein were suspended in TEG-M buffer. Protein concentration was determined with Bradford protein assay.

3.5.3. *In vitro* enzyme assay

Nicotine demethylase activity was assayed in a reaction mixture (20 µl) containing 0.5 mg ml⁻¹ microsomal protein, 2.5 mM NADPH, 25 mM Tris buffer (pH 7.5) and different amounts of (R)-, (S)- or racemic [2'-¹⁴C]nicotine. Five µM nicotine substrate was used in validation assays. Recovery of nicotine and nornicotine for all three assays ranged from 92 to 108 %. (R)- and (S)- [2'-¹⁴C]nicotine were separated from racemic [2'-¹⁴C]nicotine (Moravek Biochemicals and Radiochemicals). (R)- and (S)-nicotine were baseline separated by chiral high-performance liquid chromatography (HPLC) (Figure S3.7). (R)-nicotine was 49.8% of the original racemic [2'-¹⁴C]nicotine analyzed. Nornicotine contamination in the [2'-¹⁴C]nicotine is under 0.5 %. Reaction mixtures were incubated at room temperature for 10 min and the reactions were stopped by addition of 20 µl methanol containing 50 mM nicotine and nornicotine.

Nicotine demethylation was measured by resolving the nicotine and nornicotine in 10 µl of reaction mixture by thin layer chromatography (TLC) and ¹⁴C-nicotine and ¹⁴C-

nornicotine were quantified by liquid scintillation counter (1900 TR, Packard Instrument Company).

EF_{nic} determinations used the remaining reaction mixture of each sample to separate the nicotine and nornicotine by thin TLC, and the nornicotine was methylated to nicotine by incubating for 30 min with 50 µl formic acid and 100 µl formaldehyde at 110 °C. TLC plates were TLC Silica Gel 60 F254 (EMD Chemicals Inc.). Developing solvent for TLC was chloroform: methanol: ammonia hydroxide (85:15:2, v/v/v). The nicotine was base extracted by MTBE and collected after further separation into (R)- and (S)-enantiomer by chiral HPLC (Mesnard et al., 2001). A Perkin-Elmer series 200 HPLC was used with a Chiracel OD-H column (0.46 cm (D) × 25 cm) (Chiral Technologies Inc.) and eluted with hexanes/ methanol (98:2, v/v) at 1.0 ml min⁻¹, with detection at 252 nm. (R) and (S) collections were quantified by liquid scintillation counting. The data were analyzed by Sigmaplot 12. Enantiomer fraction (EF) (Harner et al., 2000): EF = R enantiomer / (R enantiomer + S enantiomer)

To test the specificity of three demethylases, methylanabasine was incubated with CYP82E4, CYP82E5v2 and CYP82E10 *in vitro*. After 10 h reaction, the incubations were stopped by base and extracted with MTBE containing quinoline as internal standard. Extracts were analyzed by GC-MS with a Varian CP-3800 GC coupled to a Varian Saturn 2200 MS/MS (Varian Medical Systems) using a Supelco SLB-5ms fused silica capillary column (30 m x 0.25 mm x 0.25 µM film thickness, Supelco). Initial oven temperature was set at 150 °C for 0.5 min, increased 15 °C min⁻¹ to 170 °C, then 1.5 °C min⁻¹ to 195 °C held for 2 min, then 20 °C min⁻¹ to a final temperature 300 °C, and held for 20 min.

Supplemental Material

Table S3.1. Comparison of Michaelis-Menten constants with literatures.

Table S3.2. Evolution of nicotine demethylases in *N. tabacum* L.

Figure S3.1. Competitive inhibition of CYP82E4-catalyzed (S)-nicotine demethylation by (R)-nicotine shown in Lineweaver-Burk plot.

Figure S3.2. Inability of CYP82E4 to generate leaf nornicotine composition *in vitro*.

Figure S3.3. Time course of a 10 μ M 3:97 ratio of R/S-nicotine incubated with CYP82E4, CYP82E5v2 and CYP82E10 separately or collectively.

Figure S3.4. Anabasine was identified in the incubations of methylanabasine with CYP82E4, CYP82E5v2 and CYP82E10 *in vitro*.

Figure S3.5. Nicotine demethylation inhibited by methylanabasine and ethylnornicotine catalyzed by CYP82E4, CYP82E5v2 and CYP82E10.

Figure S3.6. Two possible mechanisms in *N*-demethylation of nicotine catalyzed by cytochrome P450 enzymes (Meunier et al., 2004).

Figure S3.7. Racemic nicotine separation by chiral HPLC.

Chapter 4. (R)-nicotine biosynthesis, metabolism and translocation as determined in nicotine demethylase mutants

4.1. Introduction

Nicotine is the most abundant pyridine alkaloid in tobacco (*Nicotiana tabacum L.*), and has important biological functions including antiherbivore defense and smoking addiction (Benowitz, 2008). Nicotine biosynthesis and metabolism has been studied extensively. After biosynthesis in the tobacco root (Dawson, 1942), nicotine is translocated to the leaf via the xylem (Guthrie et al., 1962) and stored in the leaf vacuole with the help of a tonoplast localized transporter (Shitan et al., 2009). Nornicotine is the major metabolite of nicotine in tobacco, through nicotine demethylation process. Nicotine can be demethylated in both leaf (Dawson, 1945) and root (Mizusaki et al., 1965), but mainly in aging leaf (Chakrabarti et al., 2008). During curing, four main alkaloids of tobacco, nicotine, nornicotine, anabasine and anatabine, may be nitrosated to *N'*-nitrosonornicotine (NNN), 4-(methylnitrosamino)-1-(3-pyridyl)-1-butanone (NNK), *N'*-nitrosoanatabine (NAT), *N'*-nitrosoanabasine (NAB), respectively. NNK and NNN are two of the most abundant and carcinogenic of the seven tobacco-specific nitrosamines (TSNAs) identified in tobacco products (Hecht, 1998). Nicotine synthase has not been genetically or biochemically characterized. Until now only a putative enzyme mixture (Friesen and Leete, 1990) and candidate genes (A622 gene (DeBoer et al., 2009; Kajikawa et al., 2009); berberine bridge enzyme-like gene (Kajikawa et al., 2011)) were identified. Three functional nicotine demethylases in tobacco have been reported: CYP82E4 (accounts for most demethylation in senescing leaf), CYP82E5v2 and CYP82E10 (Siminszky et al., 2005; Gavilano and Siminszky, 2007; Xu et al., 2007a; Lewis et al., 2010).

Nicotine has two enantiomers which differ from each other at 2'-C position on pyrrolidine ring. (S)-nicotine is predominant form, and (R)-nicotine only accounts for 0.2% of total nicotine in cured leaf (Armstrong et al., 1998). Therefore, nicotine is considered to be equal to (S)-nicotine in most literature. Unless stated, enantiomer fraction (EF) in the following context represents (R)-enantiomer proportion of total given compound. The reports for nornicotine enantiomeric composition are inconsistent, EF of nornicotine ranging from 0.04 to 0.75 (Armstrong et al., 1999; Liu et al., 2008). It is puzzling how

0.002 of EF_{nic} results in nornicotine with 0.04-0.75 EF in tobacco leaf (Figure 4.1). Our previous characterization of nicotine demethylases *in vitro* suggests a higher EF_{nic} and selective demethylation of (R)-nicotine. Selective demethylation of nicotine was reported when feeding excised tobacco leaf (Kisaki and Tamaki, 1964) and tobacco cell culture (Mesnard et al., 2001). The questions then become how much (R)-nicotine is biosynthesized in tobacco root, and how is it demethylated in root and leaf.

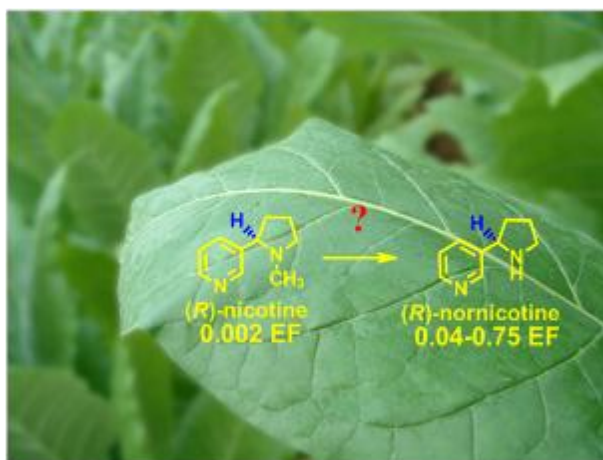


Figure 4.1. The puzzle of the discrepancy between nicotine and nornicotine enantiomeric composition. Enantiomer fraction (EF) represents the percentage of R enantiomer. (S)-nicotine accumulates to greater than 99% of the total nicotine content in leaves, yet nornicotine accumulates predominately in the R configuration. Is this because the enzyme(s) responsible for demethylation of nicotine possess sufficient specificity for (R)-nicotine, rather than (S)-nicotine?

Enantiomers of nicotine and nornicotine-nitrosated product NNN behave differently in animal models and human. The LD_{50} s for intravenous administration of (R)-nicotine in several animal species is approximately 18-times higher than that of (S)-nicotine (Pogocki et al., 2007). A significantly lower level of toxic and carcinogenic metabolites is produced from (R)-nicotine. Based on the overall cytotoxicity of the compound and its metabolites, (R)-nicotine is approximately eighty times less cytotoxic than (S)-nicotine (Yildiz et al., 1998). (S)-NNN undergoes significantly more 2-hydroxylation than (R)-

NNN in cultured rat esophagus and *in vivo* in rats. In rats treated with racemic NNN, 66% of 2-hydroxylation metabolites are from (S)-NNN, while 74% of the 5-hydroxylation products are produced from (R)-NNN (McIntee and Hecht, 2000). 2-hydroxylation of NNN is the major metabolic activation pathway, suggesting carcinogenicity of (S)-NNN may be greater than that of (R)-NNN. Understanding the mechanisms behind the nicotine and nornicotine composition will facilitate the future manipulation of enantiomeric composition of nicotine and NNN.

In this paper, we confirmed the enantioselectivity of three demethylases *in vivo* by investigating nicotine demethylase mutants at different growth and leaf curing stages. Since nicotine metabolism can occur in root and leaf, scion/stock grafts were used to dissect individual leaf and root contributions to the final nicotine and nornicotine composition in leaf.

4.2. Results

4.2.1. Effects of nicotine demethylases on enantiomeric composition of nicotine, nornicotine, and TSNA level in air-cured leaf lamina

Previously, we have shown *in vitro* three nicotine demethylases had different selectivities for nicotine enantiomers. In this study, we wanted to determine the effects of nicotine demethylases *in vivo*. Three nicotine demethylase mutant and mutant combinations (Lewis et al., 2010) were grown in the field in 2010, and the air-cured leaf were analyzed for alkaloid level and nicotine and nornicotine enantiomeric composition. The experiment was repeated in 2011, adding the widely used commercial line TN90LC (Figure 4.2, Figure S4.1 and Table S4.1). TN90LC is widely used commercial variety and was used as control.

With all three demethylases silenced (*e4e5e10*), 3% of nicotine accumulated is R enantiomer (0.03 EF_{nic}). Any of three demethylases can reduce EF_{nic} to under 0.002. Only CYP82E4 can significantly convert (S)-nicotine to (S)-nornicotine. CYP82E4 is the major demethylase and accounts for over 90 % of the demethylation in high demethylation plants. CYP82E5v2 and CYP82E10 are minor demethylases in tobacco,

probably due to the selectivity for (R)-nicotine and limitation of (R)-nicotine as substrate. All these results were consistent with the selectivity of three demethylases *in vitro*.

TSNAs in mutant air-cured leaf lamina from two years field trials were also measured (Figure 4.2.C and Figure S4.1). NNN level was closely correlated with nornicotine level, while 4-(methylnitrosamino)-1-(3-pyridyl)-1-butanone (NNK) was correlated with nicotine level. CYP82E4 changed the nicotine and nornicotine ratio in cured leaf, and dramatically affected NNN and NNK levels. No consistent conclusions, none were expected, could be drawn for the effects of demethylases on *N'*-nitrosoanatabine (NAT) and *N'*-nitrosoanabasine (NAB) level. Total TSNAs was inversely correlated with CYP82E4 activity. Without functional CYP82E4, tobacco had significantly reduced TSNAs. The triple mutant had lowest NNN among all the tobacco lines, but the total TSNAs in triple mutant was not significantly different from mutant with inactive *CYP82E4*. TN90LC in this study had similar level of individual and total TSNAs, compared to a previous report (Lewis et al., 2008).

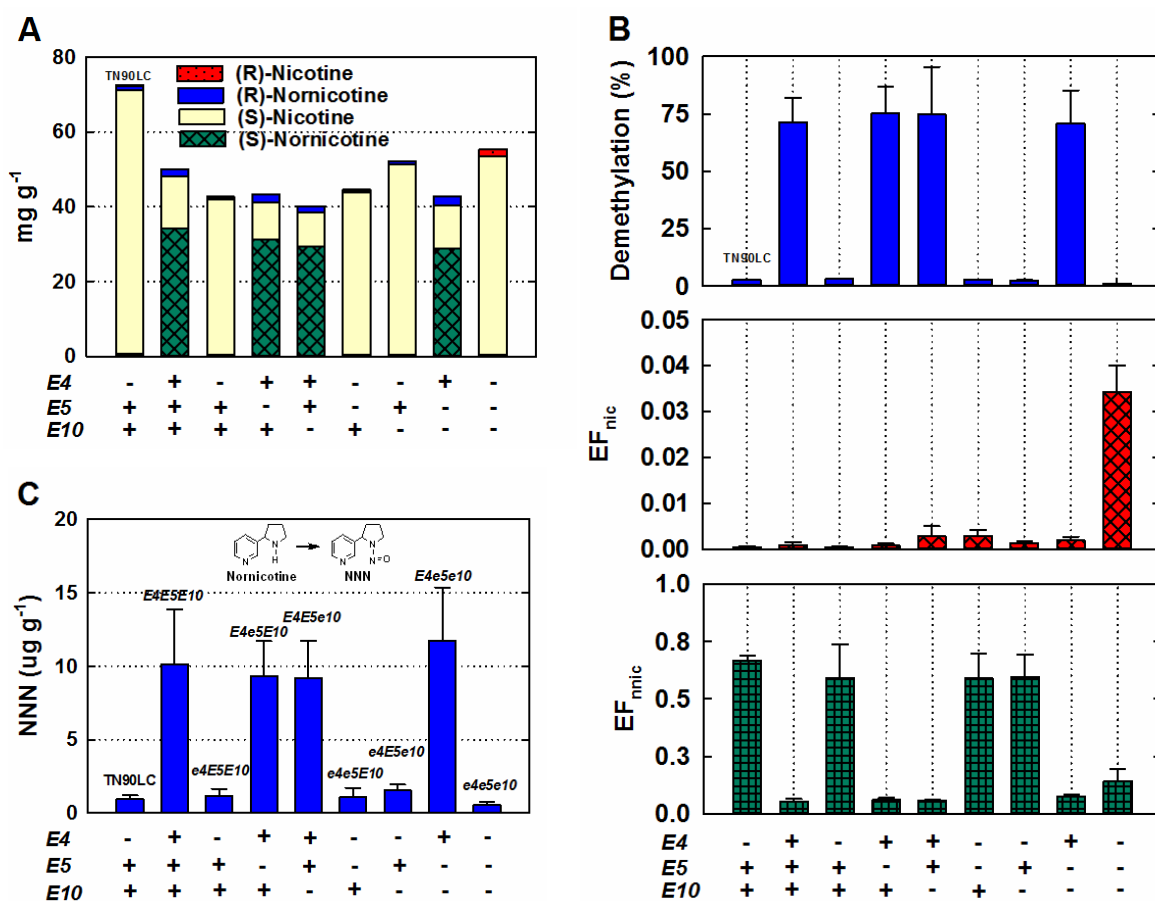


Figure 4.2. Effects of nicotine demethylases on nicotine, nornicotine and NNN in air-cured leaf laminae in 2010 and 2011. (A) Changes of enantiomers levels of nicotine and nornicotine in nicotine demethylase mutants. (B) Effects of nicotine demethylases on nicotine and nornicotine composition. (C) Effects of nicotine demethylases on NNN levels. TN90LC data is from 2011 only. Each bar is the average of two years results. The error bars represent standard deviation. +/- below the bars indicate the presence/absence of a functional demethylase gene. Demethylation reflects how much nicotine goes through the demethylation process. Demethylation (%) = nornicotine concentration (mg g^{-1}) * 100/ sum of nicotine and nornicotine concentration (mg g^{-1}).

4.2.2. Accumulation of alkaloids in mutants leaf laminae during the growth and curing

During tobacco production, levels of alkaloids significantly change at two stages, apical decapitation and harvest. Apical decapitation, typical practice in tobacco production, stimulates the alkaloid production. Since *CYP82E4* gene expression is induced in

senescing leaf, nornicotine levels increase during first two weeks of curing at the expense of nicotine. After confirming the selectivity of three demethylases in cured leaf, we wanted to know how nicotine and nornicotine enantiomers changed during growth, and to better understand the function of the three demethylases.

Nine tobacco lines were chosen to be grown in the field in 2011, and were sampled at five different sampling times during growth and air-curing process. Individual alkaloids levels were determined (Figure 4.3) at five critical times during tobacco production: after recovery from transplant shock (one month after transplant), apical decapitation (two months after transplant), harvest (three months after transplant), two weeks after harvest and cured leaf (Figure S4.4).

After apical decapitation alkaloid accumulation dramatically increased, as expected (Figure 4.3). During the two weeks of curing, nornicotine concentration increased significantly at expense of nicotine due to CYP82E4 activity. Nicotine demethylase mutations had no obvious effect on anabasine and anatabine accumulation, although nicotinic acid is shared in the biosynthesis of the four main alkaloids. Due to changes in nicotine and nornicotine levels, alkaloid profiles were changed in tobacco with active CYP82E4. For example, the parent tobacco plant (*E4E5E10*) had alkaloids level at one month after transplant nicotine > anatabine > nornicotine > anabasine; at apical decapitation nicotine > nornicotine > anatabine > anabasine; and during harvest and curing nornicotine > nicotine > anatabine > anabasine.

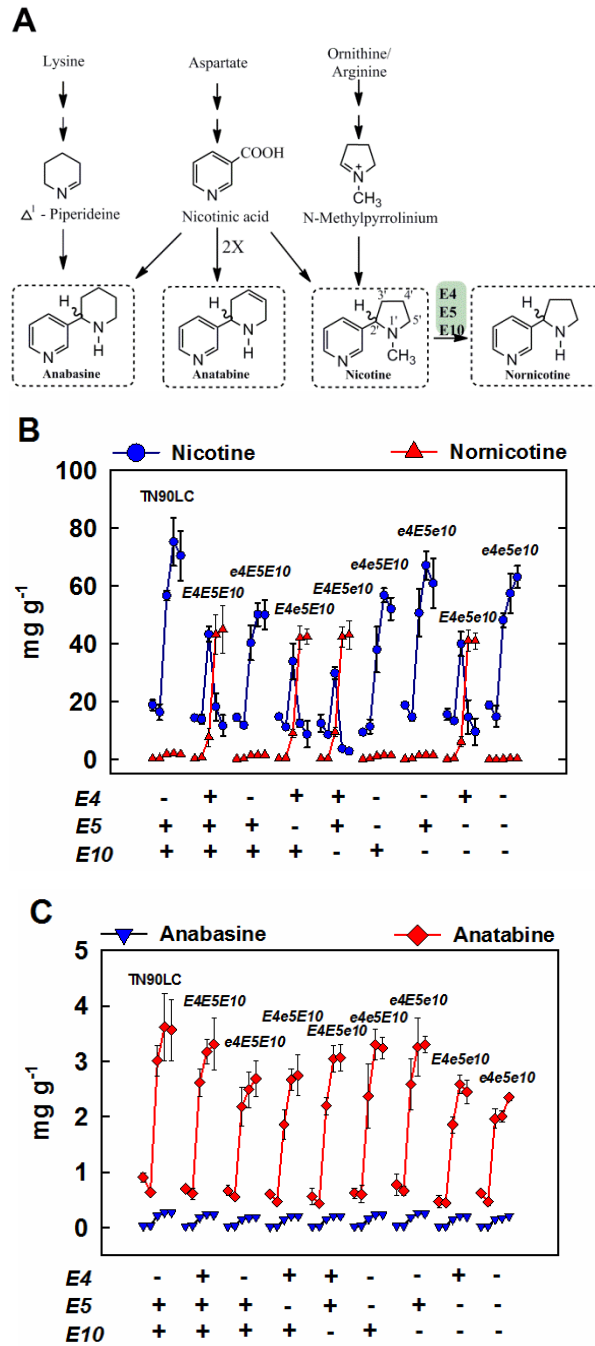


Figure 4.3. Leaf lamina alkaloids profile of different nicotine demethylase mutants during growth and curing. TN90LC (commercial variety, control) and different nicotine demethylase mutants were grown in the field and sampled five times. The sequential sampling time for each line were one month after transplant, apical decapitation, harvest, 2 weeks of curing and cured. Each data point is average of four bulk samples, and each bulk sample is a mixture of five middle leaves from five plants. The error bars represent standard deviation. +/- below the bars indicate the presence/absence of a functional demethylase gene.

4.2.3. Accumulation of nicotine and nornicotine enantiomers in mutant leaf lamina during growth and curing

Enantiomers levels (Figure 4.4) and EF (Figure 4.5) of nicotine and nornicotine were analyzed at five sampling times. (R)-nicotine levels were low throughout growth and curing in plants with active CYP82E5 or CYP82E10. The triple mutant had much higher sum of (R)-nicotine plus (R)-nornicotine than that of plants without active CYP82E4 (TN90LC, *e4E5E10*, *e4e5E10* and *e4E5e10*), indicating the loss of R form. Nornicotine has been shown to be degraded in excised leaves (Kisaki and Tamaki, 1966). Tobacco with active CYP82E4 had a different accumulation pattern of (R)-nornicotine from that of tobacco without active CYP82E4, and continued to accumulate (R)-nornicotine after harvest. (S)-nicotine demethylation occurred only in tobacco with active CYP82E4 at harvest.

Enantiomer fraction of nicotine and nornicotine changed during sampling period (Figure 4.5). EF_{nic} of all mutants had decreased trends at all sampling times. In the triple mutant, there was only a small decrease of EF_{nic} , staying around 0.04. The mutants with inactive CYP82E4 had relative stable nornicotine enantiomeric composition, while plants with active CYP82E4 had a continuous decrease in EF_{nic} , due to the larger increase in the (S)-nornicotine.

The field results from 2010 and 2011 were rearranged for analyzing the relationship between nicotine demethylation and nornicotine enantiomeric composition (Figure 4.6). With only CYP82E5 or CYP82E10 active (*e4E5e10* or *e4e5E10*), plants contained 0.50 to 0.80 EF_{nic} and demethylation in these mutants was low. When only CYP82E4 was active (*E4e5e10*), the demethylation resulted in a much wider range of EF_{nic} , 0.06 to 0.25. These results are consistent with *in vitro* enzyme assays using 0.03 EF_{nic} (Chapter 3). Triple mutant had consistently very low demethylation and 0.10 to 0.25 EF_{nic} . When more than one demethylase was present (Figure 4.6 insert), EF_{nic} spanned 0.06 to 0.80, which is consistent with the wide range and high EF_{nic} in literature reports.

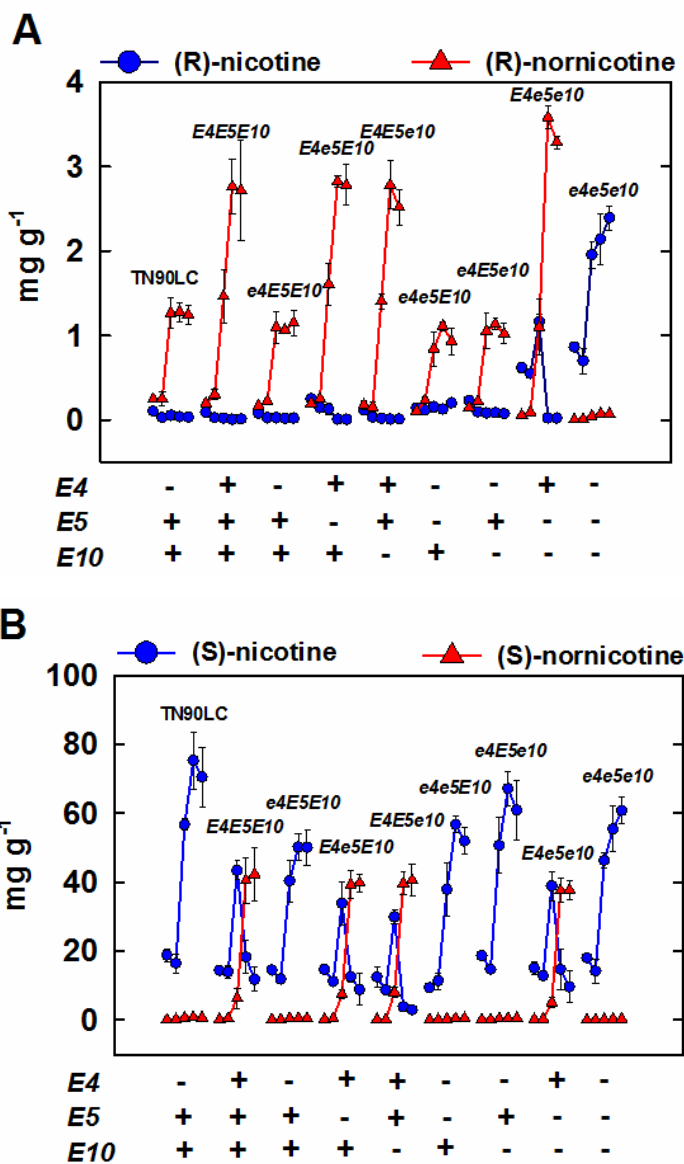


Figure 4.4. Accumulation of nicotine and nornicotine enantiomers in leaf lamina of different nicotine demethylase mutants during growth and curing. TN90LC (commercial variety, control) and different nicotine demethylase mutants were grown in the field and sampled five times. The sequential sampling time for each line were one month after transplant, apical decapitation, harvest, 2 weeks of curing and cured. Each data point is average of four bulk samples, and each bulk sample is a mixture of five middle leaves from five plants. The error bars represent standard deviation. +/- below the bars indicate the presence/absence of a functional demethylase gene.

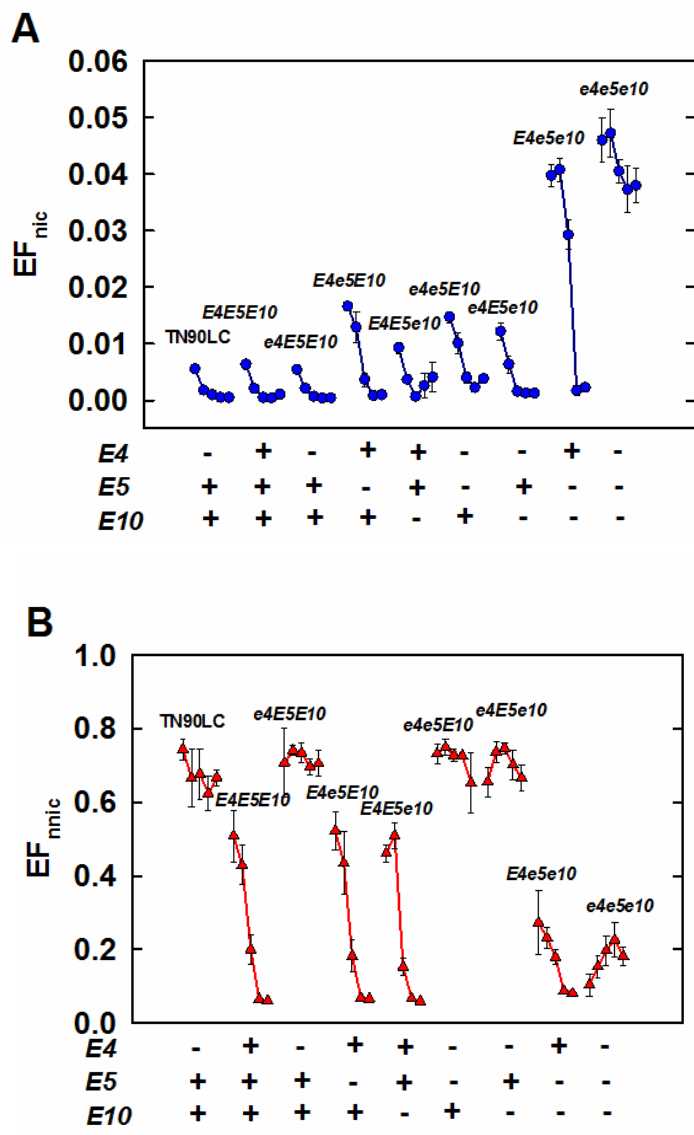


Figure 4.5. Nicotine (A) and nornicotine (B) enantiomeric composition of different nicotine demethylase mutant leaf lamina during growth and curing. TN90LC (commercial variety, control) and different nicotine demethylase mutants were grown in the field and sampled five times. The sequential sampling time for each line were one month after transplant, apical decapitation, harvest, 2 weeks of curing and cured. Each data point is average of four bulk samples, and each bulk sample is a mixture of five middle leaves from five plants. The error bars represent standard deviation. +/- below the bars indicate the presence/absence of a functional demethylase gene.

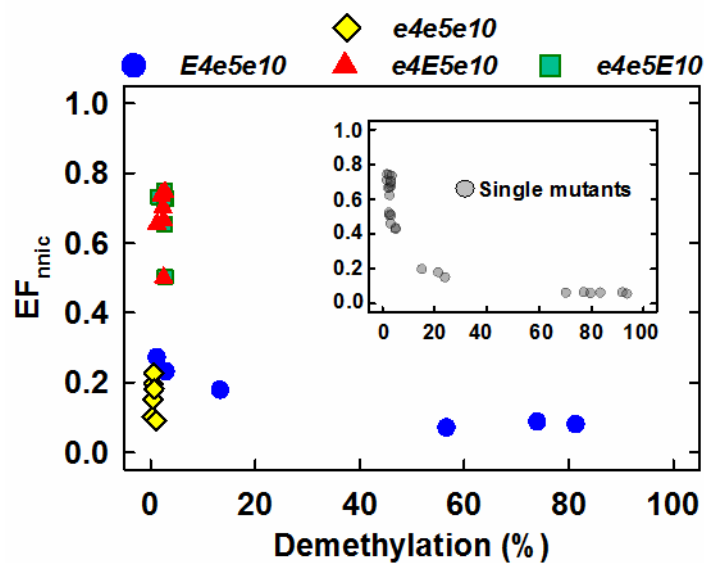


Figure 4.6. Relationships between nicotine demethylation and nornicotine enantiomeric composition from leaf lamina of demethylase mutants during growth and curing. This figure combines results of 2010 cured samples and 2011 growth and cured samples. Each data point is the average of three or four samples.

4.2.4. Contributions of three nicotine demethylases in root and leaf to the leaf nicotine and nornicotine composition

Root is the site of nicotine biosynthesis and the first place of nornicotine formation. Kisaki and Tamaki (1960) found that in root nicotine was predominantly the S enantiomer, while nornicotine was predominantly the R enantiomer. After investigating the nicotine and nornicotine enantiomer accumulation in leaf from green field plants, we tried to further understand the nicotine and nornicotine enantiomeric composition in root, and how it affected nicotine and nornicotine composition in the leaf. Scion/stock grafts were used to separate the effects of root and leaf on final nicotine and nornicotine composition in leaf (Figure 4.7 to Figure 4.9).

Tobacco plants were self-grafted to check the graft effects on nicotine and nornicotine composition (Figure 4.7). There was no difference between grafted and intact tobacco plant in terms of nicotine and nornicotine enantiomeric composition (intact plants results

not shown). For grafted plants, leaf, ethephon-treated leaf and root were analyzed. Ethephon treatment was used to enhance the aging effects after harvest. Compared to the results from field plants, nicotine and nornicotine composition in leaf laminae of grafted mutants was consistent with the enantiomeric composition in the field from apical decapitation and harvest stage. Also, after ethephon treatment grafted mutants had similar nicotine and nornicotine composition as field mutants during first two weeks of curing. Since leaf results are consistent with the results from the field, we further examined the nicotine and nornicotine compositions in root. The mutant with only CYP82E4 active (*E4e5e10*) had the same nicotine and nornicotine enantiomeric composition as *e4e5e10*, suggesting that CYP82E4 had few effects on root nicotine and nornicotine enantiomeric composition. Mutants with active CYP82E5v2 or CYP82E10 significantly reduced EF_{nic} and had predominantly (R)-nornicotine. With all three demethylases active, roots had similar nicotine and nornicotine enantiomeric composition as mutants with only CYP82E5v2 or CYP82E10 active, indicating that in root, CYP82E5v2 and CYP82E10 are major factors affecting nicotine and nornicotine enantiomeric composition. Except for triple mutants, lower EF_{nic} was found in leaves than in roots, suggesting that all demethylases actively influence nicotine enantiomeric composition in leaf.

Since the nornicotine in leaf is from leaf and root, tomato scions were grafted onto mutant roots to investigate the nicotine and nornicotine enantiomeric composition translocated to leaf (Figure 4.8). Tomato can produce small amount of nicotine (Sheen, 1988), but the amount of nicotine in tomato leaf was <1% of total nicotine translocated from tobacco root. No demethylase activity was measured when nicotine was fed to tomato leaves (data not shown). The same nicotine enantiomeric composition was found in both tomato leaves and tobacco roots, demonstrating that nicotine enantiomeric composition in root reflected the nicotine composition translocated to leaf and no selective translocation of nicotine occurs. Consistently lower EF_{nic} was found in tomato leaves. EF_{nic} of leaf lamina from tomato/tobacco grafts compared to self-grafted tobacco indicates that over 75% of the (R)-nicotine was demethylated in root, and the remainder was demethylated in leaf.

To investigate the function of three demethylases in leaf, tobacco was grafted onto triple mutant (*e4e5e10*) stock (Figure 4.9). Consequently, the same enantiomeric composition of nicotine (0.03-0.04 EF_{nic}) and nornicotine (0.10-0.25 EF_{nnic}) were supplied to mutant leaves via translocation. In leaf, CYP82E5v2 and CYP82E10 converted 0.03 EF_{nic} into 0.80 EF_{nnic}, while CYP82E4 produced 0.15 EF_{nnic}. These results are consistent with *in vitro* assays of selectivity of single demethylase.

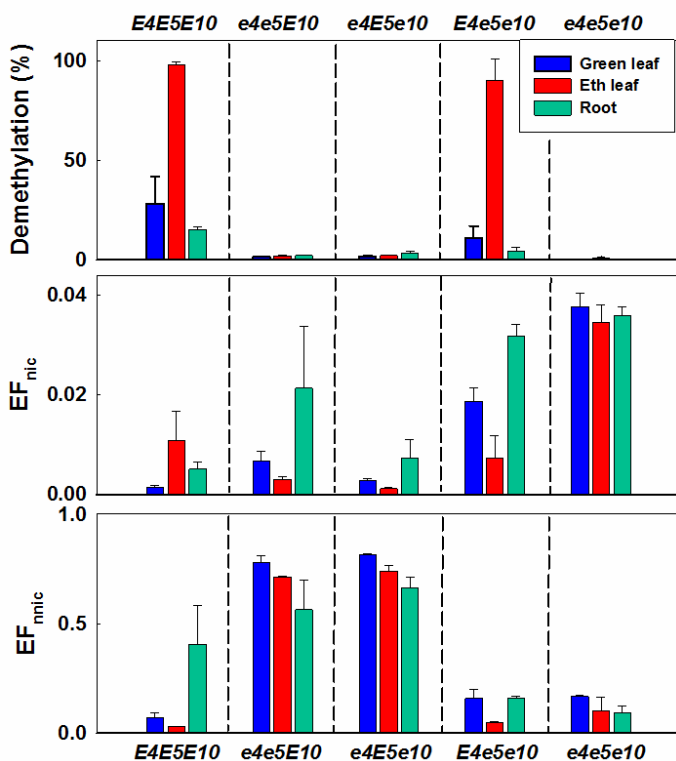


Figure 4.7. Demethylation, nicotine and nornicotine enantiomeric composition in self-grafted mutant tissues. The grafts do not influence the nicotine and nornicotine composition. Eth leaf: ethephon treated leaves which induce senescence and expression of *CYP82E4*. Data are an average of three plants. The error bars represent standard deviation.

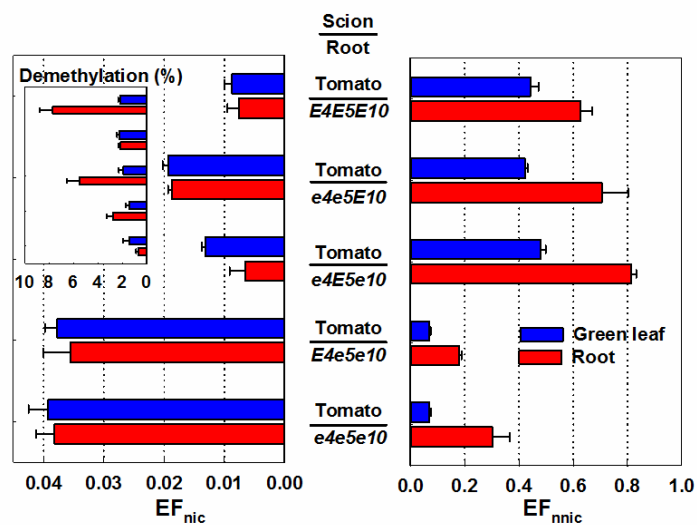


Figure 4.8. Nicotine and nornicotine composition in tomato/tobacco grafts. Each bar is an average of three replicates. The error bars represent standard deviation.

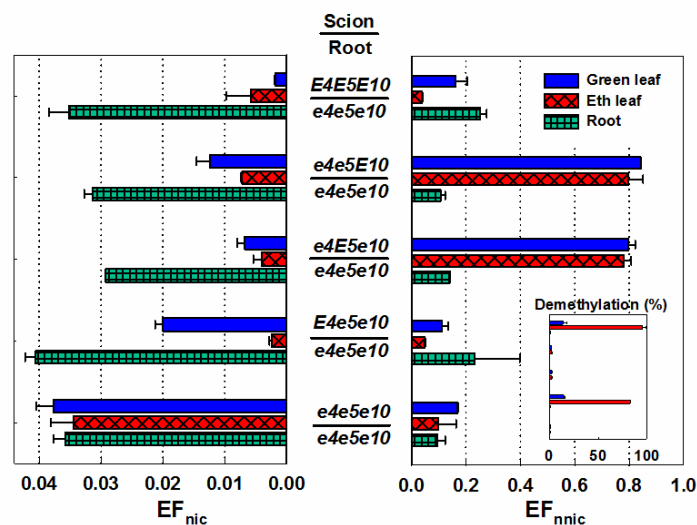


Figure 4.9. Nicotine and nornicotine enantiomeric composition in tobacco/*e4e5e10* grafts. Each bar is an average of two replicates, except that root of *e4E5e10/e4e5e10* only has one replicate. The error bars represent standard deviation.

4.3. Discussion

Previous studies of nicotine and nornicotine enantiomeric composition used cured leaf or qualitatively analytical methods. Quantitative study of nicotine and nornicotine enantiomeric composition during growth is lacking. In this study, alkaloid accumulation and enantiomeric composition of nicotine and nornicotine in different nicotine demethylase mutants were investigated during growth and curing. The discrepancy between nicotine and nornicotine enantiomeric composition was confirmed (Figure 4.10A). Previously we have shown that *in vitro* three demethylases had different selectivity for (R)-nicotine (Figure 4.10B). Both CYP82E5v2 and CYP82E10 can convert 0.04 EF_{nic} into over 0.80 EF_{nnic}, which is the reason why high EF_{nnic} is found in some tobacco samples. CYP82E4 can only produce about 0.25 EF_{nnic} from the same 0.04 EF_{nic}. However, *CYP82E4* expression is induced during senescence, and may demethylate almost all the (R)- and (S)- nicotine present in the leaf. Combination of the three demethylases could produce 0.04 to 0.75 EF_{nnic} from 0.03 EF_{nic}. In this study, we confirmed the *in vitro* observation by using nicotine demethylase mutants (Figure 4.6).

Based on the mutant graft results, we propose a model to explain the nicotine and nornicotine enantiomeric composition in the tobacco plant (Figure 4.10C). In triple mutant root (*e4e5e10*), synthesized nicotine consists of 4% of R form (0.04 EF_{nic}). CYP82E5v2 and CYP82E10 predominately determine the nicotine and nornicotine enantiomeric composition in roots whereas CYP82E4 has little impact. Soon after being synthesized, 0.04 EF_{nic} is reduced 0.01 EF_{nic}, resulting in 0.60 EF_{nnic}. Based on the EF_{nic} changes, over three fourths of (R)-nicotine is demethylated in root. After that, nicotine and nornicotine will be translocated to leaf, where the rest of (R)-nicotine is demethylated by all three demethylases. *CYP82E4* expression is induced dramatically during senescence, and (S)-nicotine is largely demethylated by CYP82E4 into (S)-nornicotine due to the limiting amount of (R)-nicotine present. Depending on *CYP82E4* expression (intensity and time), a range of EF_{nnic} was measured due to the large amount of (S)-nornicotine production, which explains the wide range of EF_{nnic} found in tobacco leaf. The general conclusion is that nicotine in tobacco consists of 4% (R)-enantiomer and may become essentially pure (S)-nicotine due to the selective demethylation of (R)-

nicotine. High selectivity of CYP82E5v2 and CYP82E10 for (R)-nicotine is the reason that there is 0.75 EF_{nic} present in some tobacco leaf. Different *CYP82E4* expression in the leaf and subsequent demethylation of (S)-nicotine to (S)-nornicotine results in a broad range of EF_{nic} .

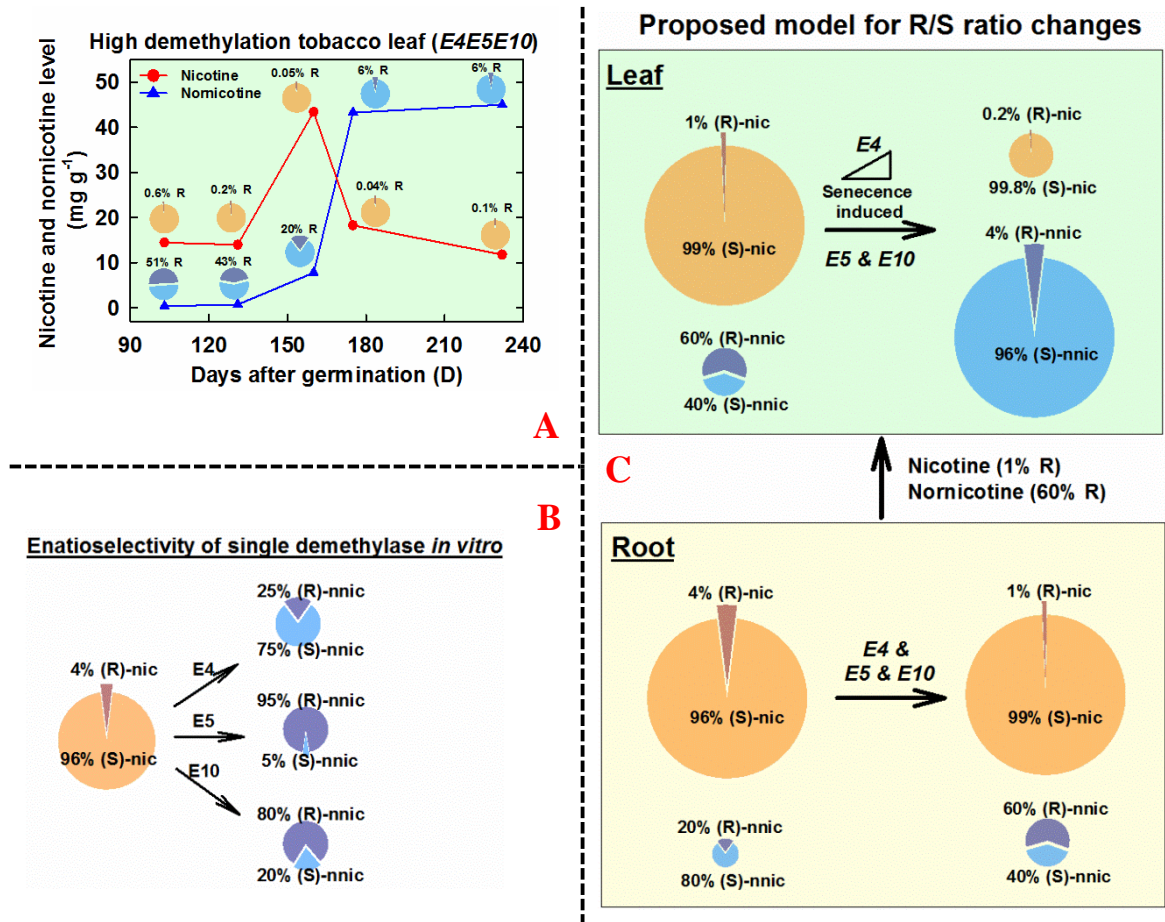


Figure 4.10. Effects of three nicotine demethylases on the enantiomeric composition of nicotine and nornicotine in high demethylation tobacco (*Nicotiana tabacum* L.). (A) Accumulation and composition of nicotine and nornicotine in converter leaf lamina during growth and curing in 2011 field. (B) Enantioselectivity of three nicotine demethylases based on *in vitro* enzyme assay. (C) Schematic diagram showing nicotine demethylases contribution on nicotine and nornicotine composition of converter leaf. When being synthesized (*-E4 -E5 -E10*) in root, EF_{nic} is 0.04. The small amount of nornicotine could be the leakage of *E4*, based on the nornicotine composition. Soon after synthesis, (R)-nicotine is selectively demethylated into (R)-nornicotine, resulting in 0.60 EF_{nic} from 0.04 EF_{nic} . Over three fourths of (R)-nicotine is selectively degraded in the root, and the rest is translocated to the leaf, where it is demethylated. *CYP82E4* expression is mainly in leaf, especially during senescence, and has little effect on the nicotine enantiomeric composition in root. Depending on *CYP82E4* expression, 0.04 to 0.60 EF_{nic} is accumulated in leaf.

The effects of *CYP82E5v2* and *CYP82E10* gene activity appeared to be dominant, rather than additive (Lewis et al., 2010). We suggest that this was due to the selectivity of these two enzymes based on *in vitro* assays. In this study, we have shown *CYP82E5v2* or *CYP82E10* alone could demethylate all (R)-nicotine by harvest time (Figure 4.4). Therefore, the limit of (R)-nicotine substrate and selectivity of the two demethylases are the reasons that *CYP82E5v2* and *CYP82E10* show a dominant effect. Substrate limitation may also be the reason why *CYP82E5v2* and *CYP82E10* are the minor demethylases in tobacco plants.

There is a change in the nicotine and nornicotine profile in tobacco over evolutionary time (Figure 4.11). Cultivated tobacco (*N. tabacum* L.) is an allotetraploid species derived from the hybridization of ancestral *N. tomentosiformis* and *N. sylvestris* (Clarkson et al., 2005). Both parents have high nicotine demethylating ability, so tobacco must also have high demethylating ability initially. However, few of tobacco lines used today have strong nicotine demethylating ability as in both parents. This change is proposed due to the selection for high nicotine content by humans (Chakrabarti et al., 2007). Because nornicotine is not desirable for smoking and harmful products may form from nornicotine, researchers are trying to reduce nornicotine through blocking the nicotine demethylation process (Lewis et al., 2008; Lewis et al., 2010). As the nicotine demethylase mutant trait is incorporated into commercial tobacco varieties (Li et al., 2011b), we will see another significant change in the nicotine and nornicotine composition, this time driven by selection for low nornicotine.

CYP82E10 was identified from root-specific cDNA libraries (Lewis et al., 2010), and not found during characterization of *CYP82E* genes expressed in leaf tissue (Siminszky et al., 2005; Gavilano et al., 2007; Xu et al., 2007a), suggesting *CYP82E10* expresses only in root. However, the graft *e4e5E10/ e4e5e10* in this study (Figure 4.9) clearly shows the functionality of *CYP82E10* in leaf.

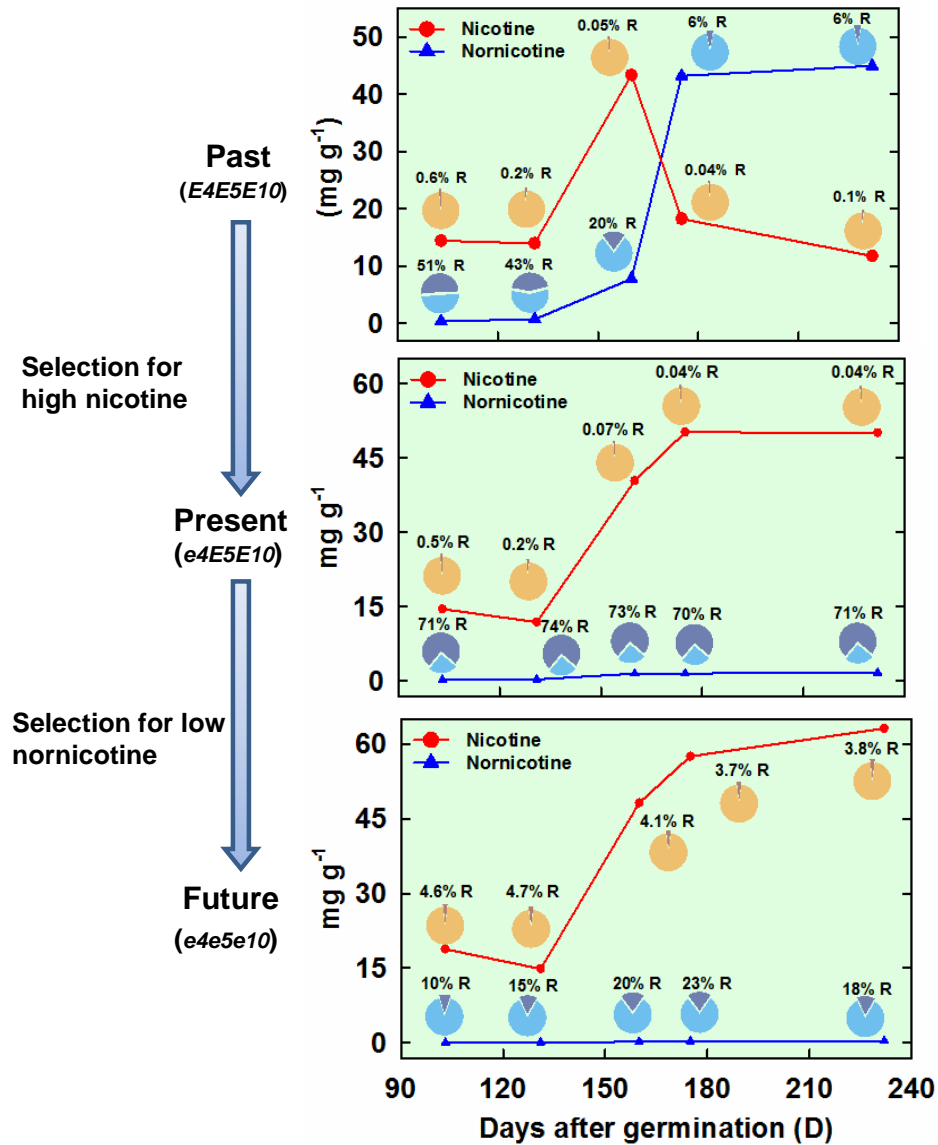


Figure 4.11. Evolution of nicotine and nornicotine enantiomeric composition in tobacco leaf, driven by human selections. All the results are from field tobacco leaf in 2011.

In this study, we also found that (R)-nornicotine accumulation increased dramatically in mutants with active CYP82E4 during the first two weeks of curing. Since *CYP82E4* expression reached maximum at that time period, and CYP82E4 can use a broad array of substrates (chapter 3) demonstrated *in vitro* assays, we propose that the (R)-nornicotine spike observed 2 weeks after harvest could come from nornicotine derivatives catalyzed by CYP82E4 through *N*-dealkylation reactions. The nornicotine derivatives could come

from (R)-nornicotine derivatization, or alternatively *de novo* biosynthesis. One piece of evidence to support this is that plants with active CYP82E5v2 or CYP82E10 have lower total R form of nicotine and nornicotine than that in *e4e5e10*, implying the (R)-nornicotine is further metabolized (Figure S4.2). Those metabolites of (R)-nornicotine could be the source which is converted back to (R)-nornicotine.

4.4. Conclusion

Enantioselectivity of three nicotine demethylases has been confirmed by investigating nicotine and nornicotine enantiomeric composition in mutant plants during growth and curing. Based on mutants and graft studies, enantioselectivity of three demethylases is enough to explain the discrepancies between nicotine and nornicotine enantiomeric composition in tobacco leaf. Nicotine consists of 4% of R form when being synthesized in root. Nicotine demethylases CYP82E5v2 and CYP82E10 selectively demethylate (R)-nicotine to (R)-nornicotine, resulting in 0.01 EF_{nic} and 0.75 EF_{nic} , while CYP82E4 decreases EF_{nic} due to the higher selectivity for (S)-nicotine than the other two demethylases. Most of (R)-nicotine is demethylated in root, and the rest is degraded in leaf. In leaf, CYP82E5v2 and CYP82E10 will still selectively use (R)-nicotine as in root, which keeps EF_{nic} high, but depending on CYP82E4 activity during senescence, 0.04 to 0.60 EF_{nic} will be produced. Although nicotine demethylases have no effect on accumulation of the other two main tobacco alkaloids, anabasine and anatabine, they change the alkaloid profiles in tobacco, due to the changes in nicotine and nornicotine levels.

4.5. MATERIALS AND METHODS

4.5.1. Plant materials

TN90LC is low demethylating line and widely used in commercial burley tobacco production. Burley tobacco breeding lines DH98-325-6 was used as parent for developing *CYP82E4*, *CYP82E5* and *CYP82E10* mutants. Development of these mutants is described previously (Lewis et al., 2010) and a scheme for their selection is in Figure S4.3.

4.5.2. Mutants grown in the field

To test nicotine demethylase selectivity, DH98-325-6 parent and seven mutants were grown in the field in North Carolina in 2010. To study the nicotine and nornicotine enantiomer accumulation, TN90LC, DH98-325-6 parent and seven mutants were grown at Spindletop Farm in Lexington (KY) in 2011. Each line or variety had 18 plants per replicate with four replicates. The arrangement of plants was in a randomized block design. The seedlings were grown in greenhouse at Spindletop Farm, and transplanted to the field (Google map location: 38.114925,-84.493119) on June 1st, 2011. Plants were sampled five times: one month after transplant (Jul. 5th), apical decapitation (Aug. 2rd), harvest (Aug. 31st), after 2 weeks of curing (Sep.15th) and cured (Nov.11st) (Figure S4.4). Plants were harvested and hung on a wagon in a curing barn to facilitate the sampling. Temperature and relative humidity were monitored during curing (Figure S4.5). Five middle leaf laminas (leaves without midrib) from five plants were sampled for each replicate per tobacco line and bulked. Some plants had been sampled at more than one sample time due to the shortage of plants. All the samples were oven-dried (55 °C), and ground to pass a 1 mm sieve for alkaloids and R/S enantiomer analysis.

4.5.3. Graft study

Tobacco lines used for grafting were: parent, three double mutants (*E4e5e10*, *e4E5e10* and *e4e5E10*) and triple mutant (*e4e5e10*). Tomato variety Rutgers was used for tomato/tobacco grafts (Jeffrey and Tso, 1964). Cleft grafting was used instead of approach grafting, which may cause the alkaloids contamination in the shoot. The grafts were shaded in high humidity environment for two weeks to recover. After four new leaves emerged, the plants were topped to induce nicotine production. Two tobacco leaves were sampled from each graft after two weeks of apical decapitation. One leaf was directly oven-dried, and the other was treated with ethephon for 2 days to induce nicotine demethylation before oven-drying. The roots were washed with water to remove potting medium, and then oven-dried.

4.5.4. Alkaloids quantification and separation of enantiomers of nicotine and nornicotine

Nicotine, nornicotine, anabasine and anatabine were quantitatively analyzed by gas chromatography (GC) (Perkin-Elmer Autosystem XL with Prevent TM) according to the 'LC-Protocol' (Jack and Bush, 2007). Alkaloids of ground tobacco samples were extracted by methyl tert-butyl alcohol (MTBE) and aqueous sodium hydroxide. The MTBE extracts was injected into GC, and quantification of alkaloids was against alkaloids standards.

Nicotine and nornicotine isomers were analyzed by chiral high-performance liquid chromatography (HPLC) (Mesnard et al., 2001). Ground tobacco leaves were extracted by MTBE and aqueous sodium hydroxide. Alkaloids from MTBE extract were dissolved into acid solution, and cleaned by MTBE wash to remove chlorophyll. The cleaned acid solution was neutralized by base and extract with MTBE. Nicotine and nornicotine from the MTBE extracts was purified by thin layer chromatography (TLC). Myosmine is the main metabolite of nornicotine and has no effects on enantiomer composition analysis of nicotine and nornicotine. TLC plates were TLC Silica Gel 60 F254 (EMD Chemicals Inc.). Purified nicotine was further separated into (R) and (S) form by HPLC (Perkin-Elmer series 200) using a Chiracel OD-H column (0.46 cm (D) × 25 cm) (Chiral Technologies Inc.), eluted with hexanes/ methanol (98:2, v/v) at 1.0 ml min⁻¹, with detection at 252 nm. Nornicotine was methylated to nicotine by incubating for 30 min with 50 µl formic acid and 100 µl formaldehyde at 110°C. Enantiomer fraction of nicotine or nornicotine ratio was calculated by peak area of the two isomers. Nicotine and nornicotine isomer amount was calculated based on total nornicotine amount and R/S ratio. Data were analyzed by Sigmaplot 12.

Enantiomer fraction (EF) (Harner et al., 2000): $EF = R \text{ enantiomer} / (R \text{ enantiomer} + S \text{ enantiomer})$

Supplemental Material

Table S4.1. Alkaloids concentrations of mutant cured leaf lamina from 2010 field trial.

Table S4.2. Nitrite and nitrate levels in mutant cured leaf lamina from 2011 field trial.

Table S4.3. Alkaloids concentration of self-grafted mutant tissues.

Table S4.4. Alkaloids concentration of tomato(scion)/ mutant(root) grafts tissues.

Table S4.5. Alkaloids concentration of mutant (scion)/ triple mutant (root) grafts tissues.

Figure S4.1. TSNAs level of mutants grown in the field in 2011.

Figure S4.2. Possible reason for the increase of (R)-nornicotine in tobacco with active CYP82E4 during the first two weeks of curing.

Figure S4.3. Selection of EMS-induced mutants in nicotine demethylase genes (Lewis et al., 2010).

Figure S4.4. Production cycle of tobacco in 2011.

Figure S4.5. Temperature and relative humidity during curing.

Chapter 5 Concluding remarks

5.1. Combining the activities of CYP82E4, CYP82E5v2 and CYP82E10 is enough to explain the enantiomeric discrepancy between nicotine and nornicotine

There are several possible reasons which can account for the discrepancy of enantiomeric composition between nicotine and nornicotine. In chapter 2, I demonstrated that nicotine enantioselective demethylation has an important role in the enantiomeric composition of nornicotine. In the following two chapters, I establish that *in vitro* and *in vivo* the combination of the three demethylases can produce the range of EF_{nic} measured in tobacco.

During the effort to study the enantioselective demethylation, other possible reasons could be inferred. In chapter 3, no racemization was found *in vitro* during demethylation. In chapter 4, the same nicotine enantiomeric composition was found in tomato leaf and tobacco root in tomato/ tobacco grafts, suggesting there is no enantioselective translocation of nicotine. In chapter 2, roots of different tobacco lines have similar nornicotine enantiomeric composition with their stalk, suggesting there is no enantioselective translocation of nornicotine. Therefore, translocation is unlikely a reason for the discrepancy. The roles of direct synthesis and enantiomeric degradation of nornicotine have not been explored in this study.

5.2. Lessons from enantioselective demethylation study

5.2.1 Nicotine composition

Leaf nicotine is reported to consist of only 0.002 EF_{nic} , and (S)-nicotine is equal to nicotine in most literature. In chapter 4, I measure EF_{nic} of 0.04 in triple mutants, suggesting the nicotine has much higher (R)-nicotine when biosynthesized in the root. The reason that only the (S)-form is found in the leaf is that (R)-nicotine is selectively demethylated soon after biosynthesis.

5.2.2. Demethylation location of nicotine enantiomers

Two nicotine enantiomers are demethylated in different tissues. Compared with nicotine enantiomeric composition in tomato/tobacco grafts (Chapter 4), over 75 % of (R)-nicotine is demethylated in root, while almost all (S)-nicotine is demethylated in leaf.

5.2.3. Lack of additive effects for CYP82E5v2 and CYP82E10

CYP82E5v2 and CYP82E10 are two minor nicotine demethylases in tobacco. Lewis (2011) reported lack of additive effects for these demethylases. In chapter 3, I establish that CYP82E5v2 and CYP82E10 have high selectivity for (R)-nicotine. In chapter 4, I demonstrate that CYP82E5v2 or CYP82E10 alone could use all the (R)-nicotine in tobacco. Therefore, it is the (R)-nicotine substrate limitation that causes the additive effect to be apparently missing.

5.2.4. Prediction of future changes of nicotine and nornicotine composition

From an evolutionary standpoint, modern tobacco initially accumulated nornicotine as main alkaloid based on the alkaloid composition of its two progenitors. It is believed due to the selection of high nicotine that resulted in the tobacco accumulating more nicotine. Due to the undesirable properties of nornicotine, researchers are trying to incorporate the demethylation mutant trait into tobacco commercial lines. Therefore, in the future the enantiomeric composition of nicotine and nornicotine in tobacco will change due to the present selection for lower nornicotine.

Appendix

Table S1.1. Pyridine alkaloids and its derivatives in tobacco plants (*Nicotiana L.*).

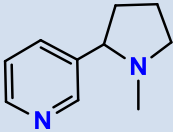
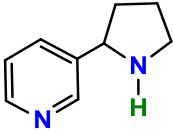
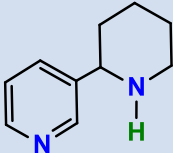
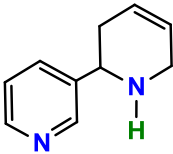
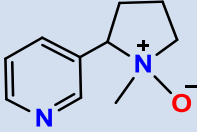
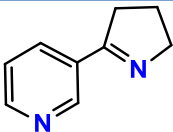
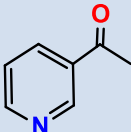
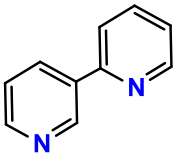
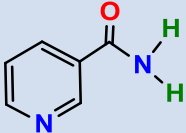
Name	CID*	Structure	Material	References
Nicotine	942		Leaf of <i>N. tabacum</i>	(Tso and Jeffrey, 1953)
Nornicotine	412		Leaf of <i>N. tabacum</i>	(Tso and Jeffrey, 1953)
Anabasine	2181		Leaf of <i>N. tabacum</i>	(Tso and Jeffrey, 1953)
Anatabine	261474		Leaf of <i>N. tabacum</i>	(Tso and Jeffrey, 1953)
Oxynicotine	409		Leaf of <i>N. tabacum</i>	(Tso and Jeffrey, 1953)
Myosmine	442649		Leaf of <i>N. tabacum</i>	(Tso and Jeffrey, 1953)
3-acetylpyridine	9589		Leaf of <i>N. tabacum</i>	(Tso and Jeffrey, 1953)
2, 3'-dipyridyl	11389		Leaf of <i>N. tabacum</i>	(Tso and Jeffrey, 1953)
Nicotinamide	936		Leaf of <i>N. tabacum</i>	(Tso and Jeffrey, 1953)

Table S.1.1 (continued)

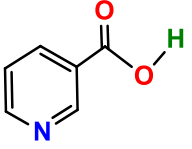
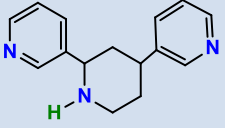
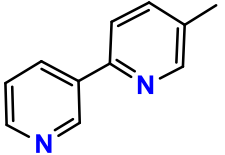
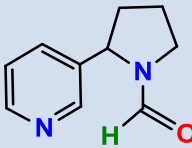
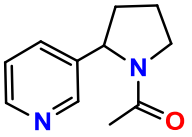
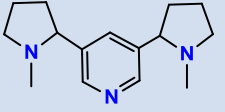
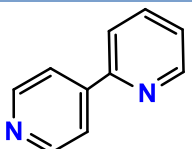
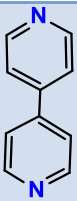
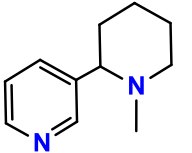
Name	CID*	Structure	Material	References
Nicotinic acid	938		Leaf of <i>N. tabacum</i>	(Tso and Jeffrey, 1953)
Anatalline	443848		Root of <i>N. tabacum</i>	(Kisaki et al., 1968)
5-methyl-2,3'-bipyridine	15543761		Leaf of <i>N. tabacum</i>	(Warfield et al., 1972)
N'-formylnornicotine	528369		Leaf of <i>N. tabacum</i>	(Warfield et al., 1972)
N'-acetylnornicotine	165384		Leaf of <i>N. tabacum</i>	(Warfield et al., 1972)
3,5-bis-(1-methyl-pyrrolidin-2-yl)-pyridine			Root of <i>N. tabacum</i>	(Wei et al., 2005)
2,4'-dipyridyl	68488		Leaf of <i>N. tabacum</i>	(Nyiredy et al., 1986)
4,4'-dipyridyl	11107		Leaf of <i>N. tabacum</i>	(Nyiredy et al., 1986)
N'-methylanabasine	29758		Leaf of <i>N. tabacum</i>	(Matsush et al., 1983)

Table S.1.1 (continued)

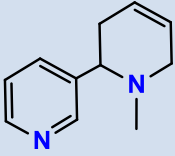
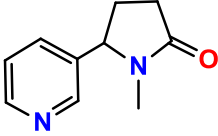
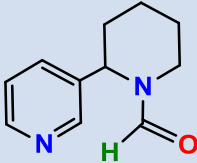
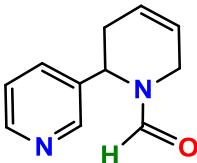
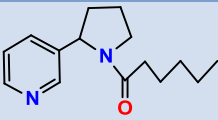
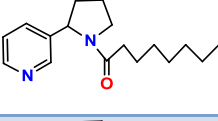
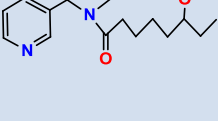
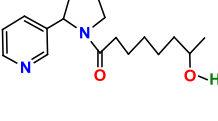
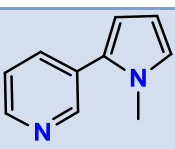
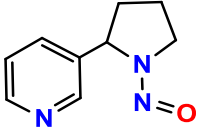
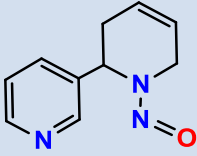
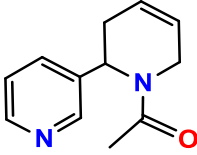
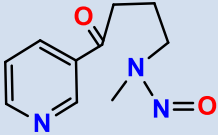
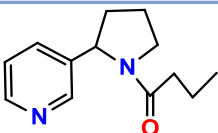
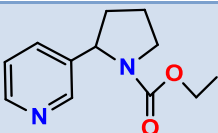
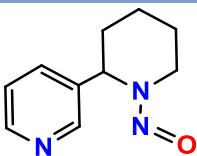
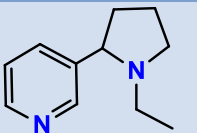
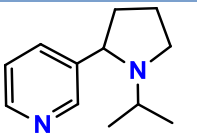
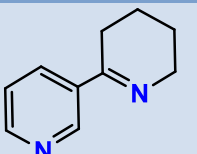
Name	CID*	Structure	Material	References
<i>N'</i>-methylanatabine	3904269		Leaf of <i>N. tabacum</i>	(Matsush et al., 1983)
Cotinine	408		Leaf of <i>N. tabacum</i>	(Matsush et al., 1983)
<i>N'</i>-formylanabasine	55250656		Leaf of <i>N. tabacum</i>	(Matsush et al., 1983)
<i>N'</i>-formylanatabine	528365		Leaf of <i>N. tabacum</i>	(Matsush et al., 1983)
<i>N'</i>-hexanoylnornicotine	528370		Leaf of <i>N. tabacum</i>	(Matsush et al., 1983)
<i>N'</i>-octanoylnornicotine	162334		Leaf of <i>N. tabacum</i>	(Matsush et al., 1983)
1'-(6-hydroxyoctanonyl)nornicotine			Leaf of <i>N. tabacum</i>	(Matsush et al., 1983)
1'-(7-hydroxyoctanonyl)nornicotine			Leaf of <i>N. tabacum</i>	(Matsush et al., 1983)
Nicotyrine	10249		Leaf of <i>N. tabacum</i>	(Matsush et al., 1983)
<i>N'</i>-nitrosonornicotine	27919		Leaf of <i>N. tabacum</i>	(Andersen et al., 1989)

Table S.1.1 (continued)

Name	CID*	Structure	Material	References
<i>N'</i>-nitrosoanatabine	528366		Leaf of <i>N. tabacum</i>	(Andersen et al., 1989)
<i>N'</i>-acetylanatabine	528364		Leaf of <i>N. tabacum</i>	(Andersen et al., 1989)
4-(<i>N</i>-methyl-<i>N</i>-nitrosamino)-1-(3-pyridyl)butanone	47289		Leaf of <i>N. tabacum</i>	(Andersen et al., 1989)
<i>N'</i>-butanoylnornicotine	528368		Leaf of <i>N. tabacum</i>	(Andersen et al., 1989)
<i>N'</i>-carboethoxynornicotine	2777155		Cell culture of <i>N. plumbaginifolia</i>	(Bartholomeusz et al., 2005a)
<i>N'</i>-nitrosoanabasine	14335		Leaf of <i>N. rustica</i> and <i>N. tabacum</i>	(Bhide et al., 1987)
<i>N'</i>-ethylnornicotine	4658388		Leaf of <i>N. tabacum</i>	(Braumann et al., 1990)
<i>N'</i>-isopropylnornicotine	21355371		Leaf of <i>N. tabacum</i>	(Leete, 1981)
Anabaseine	18985		Leaf of <i>N. tabacum</i>	(Kisaki and Tamaki, 1966)

* PubChem compound number “<http://pubchem.ncbi.nlm.nih.gov/>”

Table S1.2. *N'*-dealkylation in *Nicotiana* species, based on feeding assays.

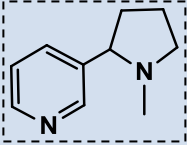
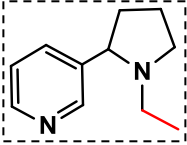
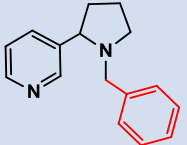
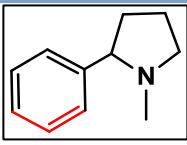
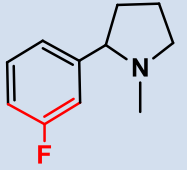
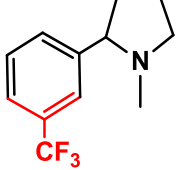
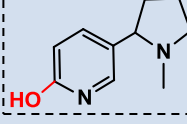
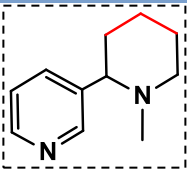
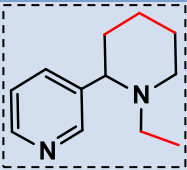
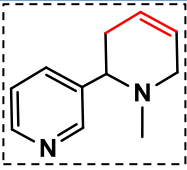
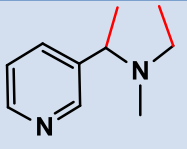
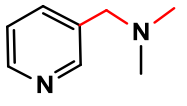
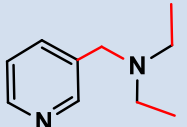
Substrate	Structure	Material	Reference
(<i>R,S</i>)-nicotine		Excised leaf of <i>N. glutinosa</i> [1] and <i>N. tabacum</i> [2], <i>N. plumbaginifolia</i> cell culture [3]	[1] (Dawson, 1951); [2] (Kisaki et al., 1978); [3] (Mesnard et al., 2001)
(<i>R,S</i>)-<i>N</i>-ethylnornicotine		Excised leaf of <i>N. glutinosa</i>	(Dawson, 1951)
2-(1-benzylpyrrolidin-3-yl)pyridine		Excised leaf of <i>N. tabacum</i>	(Kisaki et al., 1978)
(<i>R,S</i>)-1-methyl-2-phenylpyrrolidine*		<i>N. plumbaginifolia</i> cell culture	(Bartholomeusz et al., 2005b; Robins et al., 2007)
2-(3-fluorophenyl)-1-methylpyrrolidine		<i>N. plumbaginifolia</i> cell culture	(Robins et al., 2007)
1-methyl-2-(3-(trifluoromethyl)phenyl)pyrrolidine		<i>N. plumbaginifolia</i> cell culture	(Robins et al., 2007)
6-Hydroxynicotine		Excised leaf of <i>N. tabacum</i>	(Kisaki et al., 1978)

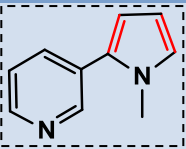
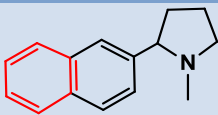
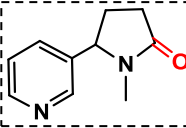

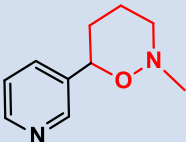
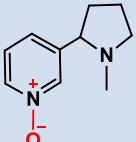
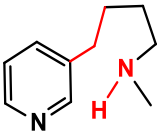
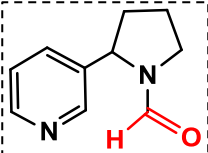
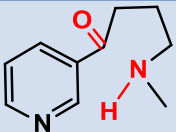
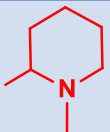
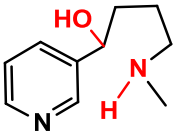
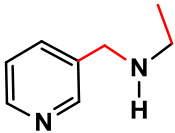
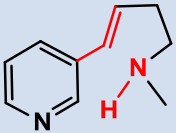
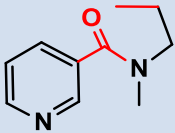
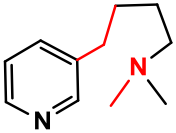
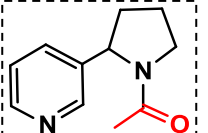
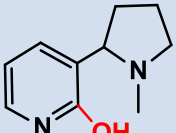
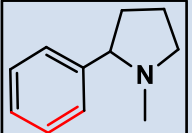
Table S.1.2 (continued)

Substrate	Structure	Material	Reference
(R,S)-N-methylanabasine		<i>N. plumbaginifolia</i> cell culture [1]; excised leaf of <i>N. glutinosa</i> [2]	[1] (Bartholomeusz et al., 2005b); [2] (Dawson, 1951)
(R,S)-N-ethylanabasine		Excised leaf of <i>N. glutinosa</i>	(Dawson, 1951)
(R,S)-N-methylanatabine		<i>N. plumbaginifolia</i> cell culture	(Bartholomeusz et al., 2005b)
N-ethyl-N-methyl-2-pyridin-3-yl-ethanamine		Excised leaf of <i>N. tabacum</i>	(Kisaki et al., 1978)
N,N-dimethyl-1-(pyridin-3-yl)methanamine		Excised leaf of <i>N. tabacum</i>	(Kisaki et al., 1978)
N,N-diethyl-1-(pyridin-3-yl)methanamine		Excised leaf of <i>N. tabacum</i>	(Kisaki et al., 1978)

*no product isolated in excised leaf (Kisaki et al., 1978).

Compounds with dashed border are found in tobacco.

Table S1.3. Compounds not *N'*-demethylated by excised leaves of *N. tabacum* (Kisaki et al., 1978).

Substrate	Structure	Substrate	Structure
Nicotyrine		1-methyl-2-(naphthalen-2-yl)pyrrolidine	
Cotinine		Dioxynicotine (102738)	
2-methyl-6-pyridin-3-ylloxazine (85906)		Nicotine N-oxide (17785)	
Dihydrometanicotine		<i>N'</i> -acetylnornicotine	
pseudooxynicotine		1,2-dimethylpiperidine	
4-(methylamino)-1-(pyridin-3-yl)butan-1-ol		N-(pyridin-3-ylmethyl)ethanamine (4716480)	
N-methyl-4-(pyridin-3-yl)but-3-en-1-amine		N-methyl-N-propylnicotinamide	
N,N-dimethyl-4-(pyridin-3-yl)butan-1-amine		<i>N'</i> -acetylnornicotine (528367)	
2-Hydroxynicotine		(<i>R,S</i>)-1-methyl-2-phenylpyrrolidine	

Note: Dashed border represent the present in tobacco.

Table S2.1. Alkaloids concentrations in different tissues of four tobacco lines. Data are average of four plants, and the numbers in parenthesis are standard deviation.

Treatment		Nic mg g ⁻¹	Nnic mg g ⁻¹	Anab mg g ⁻¹	Anat mg g ⁻¹	Dem %
DH98-325-6 RNAi #2-8	Top lamina	37.0 (6.7)	0.29 (0.10)	0.14 (0.03)	1.96 (0.33)	0.8 (0.1)
	Stalk	5.6 (0.5)	0.02 (0.01)	0.00 (0.01)	0.17 (0.02)	0.3 (0.1)
	Bottom lamina	41.3 (5.6)	0.33 (0.07)	0.15 (0.02)	2.20 (0.33)	0.8 (0.1)
	Root	7.9 (0.4)	0.06 (0.01)	0.04 (0.01)	0.28 (0.01)	0.7 (0.0)
L8	Top lamina	40.7 (7.2)	1.23 (0.23)	0.15 (0.03)	1.65 (0.27)	2.9 (0.1)
	Stalk	4.8 (1.8)	0.14 (0.03)	0.00 (0.01)	0.15 (0.04)	3.2 (1.4)
	Bottom lamina	47.2 (5.3)	1.48 (0.16)	0.16 (0.02)	1.84 (0.17)	3.1 (0.4)
	Root	6.7 (1.3)	0.25 (0.09)	0.05 (0.01)	0.34 (0.11)	3.5 (0.7)
TN90LC	Top lamina	35.5 (6.1)	1.11 (0.28)	0.13 (0.01)	1.82 (0.51)	3.0 (0.2)
	Stalk	7.2 (0.2)	0.16 (0.00)	0.02 (0.00)	0.25 (0.12)	2.2 (0.0)
	Bottom lamina	39.4 (6.8)	1.44 (0.44)	0.16 (0.01)	2.11 (0.28)	3.5 (0.5)
	Root	6.8 (1.2)	0.20 (0.04)	0.04 (0.00)	0.26 (0.00)	2.9 (0.0)
RM52	Top lamina	33.1 (3.1)	1.75 (0.15)	0.14 (0.01)	1.42 (0.16)	5.0 (0.2)
	Stalk	5.7 (0.7)	0.15 (0.03)	0.00 (0.01)	0.21 (0.05)	2.5 (0.2)
	Bottom lamina	24.1 (1.6)	9.92 (2.01)	0.15 (0.01)	2.37 (0.29)	29.1 (5.3)
	Root	7.8 (1.9)	0.44 (0.11)	0.07 (0.02)	0.59 (0.15)	5.3 (0.4)

Note: Nic: nicotine; Nnic: nornicotine; Anab: anabasine; Anat: anatabine; Dem: Demethylation.

Table S2.2. Alkaloids concentrations in ethephon-treated tobacco. Data are average of two replicates.

Treatment		Nic	Nnic	Anab	Anat	Dem
		mg g ⁻¹	mg g ⁻¹	mg g ⁻¹	mg g ⁻¹	%
Freeze-dried leaf	DH98-325-6 RNAi#2-8	28.9	0.18	0.10	1.17	0.7
	DH98-325-5	17.2	0.50	0.06	0.78	2.9
	DH98-325-6	22.6	1.24	0.09	0.93	5.2
Ethylene-treated leaf	DH98-325-6 RNAi#2-8	36.1	0.22	0.13	1.47	0.6
	DH98-325-5	19.0	0.92	0.07	0.84	6.0
	DH98-325-6	11.7	13.90	0.10	1.08	54.3
Root	DH98-325-6 RNAi#2-8	5.2	0.08	0.05	0.39	1.5
	DH98-325-5	6.6	0.22	0.07	0.68	3.4
	DH98-325-6	5.4	0.31	0.08	0.52	5.3

Note: Nic: nicotine; Nnic: nornicotine; Anab: anabasine; Anat: anatabine; Dem: Demethylation.

Table S2.3. Alkaloids concentrations in *e4* mutants. Data are single replicate.

Treatment	Mutation	Nic	Nnic	Anab	Anat	Dem
		mg g ⁻¹	mg g ⁻¹	mg g ⁻¹	mg g ⁻¹	%
TN90LC		32.1	1.10	0.17	1.38	3.4
DH98-325-6 (parent, P)		9.3	22.77	0.17	1.51	71.2
<i>e4</i> #1	G986A	22.8	0.70	0.10	0.81	3.1
<i>e4</i> #2	C1372T	22.7	0.90	0.13	0.97	4.0
<i>e4</i> #3	G1375A	26.9	1.12	0.18	1.63	4.1
<i>e4</i> #4	G1092T	21.1	1.19	0.15	0.91	5.2
<i>e4</i> #4x P; F1		19.1	5.97	0.14	1.06	23.7
<i>e4</i> #5	G886A	23.1	7.84	0.12	1.29	25.2
<i>e4</i> #1x P; F1		16.3	8.22	0.12	1.03	32.9
<i>e4</i> #2x P; F1		17.1	9.54	0.10	0.84	38.7
<i>e4</i> #3x P; F1		19.0	14.35	0.20	1.81	43.8
<i>e4</i> #6	C1280T	8.5	20.55	0.14	1.32	70.7
<i>e4</i> #7	G601A	9.8	25.90	0.16	1.28	72.5
<i>e4</i> #8	C113T	5.0	17.56	0.14	1.37	77.5
<i>e4</i> #9	G511A	3.9	22.82	0.12	1.10	85.8

Note: Nic: nicotine; Nnic: normicotine; Anab: anabasine; Anat: anatabine; Dem: Demethylation.

Table S2.4. Alkaloids concentrations in RNAi plants. Data are single replicate.

Treatment	Nic	Nnic	Anab	Anat	Dem
	mg g ⁻¹	mg g ⁻¹	mg g ⁻¹	mg g ⁻¹	%
TN90H (high converter)	6.7	26.33	0.21	1.92	79.8
TN90L (low converter)	31.4	0.81	0.13	0.99	2.5
L8L (low converter)	39.7	1.10	0.21	1.48	2.7
DH98-325-5 (Non-Converter)	41.8	0.90	0.17	1.31	2.1
DH98-325-5 RNAi #1-1	41.3	1.19	0.19	1.42	2.8
DH98-325-5 RNAi #2-1	50.3	0.33	0.23	1.55	0.6
DH98-325-5 RNAi #1-2	40.7	0.31	0.17	1.31	0.8
DH98-325-5 RNAi #3-1	40.5	0.38	0.21	1.42	0.9
DH98-325-5 RNAi #1-3	37.4	0.31	0.16	1.20	0.8
DH98-325-5 RNAi #1-4	48.9	0.42	0.27	1.79	0.8
DH98-325-5 RNAi #1-5	41.6	2.44	0.19	1.44	5.5
DH98-325-6 (Converter)	8.8	39.80	0.27	2.31	81.9
DH98-325-6 RNAi #1-1	24.8	11.00	0.21	1.66	30.7
DH98-325-6 RNAi #2-1	29.2	4.33	0.17	1.25	12.9
DH98-325-6 RNAi #2-2	35.6	2.97	0.16	1.10	7.7
DH98-325-6 RNAi #1-2	42.4	0.46	0.19	1.47	1.1
DH98-325-6 RNAi #2-3	30.7	3.31	0.14	0.89	9.7
DH98-325-6 RNAi #1-3	46.7	0.33	0.20	1.50	0.7
DH98-325-6 RNAi #2-4	43.8	0.49	0.20	1.39	1.1
DH98-325-6 RNAi #2-5	39.9	2.45	0.19	1.35	5.8
DH98-325-6 RNAi #2-6	37.2	0.34	0.18	1.19	0.9
DH98-325-6 RNAi #2-7	39.2	0.75	0.18	1.22	1.9
DH98-325-6 RNAi #2-8	45.1	0.44	0.21	1.41	1.0
DH98-325-6 RNAi #2-9	44.0	1.55	0.21	1.45	3.4
DH98-325-6 RNAi #3-1	33.4	0.71	0.16	1.17	2.1
DH98-325-6 RNAi #3-2	33.8	0.60	0.18	1.22	1.7

Note: Nic: nicotine; Nnic: normicotine; Anab: anabasine; Anat: anatabine; Dem: Demethylation.

Table S3.1. Comparison of Michaelis-Menten constants with literatures.

		This study		Report	References
		R	S	RS	
CYP82E4	K_m	1.90 ± 0.36	2.76 ± 0.65	3.9*	(Xu et al., 2007a)
	V_{max}	0.55 ± 0.02	0.17 ± 0.01	0.54*	
CYP82E5v2	K_m	3.02 ± 1.27	2.3 ± 2.37	5.6 ± 1.4	(Gavilano and Siminszky, 2007)
	V_{max}	0.04 ± 0.004	0.003 ± 0.0007	0.7 ± 0.02	
CYP82E10	K_m	0.78 ± 0.24	3.70 ± 5.22	3.9	(Lewis et al., 2010)
	V_{max}	0.12 ± 0.01	0.001 ± 0.002		

Note: Units for K_m: μM; units for V_{max}: nmol min⁻¹ mg⁻¹ protein.

*Results are from leaf microsome of high expressed CYP82E4.

Table S3.2. Evolution of nicotine demethylases in *N. tabacum* L.

Demethylase	Originality	Function	References
<i>CYP82E2</i>	<i>N. sylvestris</i>	Inactive, E375K and W422 mutations	(Chakrabarti et al., 2007)
<i>CYP82E3</i>	<i>N. tomentosiformis</i>	Inactive, W330C	(Gavilano et al., 2007)
<i>CYP82E4</i>	<i>N. tomentosiformis</i>	Active, Unstable mutation	(Gavilano et al., 2007)
<i>CYP82E5v2</i>	<i>N. tomentosiformis</i>	Active	(Gavilano and Siminszky, 2007)
<i>CYP82E10</i>	<i>N. sylvestris</i>	Active	(Lewis et al., 2010)

Table S4.1. Alkaloid concentrations of mutant cured leaf lamina from 2010 field trial. Data are average of three replicates, and the numbers in parenthesis are standard deviation.

Treatment	Nic mg g⁻¹	Nnic mg g⁻¹	Anab mg g⁻¹	Anat mg g⁻¹	Dem %
Parent	16.2 (3.5)	24.80 (2.28)	0.22 (0.01)	1.67 (0.10)	60.8 (3.2)
<i>e4E5E10</i>	29.7 (7.7)	0.88 (0.22)	0.13 (0.03)	1.00 (0.18)	2.9 (0.1)
<i>E4e5E10</i>	11.5 (1.7)	20.86 (2.35)	0.18 (0.01)	1.46 (0.13)	64.4 (5.6)
<i>E4E5e10</i>	15.0 (2.1)	19.30 (4.00)	0.15 (0.03)	1.35 (0.48)	56.0 (1.6)
<i>e4e5E10</i>	31.7 (2.5)	0.90 (0.11)	0.18 (0.03)	1.57 (0.23)	2.7 (0.1)
<i>e4E5e10</i>	37.6 (3.8)	0.95 (0.11)	0.15 (0.03)	1.22 (0.31)	2.5 (0.0)
<i>E4e5e10</i>	14.0 (0.5)	18.34 (1.95)	0.15 (0.01)	0.89 (0.13)	56.6 (3.5)
<i>e4e5e10</i>	44.2 (1.2)	0.48 (0.04)	0.17 (0.01)	1.32 (0.26)	1.1 (0.1)

Note: Nic: nicotine; Nnic: nornicotine; Anab: anabasine; Anat: anatabine; Dem: Demethylation.

Table S4.2. Nitrite and nitrate levels in mutant cured leaf lamina from 2011 field trial. Data are average of four replicates, and the numbers in parenthesis are standard deviation.

Treatment	[NO₂]⁻N µg/g	[NO₃]⁻N µg/g	Total N %
TN90LC	2.7 (0.6)	878 (250)	4.0 (0.1)
Parent	2.4 (0.2)	1182 (748)	4.0 (0.3)
<i>e4E5E10</i>	3.0 (0.6)	3389(1243)	4.5 (0.2)
<i>E4e5E10</i>	2.8 (0.4)	2075 (956)	4.5 (0.2)
<i>E4E5e10</i>	2.6 (0.2)	1510 (335)	4.7 (0.3)
<i>e4e5E10</i>	2.8 (0.4)	1002 (725)	4.1 (0.6)
<i>e4E5e10</i>	3.6 (0.9)	2617 (826)	4.7 (0.5)
<i>E4e5e10</i>	2.7 (0.3)	1755 (581)	4.6 (0.3)
<i>e4e5e10</i>	2.9 (0.1)	2679(1090)	4.6 (0.1)

Table S4.3. Alkaloids concentration of self-grafted mutant tissues. Data are average of three replicates, and the numbers in parenthesis are standard deviation.

Treatment		Nic mg g ⁻¹	Nnic mg g ⁻¹	Anab mg g ⁻¹	Anat mg g ⁻¹	Dem %
Green leaf lamina	<i>E4E5E10</i>	12.1 (5.2)	4.25 (0.85)	0.03 (0.00)	0.67 (0.25)	28.4(13.6)
	<i>e4e5E10</i>	28.0(17.0)	0.48 (0.29)	0.05 (0.03)	1.11 (0.42)	1.7 (0.1)
	<i>e4E5e10</i>	18.8 (5.3)	0.36 (0.08)	0.02 (0.00)	0.44 (0.07)	1.9 (0.1)
	<i>E4e5e10</i>	19.8 (2.1)	2.39 (1.32)	0.03 (0.00)	0.48 (0.07)	10.8 (6.3)
	<i>e4e5e10</i>	18.9 (9.8)	0.08 (0.04)	0.02 (0.01)	0.26 (0.17)	0.4 (0.0)
Ethephon treated leaf lamina	<i>E4E5E10</i>	0.5 (0.4)	17.68 (5.03)	0.04 (0.01)	0.98 (0.42)	97.8 (1.7)
	<i>e4e5E10</i>	42.2 (8.9)	0.85 (0.08)	0.08 (0.01)	1.75 (0.22)	2.0 (0.4)
	<i>e4E5e10</i>	27.2 (8.4)	0.64 (0.18)	0.03 (0.01)	0.67 (0.15)	2.3 (0.1)
	<i>E4e5e10</i>	2.0 (2.0)	20.38 (5.77)	0.04 (0.01)	0.70 (0.21)	90.3(10.7)
	<i>e4e5e10</i>	25.7(11.7)	0.26 (0.03)	0.02 (0.02)	0.37 (0.22)	1.1 (0.4)
Root	<i>E4E5E10</i>	3.6 (0.2)	0.20 (0.07)	0.03 (0.01)	0.35 (0.03)	5.3 (1.6)
	<i>e4e5E10</i>	5.0 (2.5)	0.11 (0.04)	0.03 (0.02)	0.48 (0.32)	2.2 (0.3)
	<i>e4E5e10</i>	4.7 (1.8)	0.18 (0.10)	0.02 (0.01)	0.23 (0.06)	3.6 (0.7)
	<i>E4e5e10</i>	4.2 (0.5)	0.20 (0.06)	0.02 (0.01)	0.21 (0.01)	4.6 (1.8)
	<i>e4e5e10</i>	5.1 (0.0)	0.03 (0.00)	0.02 (0.00)	0.17 (0.06)	0.7 (0.1)

Note: Nic: nicotine; Nnic: nornicotine; Anab: anabasine; Anat: anatabine; Dem: Demethylation.

Table S4.4. Alkaloids concentration of tomato(scion)/ mutant(root) grafts tissues.
Data are average of three replicates, and the numbers in parenthesis are standard deviation.

Treatment		Nic mg g ⁻¹	Nnic mg g ⁻¹	Anab mg g ⁻¹	Anat mg g ⁻¹	Dem %
Green leaf lamina	Tom/E4E5E10	18.2 (5.1)	0.40 (0.09)	0.02 (0.00)	0.44 (0.08)	2.2 (0.2)
	Tom/e4e5E10	10.1 (1.4)	0.23 (0.02)	0.02 (0.00)	0.44 (0.06)	2.3 (0.2)
	Tom/e4E5e10	12.8 (3.5)	0.26 (0.11)	0.01 (0.01)	0.30 (0.01)	1.9 (0.4)
	Tom/E4e5e10	19.1 (7.3)	0.27 (0.07)	0.01 (0.01)	0.18 (0.08)	1.4 (0.3)
	Tom/e4e5e10	16.0(11.1)	0.20 (0.09)	0.01 (0.01)	0.17 (0.11)	1.4 (0.5)
Root	Tom/E4E5E10	4.0 (0.4)	0.34 (0.08)	0.02 (0.00)	0.33 (0.05)	7.7 (1.1)
	Tom/e4e5E10	4.3 (0.8)	0.09 (0.02)	0.02 (0.00)	0.43 (0.09)	2.1 (0.2)
	Tom/e4E5e10	3.2 (0.3)	0.19 (0.05)	0.01 (0.00)	0.15 (0.01)	5.5 (1.0)
	Tom/E4e5e10	3.9 (0.4)	0.11 (0.02)	0.02 (0.01)	0.19 (0.10)	2.7 (0.5)
	Tom/e4e5e10	2.8 (1.0)	0.02 (0.01)	0.01 (0.01)	0.12 (0.05)	0.7 (0.2)

Note: Nic: nicotine; Nnic: nornicotine; Anab: anabasine; Anat: anatabine; Dem: Demethylation.

Table S4.5. Alkaloids concentration of mutant (scion)/ triple mutant (root) grafts tissues. Data are average of two replicates, and the numbers in parenthesis are standard deviation.

Treatment		Nic mg g ⁻¹	Nnic mg g ⁻¹	Anab mg g ⁻¹	Anat mg g ⁻¹	Dem %
Green leaf lamina	<i>E4E5E10/e4e5e10</i>	19.2 (6.6)	3.28 (2.21)	0.03 (0.00)	0.50 (0.00)	13.7 (4.5)
	<i>e4e5E10/e4e5e10</i>	27.5 (4.5)	0.58 (0.07)	0.03 (0.00)	0.55 (0.06)	2.1 (0.1)
	<i>e4E5e10/e4e5e10</i>	21.6(11.5)	0.48 (0.19)	0.02 (0.01)	0.38 (0.20)	2.3 (0.4)
	<i>E4e5e10/e4e5e10</i>	21.0 (4.8)	3.67 (0.60)	0.03 (0.01)	0.43 (0.15)	15.0 (0.9)
Ethephon treated leaf lamina	<i>E4E5E10/e4e5e10</i>	1.3 (1.3)	20.20 (8.03)	0.05 (0.01)	0.71 (0.03)	94.9 (3.6)
	<i>e4e5E10/e4e5e10</i>	33.6 (4.7)	0.84 (0.08)	0.04 (0.00)	0.67 (0.02)	2.5 (0.6)
	<i>e4E5e10/e4e5e10</i>	26.2(13.0)	0.57 (0.18)	0.03 (0.02)	0.48 (0.27)	2.2 (0.5)
	<i>E4e5e10/e4e5e10</i>	4.7 (0.6)	22.38 (2.44)	0.04 (0.01)	0.61 (0.15)	82.7 (0.4)
Root	<i>E4E5E10/e4e5e10</i>	4.5 (2.5)	0.03 (0.02)	0.04 (0.02)	0.32 (0.11)	0.7 (0.1)
	<i>e4e5E10/e4e5e10</i>	5.2 (0.6)	0.03 (0.00)	0.02 (0.00)	0.23 (0.04)	0.6 (0.0)
	<i>e4E5e10/e4e5e10</i>	4.1 (0.8)	0.02 (0.00)	0.01 (0.00)	0.16 (0.02)	0.6 (0.1)
	<i>E4e5e10/e4e5e10</i>	4.5 (1.9)	0.03 (0.01)	0.03 (0.01)	0.21 (0.06)	0.7 (0.1)

Note: Nic: nicotine; Nnic: nornicotine; Anab: anabasine; Anat: anatabine; Dem: Demethylation.

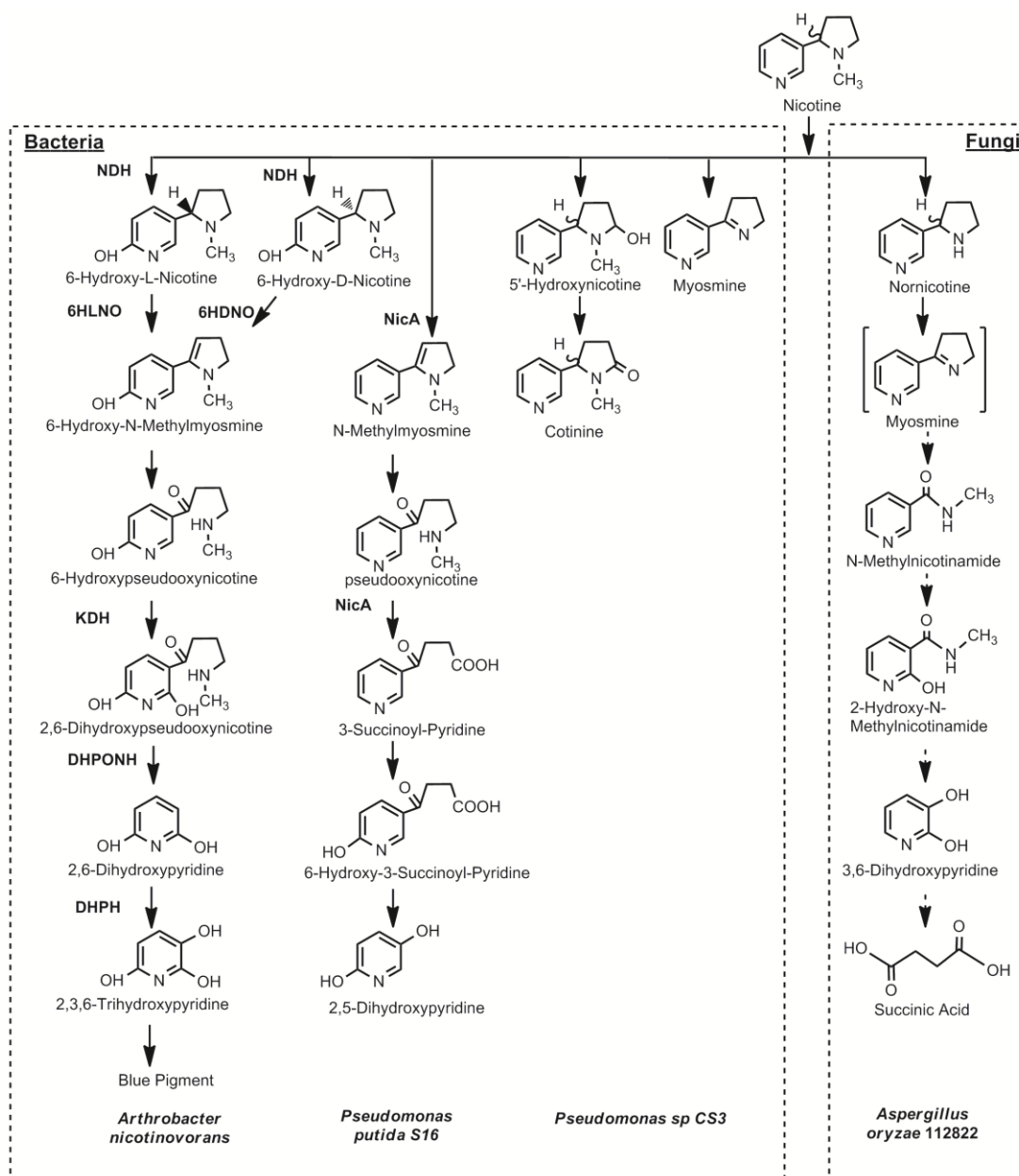


Figure S1.1. Nicotine degradation in bacteria and fungi. *Arthrobacter nicotinovorans* (Brandsch, 2006), *Pseudomonas putida S16* (Tang et al., 2009), *Pseudomonas sp CS3* (Wang et al., 2012), *Aspergillus oryzae 112822* (Meng et al., 2010). Enzymes listed: NDH: nicotine dehydrogenase; 6HLNO and 6HDNO: 6-hydroxy-L- and 6-hydroxy-D-nicotine oxidases; KDH: ketone dehydrogenase; DHPONH: 2, 6-dihydroxypseudooxynicotine hydrolase. Compounds in bracket were postulated by referring to published reports.

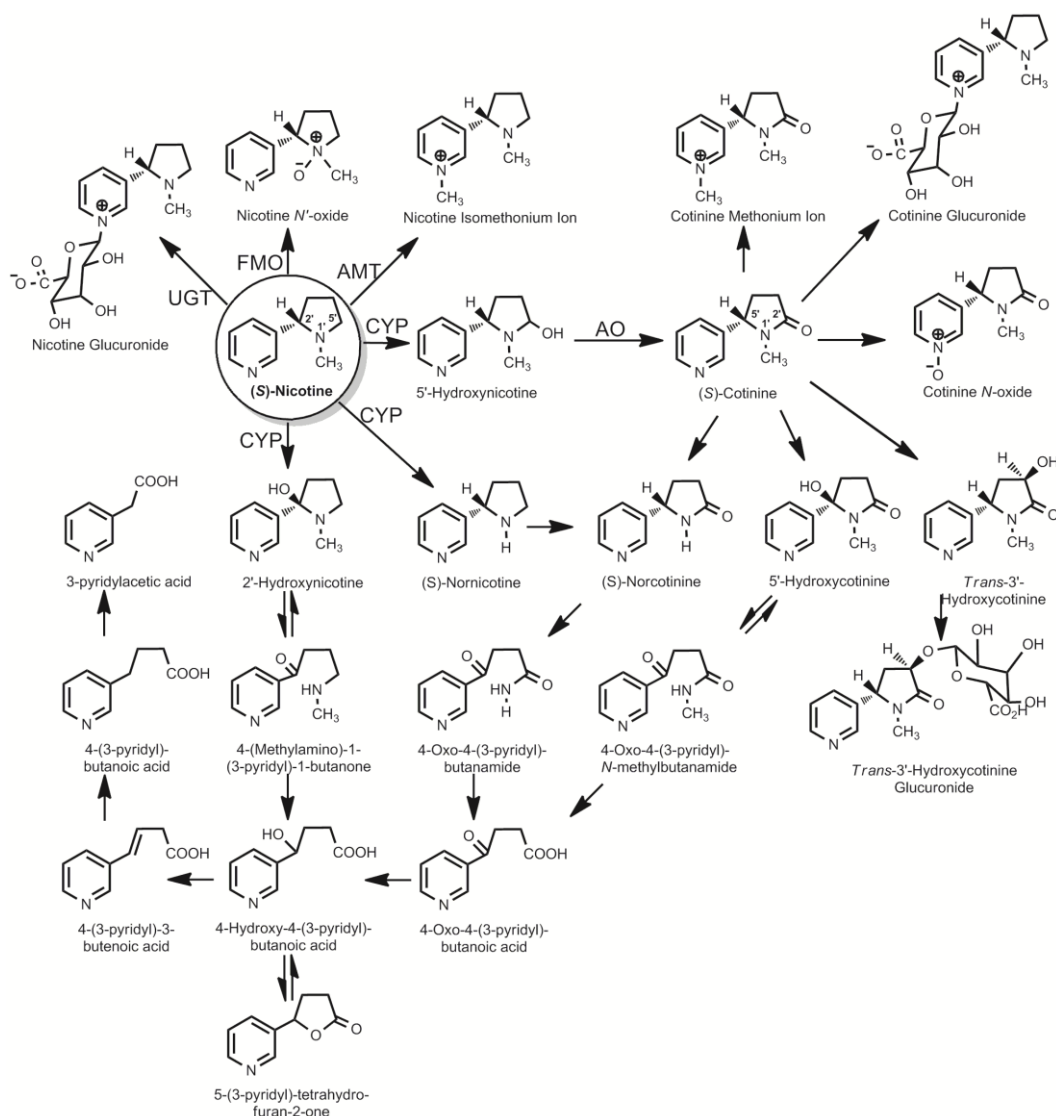


Figure S1.2. Nicotine degradation in human based on urinary metabolites (Hukkanen et al., 2005). Enzymes listed: CYP: cytochrome P450 enzymes; AO: aldehyde oxidase; FMO: Flavin-containing monooxygenase; AMT: amine N-methyltransferase; UGT: UDP-glucuronosyltransferase. Detailed primary routes of CYP catalyzed nicotine metabolism can be found in previous papers (Dicke et al., 2005; Pogocki et al., 2007)

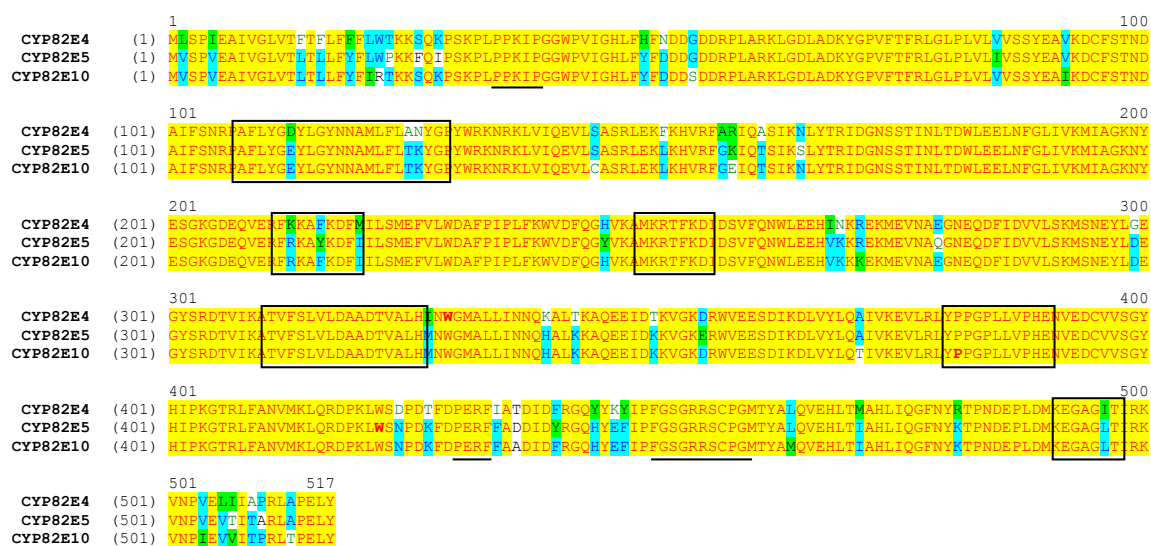


Figure S1.3. Alignment of the CYP82E4, CYP82E5 and CYP82E10 predicted protein sequences. Domains predicted to be involved in substrate recognition are boxed. Sequences that are highly conserved in a diversity of plant P450 enzymes are underlined (Xu et al., 2007a).

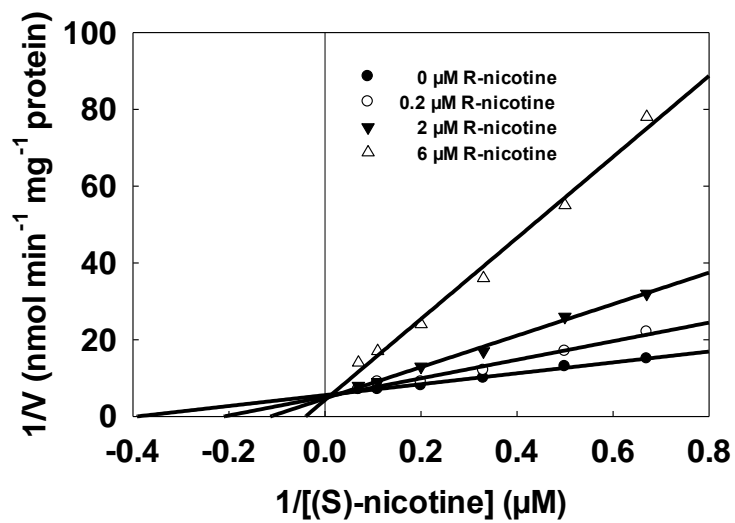


Figure S3.1. Competitive inhibition of CYP82E4-catalyzed (S)-nicotine demethylation by (R)-nicotine shown in Lineweaver-Burk plot. R^2 for all four fitted lines are over 0.97.

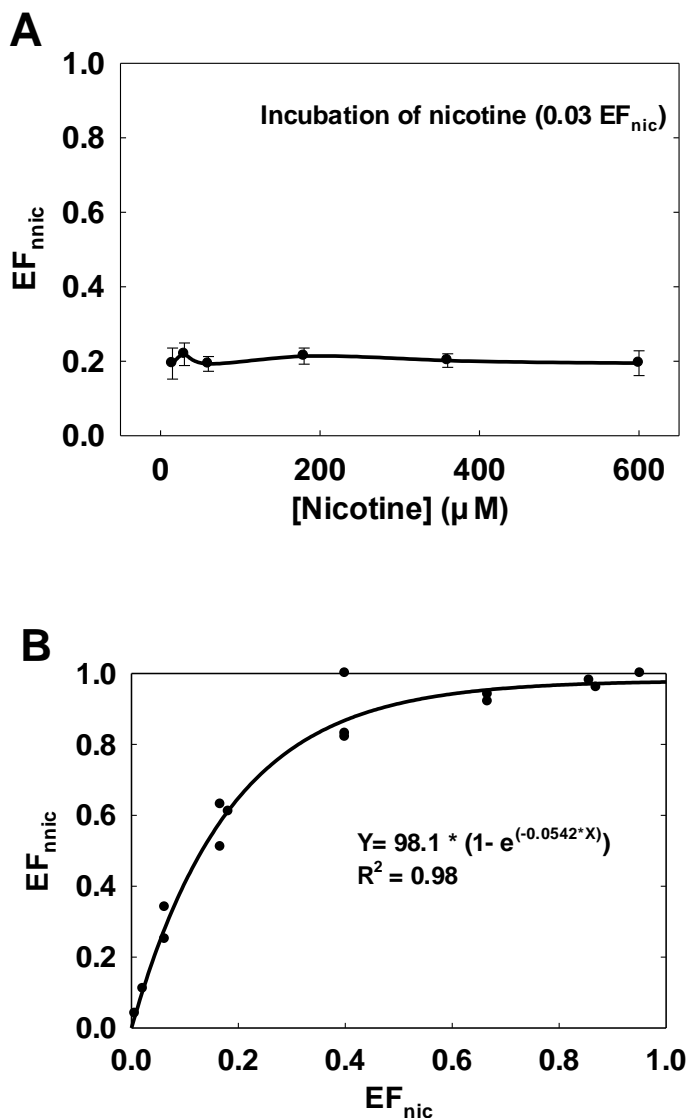


Figure S3.2. Inability of CYP82E4 to generate leaf nornicotine enantiomeric composition *in vitro*. (A) CYP82E4 produces stable EF_{nnic} from varying concentration of nicotine substrate (0.03 EF_{nic}). (B) EF_{nnic} produced from different nicotine enantiomeric compositions by recombinant CYP82E4 *in vitro*. Data points in (A) are the average of three independent assays, and the bars represent the standard deviation. In (B), the nicotine mixtures were prepared with 0.2 μM , 2 μM and 6 μM of (R)-nicotine in combination with 0.3 μM , 1 μM , 3 μM , 9 μM and 30 μM of (S)-nicotine to cover the substrate range. The results were fit into Exponential Rise to Maximum Equation by Sigmaplot 12.

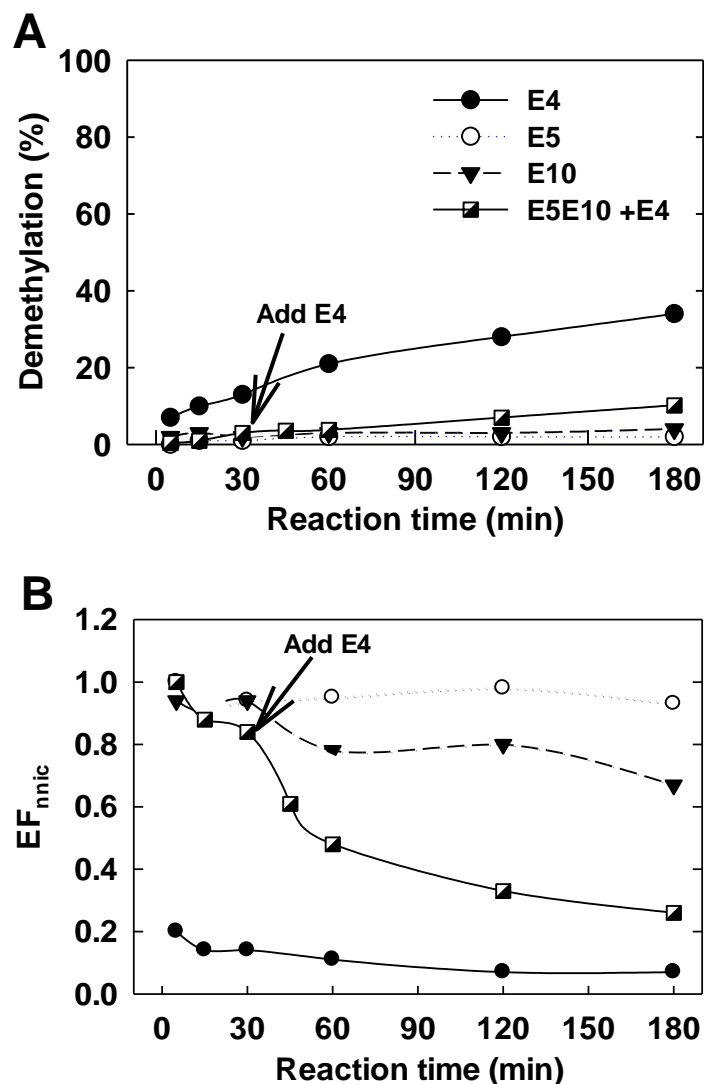


Figure S3.3. Time course of the demethylation of 10 μM nicotine ($0.03 \text{ EF}_{\text{nic}}$) incubated with CYP82E4, CYP82E5v2 or CYP82E10 separately, or all together as measured as demethylation (A) or nornicotine composition (B). For collective incubation, same amount of E5 and E10 were mixed and incubated with substrate, and at 30 min equal amount of E4 was added into mixture for incubation. Total protein in single and collective enzyme incubation are same. Each data are average of two independent assays.

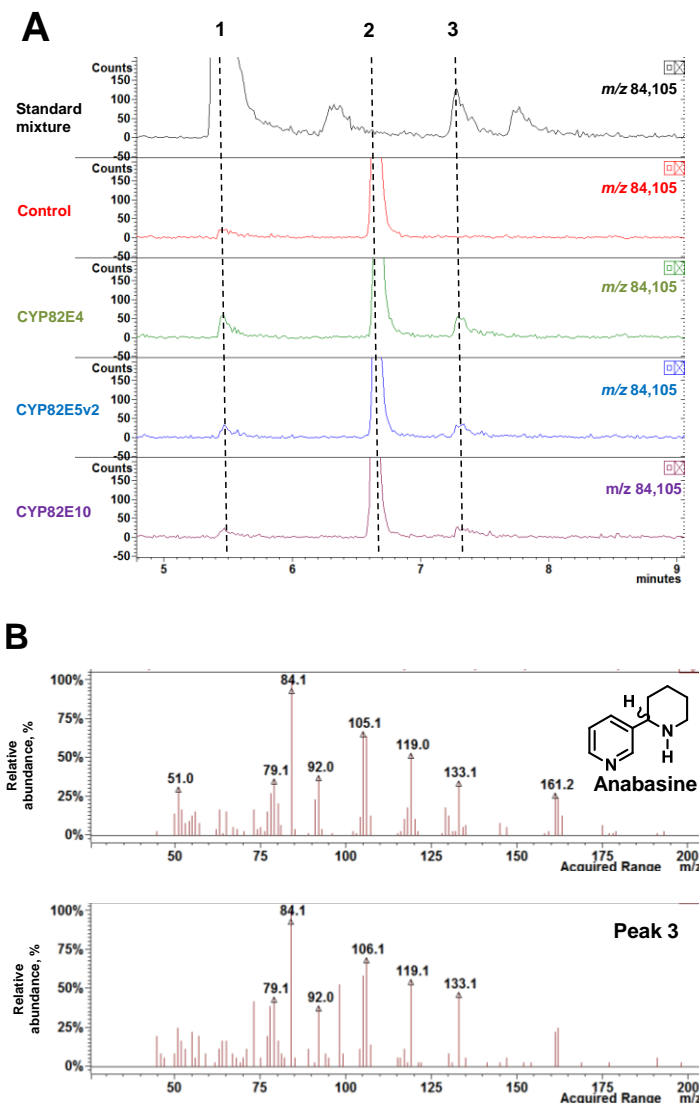


Figure S3.4. Anabasine was identified in the incubations of methylanabasine with CYP82E4, CYP82E5v2 and CYP82E10 *in vitro*. Microsomes were isolated from yeast not expressing any introduced P450s or the indicated tobacco genes, and incubated with methylanabasine. The reaction mixtures were extracted and analyzed by GC-MS. (A) Extracted GC-MS chromatographs of incubations of methylanabasine with CYP82E4, CYP82E5v2 and CYP82E10 *in vitro*. Peak 1: quinoline (internal standard); peak 2: methylanabasine; peak 3: anabasine. (B) The identity of anabasine (peak 3) is confirmed by mass spectrum.

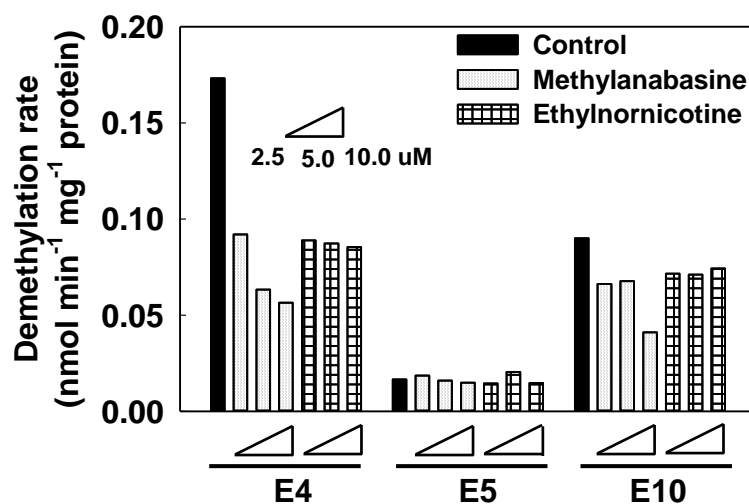


Figure S3.5. Nicotine demethylation inhibited by methylanabasine and *N'*-ethylnornicotine catalyzed by CYP82E4, CYP82E5v2 and CYP82E10. 10 μM racemic nicotine was incubated with CYP82E4, CYP82E5v2 and CYP82E10, respectively, and 2.5 μM, 5 μM and 10 μM of methylanabasine or ethylnornicotine was added to the reaction mixture. Each bar is the average of two independent assays.

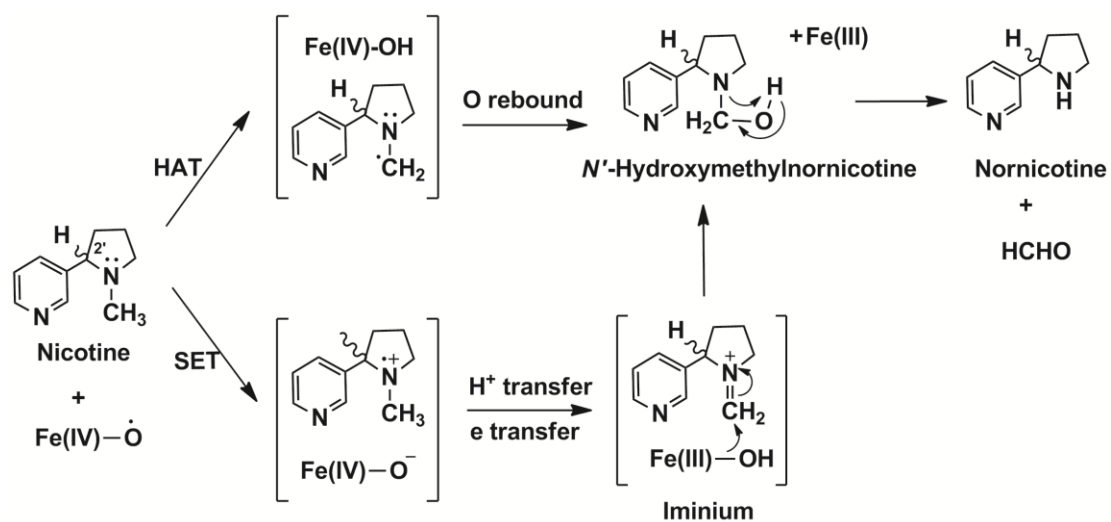


Figure S3.6. Two possible mechanisms in *N*-demethylation of nicotine catalyzed by cytochrome P450 enzymes (Meunier et al., 2004): hydrogen atom transfer (HAT) versus single electron transfer (SET). Presumably (R)-nicotine is demethylated into (R)-nornicotine, and (S)-nicotine is converted into (S)-nornicotine. Note the hydrogen atom at the 2'-C position is not involved in either mechanism.

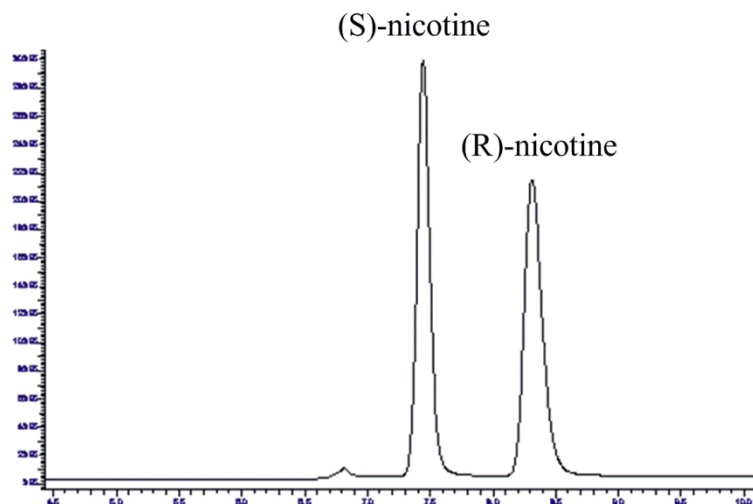


Figure S3.7. Racemic nicotine separation by chiral HPLC. Retention time for (S)-nicotine was 7.45 min and for (R)-nicotine was 8.31 min. Nornicotine was chemically methylated back to nicotine and separated by this method.

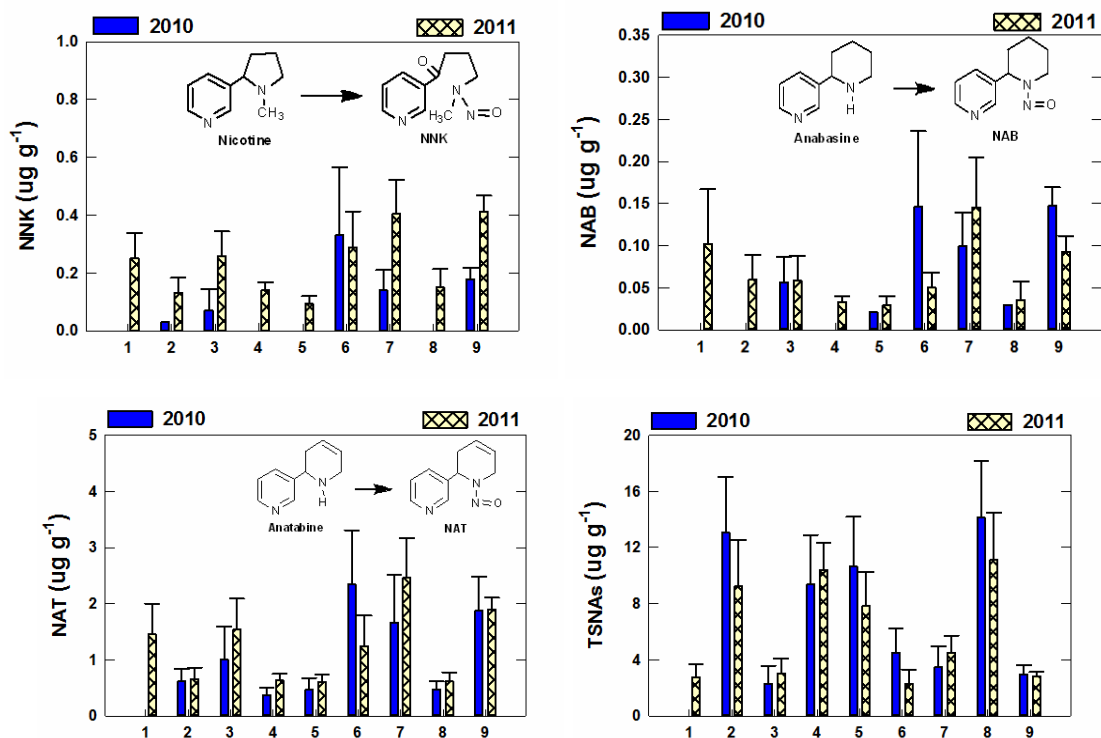


Figure S4.1. TSNA level of mutants grown in the field in 2010 and 2011. 1: TN90LC (2011 data only); 2: Parent; 3: e4E5E10; 4: E4e5E10; 5: E4E5e10; 6: e4e5E10; 7: e4E5e10; 8: E4e5e10; 9: e4e5e10. Each data is the average of three (2010) or four (2011) replicates. The error bars represent standard deviation. The error bars represent standard deviation.

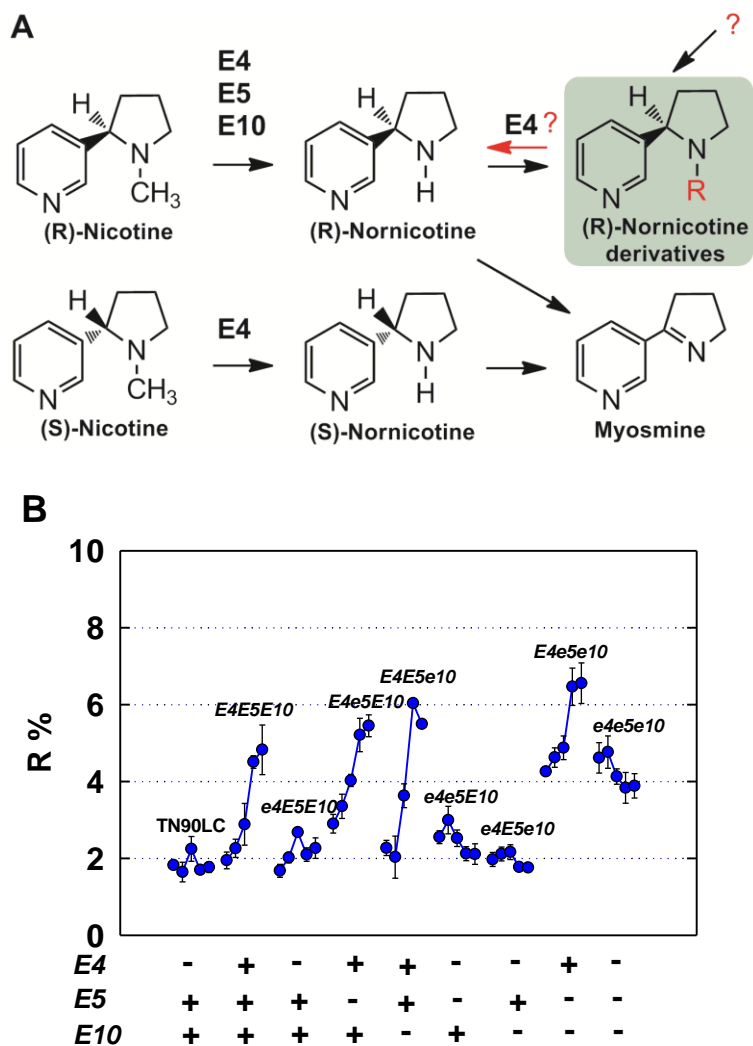


Figure S4.2. Possible reason for the increase of (R)-nornicotine in tobacco with active CYP82E4 during the first two weeks of curing. (A) (R)-nornicotine derivatives could be the source of (R)-nornicotine during first two weeks of curing. (B) Total (R) enantiomer percentage changes of nicotine plus nornicotine in nicotine demethylase mutants throughout growth and curing. Each data point is average of four bulk samples, and each bulk sample is a mixture of five middle leaves from five plants. The error bars represent standard deviation. +/- below the bars indicate the presence/absence of a functional demethylase gene.

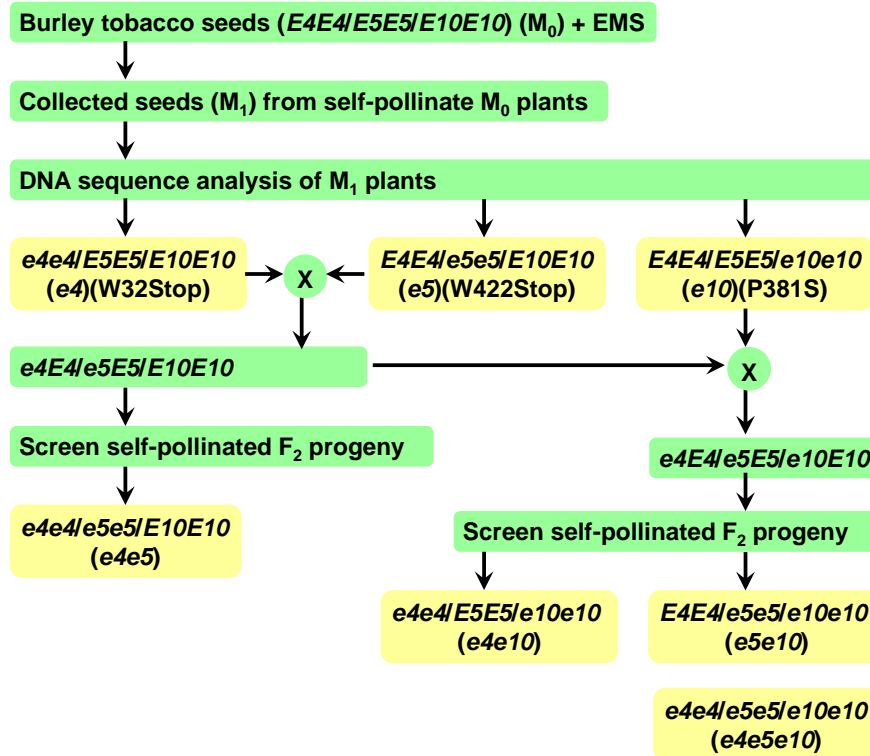


Figure S4.3. Selection of EMS-induced mutants in nicotine demethylase genes (Lewis et al., 2010). Mutants used in this study are highlighted in yellow. The particular amino acid mutation in each of non-functional demethylases (amino acid position substitution), and the zygosity at each locus noted (e4e4 – homozygous knock-out mutation) are also indicated.

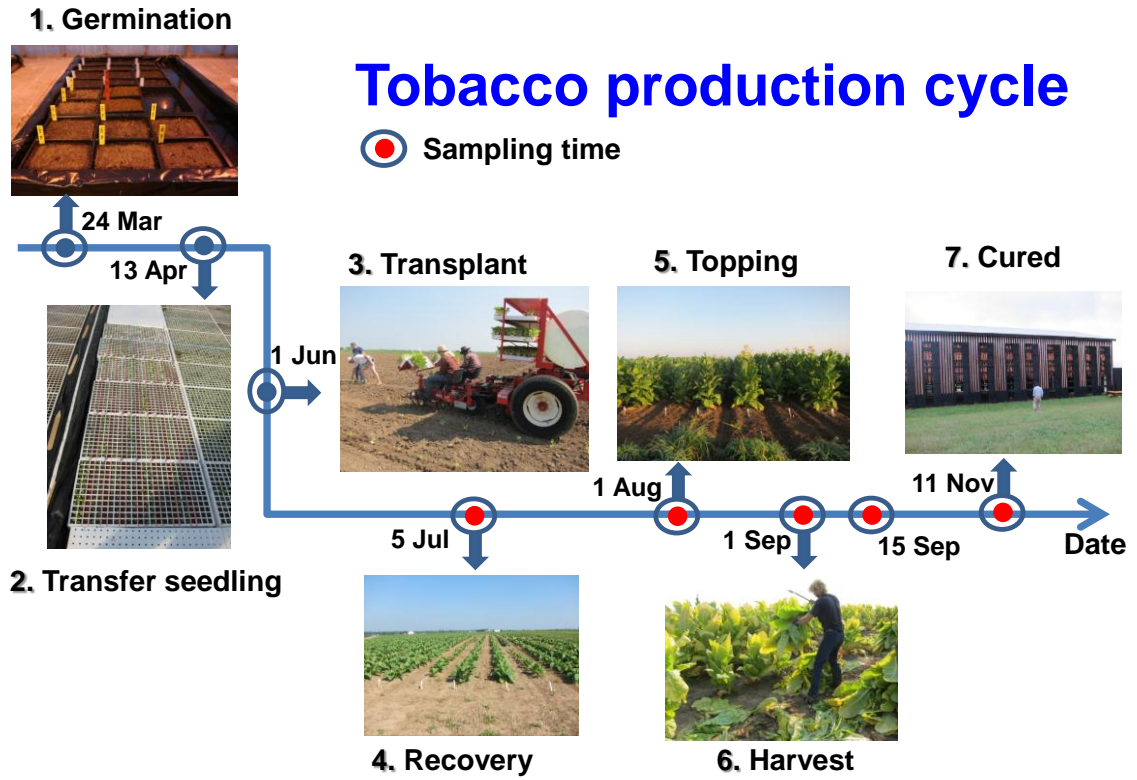


Figure S4.4. Production cycle of tobacco in 2011. Red dots represent sampling time.

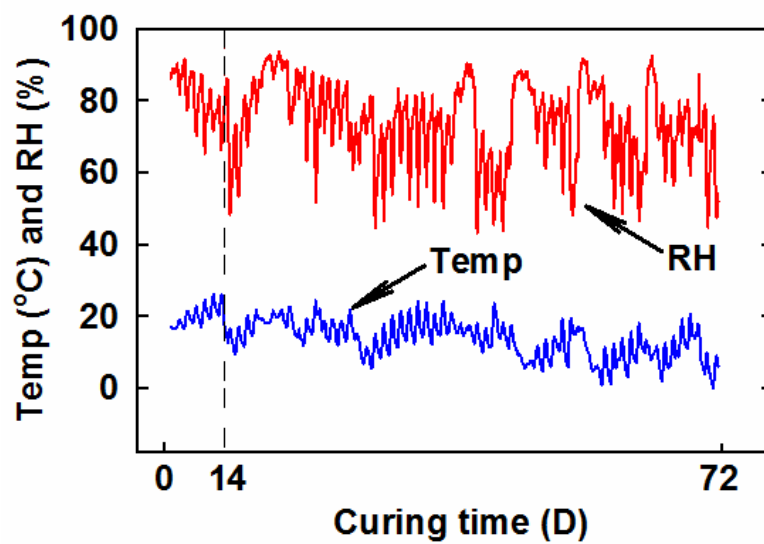


Figure S4.5. Temperature and relative humidity during curing. Cut tobacco plants were hung on a wagon in the air-curing barn. Tobacco plants were sampled at 0d (harvest), 14d and 72d (cured).

Literature Cited

- Andersen RA, Fleming PD, Burton HR, Hamilton-Kemp TR, Sutton TG** (1989) N²-Acyl and N'-nitroso pyridine alkaloids in alkaloid lines of burley tobacco during growth and air-curing. *Journal of Agricultural and Food Chemistry* **37**: 44–50
- Armstrong DW, Wang XD, Ercal N** (1998) Enantiomeric composition of nicotine in smokeless tobacco, medicinal products, and commercial reagents. *Chirality* **10**: 587–591
- Armstrong DW, Wang XD, Lee JT, Liu YS** (1999) Enantiomeric composition of nornicotine, anatabine, and anabasine in tobacco. *Chirality* **11**: 82–84
- Baldwin IT** (1989) Mechanism of damage-induced alkaloid production in wild tobacco. *Journal of Chemical Ecology* **15**: 1661–1680
- Bandell M, Lolkema JS** (1999) Stereoselectivity of the membrane potential-generating citrate and malate transporters of lactic acid bacteria. *Biochemistry* **38**: 10352–60
- Bao Z, He X, Ding X, Prabhu S, Hong J** (2005) Metabolism of nicotine and cotinine by human cytochrome P450 2A13. *Drug metabolism and disposition: the biological fate of chemicals* **33**: 258–61
- Bartholomeusz TA, Bhogal RK, Molini éR, Felpin FX, Mathe-Allainmat M, Meier AC, Drager B, Lebreton J, Roscher A, Richard RJ, et al** (2005a) Nicotine demethylation in *Nicotiana* cell suspension cultures: N²-formylnornicotine is not involved. *Phytochemistry* **66**: 2432–2440
- Bartholomeusz TA, Molinie R, Roscher A, Felpin FX, Gillet F, Lebreton J, Mesnard F, Robins RJ** (2005b) Stereoselectivity of the demethylation of nicotine piperidine homologues by *Nicotiana plumbaginifolia* cell suspension cultures. *Phytochemistry* **66**: 1890–1897
- Benowitz NL** (2008) Clinical pharmacology of nicotine: implications for understanding, preventing, and treating tobacco addiction. *Clinical Pharmacology & Therapeutics* **83**: 531–541
- Bernhardt R** (2006) Cytochromes P450 as versatile biocatalysts. *Journal of biotechnology* **124**: 128–45
- Bhide S, Nair J, Maru G, Nair U, Rao B, Chakraborty M, Brunnemann K** (1987) Tobacco-specific N-Nitrosamines [TSNA] in Green Mature and Processed Tobacco Leaves from India. *Beitrag Zur Tabakforschung International* **14**: 29–32

- Botte M, Mabon F, Le Mouillour M, Robins RJ** (1997) Biosynthesis of nornicotine in root cultures of *Nicotiana glauca* does not involve oxidation at C-5' of nicotine. *Phytochemistry* **46**: 117–122
- Brandsch R** (2006) Microbiology and biochemistry of nicotine degradation. *Applied Microbiology and Biotechnology* **69**: 493–498
- Braumann T, Nicolaus G, Hahn W, Elmenhorst H** (1990) N'-ethylnornicotine from burley tobacco. *Phytochemistry* **29**: 3693–3694
- Brown CM, Reisfeld B, Mayeno AN** (2008) Cytochromes p450: A structure-based summary of biotransformations using representative substrates. *Drug Metabolism Reviews* **40**: 1–100
- Burton HR, Dye NK, Bush LP** (1992) Distribution of tobacco constituents in tobacco leaf tissue. 1. Tobacco-specific nitrosamines, nitrate, nitrite, and alkaloids. *Journal of Agricultural and Food Chemistry* **40**: 1050–1055
- Bush L, Luo L, Wang J, Fannin FF, Burton HR** (2003) Nicotine demethylation and nornicotine racemization in *Nicotiana*. *American Society of Plant Biologists*
- Carlson TJ, Jones JP, Peterson L, Castagnoli N, Iyer KR, Trager WF** (1995) Stereoselectivity and isotope effects associated with cytochrome P450-catalyzed oxidation of (S)-nicotine. The possibility of initial hydrogen atom abstraction in the formation of the delta 1', 5-nicotinium ion. *Drug Metabolism and Disposition* **23**: 749–756
- Carmella SG, McIntee EJ, Chen M, Hecht SS** (2000) Enantiomeric composition of N'-nitrosornicotine and N'-nitrosoanatabine in tobacco. *Carcinogenesis* **21**: 839–43
- Chakrabarti M, Bowen SW, Coleman NP, Meekins KM, Dewey RE, Siminszky B** (2008) CYP82E4-mediated nicotine to nornicotine conversion in tobacco is regulated by a senescence-specific signaling pathway. *Plant Molecular Biology* **66**: 415–427
- Chakrabarti M, Meekins KM, Gavilano LB, Siminszky B** (2007) Inactivation of the cytochrome P450 gene CYP82E2 by degenerative mutations was a key event in the evolution of the alkaloid profile of modern tobacco. *New Phytologist* **175**: 565–574
- Chapple C** (1998) Molecular-genetic analysis of plant cytochrome P450-dependent monooxygenases. *Annual review of plant physiology and plant molecular biology* **49**: 311–343
- Chelvarajan RL, Fannin FF, Bush LP** (1993) Study of nicotine demethylation in *Nicotiana glauca*. *Journal of Agricultural and Food Chemistry* **41**: 858–862

- Clarkson JJ, Lim KY, Kovarik A, Chase MW, Knapp S, Leitch AR** (2005) Long-term genome diploidization in allopolyploid *Nicotiana* section *Repandae* (Solanaceae). *The New phytologist* **168**: 241–52
- Crooks PA, Godin CS** (1988) N-Methylation of nicotine enantiomers by human liver cytosol. *Journal of Pharmacy and Pharmacology* **40**: 153–154
- Davis RA, Stiles MF, DeBethizy JD, Reynolds JH** (1991) Dietary nicotine: A source of urinary cotinine. *Food and Chemical Toxicology* **29**: 821–827
- Dawson RF** (1951) Alkaloid biogenesis III. specificity of the nicotine-nornicotine conversion. *Journal of the American Chemical Society* **73**: 4218–4221
- Dawson RF** (1945) An experimental analysis of alkaloid production in *Nicotiana*: the origin of nornicotine. *American Journal of Botany* **32**: 416–423
- Dawson RF** (1942) Nicotine synthesis in excised tobacco roots. *American Journal of Botany* **29**: 813–815
- DeBoer KD, Lye JC, Aitken CD, Su AKK, Hamill JD** (2009) The A622 gene in *Nicotiana glauca* (tree tobacco): evidence for a functional role in pyridine alkaloid synthesis. *Plant Molecular Biology* **69**: 299–312
- DeVore NM, Scott EE** (2012) Nicotine and 4-(methylnitrosamino)-1-(3-pyridyl)-1-butanone (NNK) binding and access channel in human cytochrome P450 2A6 and 2A13 enzymes. *Journal of Biological Chemistry*. doi: 10.1074/jbc.M112.372813
- Denisov IG, Makris TM, Sligar SG, Schlichting I** (2005) Structure and Chemistry of Cytochrome P450. *Chemical Reviews* **105**: 2253–2278
- Dicke KE, Skrlin SM, Murphy SE** (2005) Nicotine and 4-(methylnitrosamino)-1-(3-pyridyl)-butanone metabolism by cytochrome p450 2B6. *Drug Metabolism and Disposition* **33**: 1760–1764
- Edwards WB, McCuen R** (1983) Preparation of optically pure R-(+)-nicotine studies on the microbial degradation of nicotinoids. *The Journal of Organic Chemistry* **48**: 2484–2487
- Fannin FF, Wei X, Bush L** (1996) Mechanism for partial racemization of nornicotine in tobacco. *Tobacco Chemists' Research Conference*. Richmond, Virginia USA, p 39
- Flammang A, Gelboin H, Aoyama T** (1992) Nicotine metabolism by cDNA-expressed human cytochrome P-450s. *Biochemical archives* **8**: 1–8

- Freudenberg W, König K, Andreessen JR** (1988) Nicotine dehydrogenase from *Arthrobacter oxidans*: A molybdenum-containing hydroxylase. *FEMS Microbiology Letters* **52**: 13–17
- Friesen JB, Leete E** (1990) Nicotine synthase: an enzyme from *Nicotiana* species which catalyzes the formation of (S)-nicotine from nicotinic acid and 1-methyl- Δ^2 -pyrrolinium chloride. *Tetrahedron Letters* **31**: 6295–6298
- Gavilano LB, Coleman NP, Bowen SW, Siminszky B** (2007) Functional analysis of nicotine demethylase genes reveals insights into the evolution of modern tobacco. *Journal of Biological Chemistry* **282**: 249–256
- Gavilano LB, Coleman NP, Burnley LE, Bowman ML, Kalengamaliro NE, Hayes A, Bush L, Siminszky B** (2006) Genetic engineering of *Nicotiana tabacum* for reduced nornicotine content. *Journal of Agricultural and Food Chemistry* **54**: 9071–9078
- Gavilano LB, Siminszky B** (2007) Isolation and characterization of the cytochrome P450 gene CYP82E5v2 that mediates nicotine to nornicotine conversion in the green leaves of tobacco. *Plant and Cell Physiology* **48**: 1567–1574
- Guthrie FE, Campbell WV, Baron RL** (1962) Feeding sites of the green peach aphid with respect to its adaptation to tobacco. *Annals of the Entomological Society of America* **55**: 42–46
- Hakkinen ST, Tilleman S, Swiatek A, De Sutter V, Rischer H, Vanhoutte I, Van Onckelen H, Hilson P, Inze D, Oksman-Caldentey KM, et al** (2007) Functional characterisation of genes involved in pyridine alkaloid biosynthesis in tobacco. *Phytochemistry* **68**: 2773–2785
- Hao DY, Yeoman MM** (1996) Mechanism of nicotine N-demethylation in tobacco cell suspension cultures. *Phytochemistry* **41**: 477–482
- Harner T, Wiberg K, Norstrom R** (2000) Enantiomer Fractions Are Preferred to Enantiomer Ratios for Describing Chiral Signatures in Environmental Analysis. *Environmental Science & Technology* **34**: 218–220
- Hecht SS** (1998) Biochemistry, biology, and carcinogenicity of tobacco-specific N-nitrosamines. *Chemical research in toxicology* **11**: 559–603
- Hecht SS** (2008) Progress and challenges in selected areas of tobacco carcinogenesis. *Chemical research in toxicology* **21**: 160–71
- Hecht SS, Hochalter JB, Villalta PW, Murphy SE** (2000) 2'-Hydroxylation of nicotine by cytochrome P450 2A6 and human liver microsomes: formation of a lung carcinogen precursor. *Proceedings of the National Academy of Sciences of the United States of America* **97**: 12493–7

- Hibi N, Higashiguchi S, Hashimoto T, Yamada Y** (1994) Gene expression in tobacco low-nicotine mutants. *The Plant Cell Online* **6**: 723–735
- Hukkanen J, Jacob P, Benowitz NL** (2005) Metabolism and disposition kinetics of nicotine. *Pharmacological reviews* **57**: 79–115
- Jack A, Bush L** (2007) The “LC” protocol. <http://www.uky.edu/Ag/Tobacco/Pdf/LC-Protocol.pdf>
- Jacob P** (1996) Facile Pyridoxal-Catalyzed Racemization of Nornicotine and Related Compounds. *The Journal of organic chemistry* **61**: 2916–2917
- Jeffrey RN, Tso TC** (1964) Influences of stock and scion on alkaloid synthesis and transformation. *Plant Physiology* **39**: 480
- Jones JP, Trager WF, Carlson TJ** (1993) The binding and regioselectivity of reaction of (R)- and (S)-nicotine with cytochrome P-450cam: parallel experimental and theoretical studies. *Journal of the American Chemical Society* **115**: 381–387
- Kachalova GS, Bourenkov GP, Mengesdorf T, Schenk S, Maun HR, Burghammer M, Riekel C, Decker K, Bartunik HD** (2010) Crystal Structure Analysis of Free and Substrate-Bound 6-Hydroxy-L-Nicotine Oxidase from *Arthrobacter nicotinovorans*. *Journal of Molecular Biology* **396**: 785–799
- Kajikawa M, Hirai N, Hashimoto T** (2009) A PIP-family protein is required for biosynthesis of tobacco alkaloids. *Plant Molecular Biology* **69**: 287–298
- Kajikawa M, Shoji T, Kato A, Hashimoto T** (2011) Vacuole-localized berberine bridge enzyme-like proteins are required for a late step of nicotine biosynthesis in tobacco. *Plant physiology* **155**: 2010–22
- Katoh A, Hashimoto T** (2004) Molecular biology of pyridine nucleotide and nicotine biosynthesis. *Front Biosci* **9**: 1577–1586
- Katoh A, Shoji T, Hashimoto T** (2007) Molecular cloning of N-methylputrescine oxidase from tobacco. *Plant and Cell Physiology* **48**: 550–554
- Kisaki T, Maeda S, Koiwai A, Mikami Y, Sasaki T, Matsushita H** (1978) Transformation of Tobacco Alkaloids. *Beitrag Zur Tabakforschung International* **9**: 308–316
- Kisaki T, Mizusaki S, Tamaki E** (1968) Phytochemical studies on tobacco alkaloids—XI: A new alkaloid in *Nicotiana tabacum* roots. *Phytochemistry* **7**: 323–327

- Kisaki T, Tamaki E** (1960) The phytochemistry on the tobacco alkaloids. II Isolation of d-form predominant nornicotine from the roots of *Nicotiana tabacum* L. *Naturwissenschaften* **47**: 540–541
- Kisaki T, Tamaki E** (1961a) Phytochemical studies on the tobacco alkaloids III. Observations on the interconversion of DL-nicotine and DL-nornicotine in excised tobacco leaves. *Archives of Biochemistry and Biophysics* **94**: 252–256
- Kisaki T, Tamaki E** (1961b) Phytochemical studies on the tobacco alkaloids. I. Optical rotatory power of nornicotine. *Archives of Biochemistry and Biophysics* **92**: 351–355
- Kisaki T, Tamaki E** (1964) Phytochemical studies on tobacco alkaloids IV. Stereospecific demethylation of nicotine in tobacco leaves. *Agricultural and Biological Chemistry* **28**: 492–495
- Kisaki T, Tamaki E** (1966) Phytochemical studies on the tobacco alkaloids X. Degradation of the tobacco alkaloids and their optical rotatory changes in tobacco plants. *Phytochemistry* **5**: 293–300
- Koetter JW a, Schulz GE** (2005) Crystal structure of 6-hydroxy-D-nicotine oxidase from *Arthrobacter nicotinovorans*. *Journal of molecular biology* **352**: 418–28
- Kuehl GE, Murphy SE** (2003) N-glucuronidation of nicotine and cotinine by human liver microsomes and heterologously expressed UDP-glucuronosyltransferases. *Drug metabolism and disposition: the biological fate of chemicals* **31**: 1361–8
- Lao Y, Yu N, Kassie F, Villalta PW, Hecht SS** (2007) Analysis of pyridyloxobutyl DNA adducts in F344 rats chronically treated with (R)- and (S)-N⁷-nitrosornicotine. *Chemical research in toxicology* **20**: 246–56
- Leete E** (1992) The biosynthesis of nicotine and related alkaloids in intact plants, isolated plant parts, tissue cultures, and cell-free systems. *In* RJ Petroski, SP McCormick, eds, *Secondary-Metabolite Biosynthesis and Metabolism*. Plenum Press, New York, pp 121–140
- Leete E** (1981) N'-isopropylornicotine: Its formation from nicotine in aged leaves of *Nicotiana tabacum*. *Phytochemistry* **20**: 1037–1040
- Leete E, Chedekel MR** (1974) Metabolism of nicotine in *Nicotiana glauca*. *Phytochemistry* **13**: 1853–1859
- Leete E, Chedekel MR** (1972) The aberrant formation of (–)-N-methylanabasine from N-methyl- Δ 1-piperideinium chloride in *Nicotiana tabacum* and *N. Glauca*. *Phytochemistry* **11**: 2751–2756

- Lewis RS, Bowen SW, Keogh MR, Dewey RE** (2010) Three nicotine demethylase genes mediate nornicotine biosynthesis in *Nicotiana tabacum* L.: Functional characterization of the CYP82E10 gene. *Phytochemistry* **71**: 1988–1998
- Lewis RS, Jack AM, Morris JW, Robert VJM, Gavilano LB, Siminszky B, Bush LP, Hayes AJ, Dewey RE** (2008) RNA interference (RNAi)-induced suppression of nicotine demethylase activity reduces levels of a key carcinogen in cured tobacco leaves. *Plant Biotechnology Journal* **6**: 346–354
- Li D, Huang X, Han K, Zhan C-G** (2011a) Catalytic mechanism of cytochrome P450 for 5'-hydroxylation of nicotine: fundamental reaction pathways and stereoselectivity. *Journal of the American Chemical Society* **133**: 7416–27
- Li D, Lewis RS, Jack AM, Dewey RE, Bowen SW, Miller RD** (2011b) Development of CAPS and dCAPS markers for CYP82E4, CYP82E5v2 and CYP82E10 gene mutants reducing nicotine to nornicotine conversion in tobacco. *Molecular Breeding* **29**: 589–599
- Li D, Wang Y, Han K, Zhan C-G** (2010) Fundamental reaction pathways for cytochrome P450-catalyzed 5'-hydroxylation and N-demethylation of nicotine. *The journal of physical chemistry B* **114**: 9023–30
- Liu BZ, Chen CY, Wu D, Su QD** (2008) Enantiomeric analysis of anatabine, nornicotine and anabasine in commercial tobacco by multi-dimensional gas chromatography and mass spectrometry. *Journal of Chromatography B-Analytical Technologies in the Biomedical and Life Sciences* **865**: 13–17
- Lochmann H, Bazzanella A, Kropsch S, Bächmann K** (2001) Determination of tobacco alkaloids in single plant cells by capillary electrophoresis. *Journal of chromatography A* **917**: 311–7
- Luurtsema G, de Lange ECM, Lammertsma AA, Franssen EJJ** (2004) Transport across the blood-brain barrier: stereoselectivity and PET-tracers. *Molecular imaging and biology* **6**: 306–18
- Matsush S, Ohstjmi T, Sugawara S** (1983) Composition of trace alkaloids in tobacco leaf lamina. *Agricultural and biological chemistry* **47**: 507–10
- McIntee EJ, Hecht SS** (2000) Metabolism of N'-nitrosonornicotine enantiomers by cultured rat esophagus and in vivo in Rats. *Chemical Research in Toxicology* **13**: 192–199
- Meng XJ, Lu LL, Gu GF, Xiao M** (2010) A novel pathway for nicotine degradation by *Aspergillus oryzae* 112822 isolated from tobacco leaves. *Research in Microbiology* **161**: 626–633

- Mesnard F, Girard S, Fliniaux O, Bhogal RK, Gillet F, Lebreton J, Fliniaux MA, Robins RJ** (2001) Chiral specificity of the degradation of nicotine by *Nicotiana glauca* cell suspension cultures. *Plant Science (Amsterdam, Netherlands)* **161**: 1011–1018
- Mesnard F, Roscher A, Garlick AP, Girard S, Baguet E, Arrou RRJ, Lebreton J, Robins RJ, Ratcliffe RG** (2002) Evidence for the involvement of tetrahydrofolate in the demethylation of nicotine by *Nicotiana glauca* cell-suspension cultures. *Planta* **214**: 911–919
- Meunier B, de Visser SP, Shaik S** (2004) Mechanism of Oxidation Reactions Catalyzed by Cytochrome P450 Enzymes. *Chemical Reviews* **104**: 3947–3980
- Mizusaki S, Kisaki T, Tamaki E** (1965) Transformation of nicotine to nornicotine in excised tobacco root culture. *Agricultural and Biological Chemistry* **29**: 78–79
- Molinié R, Kwiecień R a, Paneth P, Hatton W, Lebreton J, Robins RJ** (2007) Investigation of the mechanism of nicotine demethylation in *Nicotiana glauca* through ²H and ¹⁵N heavy isotope effects: implication of cytochrome P450 oxidase and hydroxyl ion transfer. *Archives of biochemistry and biophysics* **458**: 175–83
- Morita M, Shitan N, Sawada K, Van Montagu MCE, Inzé D, Rischer H, Goossens A, Oksman-Caldentey K-M, Moriyama Y, Yazaki K** (2009) Vacuolar transport of nicotine is mediated by a multidrug and toxic compound extrusion (MATE) transporter in *Nicotiana glauca*. *Proceedings of the National Academy of Sciences of the United States of America* **106**: 2447–52
- Murphy SE, Raulinaitis V, Brown KM** (2005) Nicotine 5'-oxidation and methyl oxidation by P450 2A enzymes. *Drug metabolism and disposition: the biological fate of chemicals* **33**: 1166–73
- Nyiredy S, Gross GA, Sticher O** (1986) Minor Alkaloids from *Nicotiana glauca*. *Journal of Natural Products* **49**: 1156–1157
- Park SB, Jacob P, Benowitz NL, Cashman JR** (1993) Stereoselective metabolism of (S)-(-)-nicotine in humans: formation of trans-(S)-(-)-nicotine N-1'-oxide. *Chemical research in toxicology* **6**: 880–8
- Perfetti TA, Coleman WMI** (1998) Chiral-Gas Chromatography-Selected Ion Monitoring/Mass Selective Detection Analysis of Secondary Alkaloids in Tobacco and Tobacco Smoke. *Beitrage Zur Tabakforschung International* 35–42
- Pogocki D, Ruman T, Danilczuk M, Celuch M, Walajtys-Rode E** (2007) Application of nicotine enantiomers, derivatives and analogues in therapy of neurodegenerative disorders. *European Journal of Pharmacology* **563**: 18–39

- Pompon D, Louerat B, Bronine A, Urban P** (1996) Yeast expression of animal and plant P450s in optimized redox environments. *In* FJ Eric, RW Michael, eds, *Methods in Enzymology*. Academic Press, pp 51–64
- Pylypenko O, Schlichting I** (2004) Structural aspects of ligand binding to and electron transfer in bacterial and fungal P450s. *Annual review of biochemistry* **73**: 991–1018
- Robins RJ, Molini é Kwiecie RA, Paneth P, Lebreton J, Bartholomeusz TA, Roscher A, Dr äger B, Meier AC, Mesnard F** (2007) Progress in understanding the N-demethylation of alkaloids by exploiting isotopic techniques. *Phytochemistry Reviews* **6**: 51–63
- Sachan N, Falcone DL** (2002) Wound-induced gene expression of putrescine N-methyltransferase in leaves of *Nicotiana tabacum*. *Phytochemistry* **61**: 797–805
- Saitoh F, Noma M, Kawashima N** (1985) The alkaloid contents of sixty *Nicotiana* species. *Phytochemistry* **24**: 477–480
- Sato F, Inai K, Hashimoto T** (2007) Metabolic Engineering in Alkaloid Biosynthesis: Case Studies in Tyrosine- and Putrescine-Derived Alkaloids. *In* R Verpoorte, ed, *Applications of Plant Metabolic Engineering*. Springer, pp 145–173
- Schlicht KE, Berg JZ, Murphy SE** (2009) Effect of CYP2A13 active site mutation N297A on metabolism of coumarin and tobacco-specific nitrosamines. *Drug metabolism and disposition: the biological fate of chemicals* **37**: 665–71
- Seifert R, Dove S** (2009) Functional selectivity of GPCR ligand stereoisomers: new pharmacological opportunities. *Molecular pharmacology* **75**: 13–8
- Sheen SJ** (1988) Detection of nicotine in foods and plant materials. *Journal of Food Science* **53**: 1572–1573
- Shitan N, Morita M, Yazaki K** (2009) Identification of a nicotine transporter in leaf vacuoles of *Nicotiana tabacum*. *Plant Signaling & Behavior* **4**: 530–532
- Shitan N, Yazaki K** (2007) Accumulation and Membrane Transport of Plant Alkaloids. *Current Pharmaceutical Biotechnology* **8**: 244–252
- Shoji T, Hashimoto T** (2011) Nicotine Biosynthesis. *Plant Metabolism and Biotechnology*. John Wiley & Sons, Ltd, pp 191–216
- Shoji T, Inai K, Yazaki Y, Sato Y, Takase H, Shitan N, Yazaki K, Goto Y, Toyooka K, Matsuoka K, et al** (2009) Multidrug and toxic compound extrusion-type transporters implicated in vacuolar sequestration of nicotine in tobacco roots. *Plant physiology* **149**: 708–18

- Shoji T, Winz R, Iwase T, Nakajima K, Yamada Y, Hashimoto T** (2002) Expression patterns of two tobacco isoflavone reductase-like genes and their possible roles in secondary metabolism in tobacco. *Plant Molecular Biology* **50**: 427–440
- Siegmund B, Leitner E, Pfannhauser W** (1999) Determination of the nicotine content of various edible nightshades (Solanaceae) and their products and estimation of the associated dietary nicotine intake. *Journal of agricultural and food chemistry* **47**: 3113–20
- Siminszky B, Gavilano L, Bowen SW, Dewey RE** (2005) Conversion of nicotine to nornicotine in *Nicotiana tabacum* is mediated by CYP82E4, a cytochrome P450 monooxygenase. *Proceedings of the National Academy of Sciences of the United States of America* **102**: 14919–14924
- Sinclair SJ, Johnson R, Hamill JD** (2004) Analysis of wound-induced gene expression in *Nicotiana* species with contrasting alkaloid profiles. *Functional Plant Biology* **31**: 721
- Sinclair SJ, Murphy KJ, Birch CD, Hamill JD** (2000) Molecular characterization of quinolinate phosphoribosyltransferase (QPRTase) in *Nicotiana*. *Plant Molecular Biology* **44**: 603–617
- Sisson VA, Severson RF** (1990) Alkaloid composition of the *Nicotiana* species. *Beiträge zur Tabakforschung International* **14**: 327–339
- Solt ML** (1957) Nicotine Production and Growth of Excised Tobacco Root Cultures. *Plant Physiology* **32**: 480
- Steppuhn A, Gase K, Krock B, Halitschke R, Baldwin IT** (2004) Nicotine's defensive function in nature. *PLoS Biology* **2**: e217
- Strickler M, Goldstein BM, Maxfield K, Shireman L, Kim G, Matteson DS, Jones JP** (2003) Crystallographic studies on the complex behavior of nicotine binding to P450cam (CYP101). *Biochemistry* **42**: 11943–11950
- Tang H, Wang L, Meng X, Ma L, Wang S, He X, Wu G, Xu P** (2009) Novel nicotine oxidoreductase-encoding gene involved in nicotine degradation by *Pseudomonas putida* strain S16. *Applied and environmental microbiology* **75**: 772–8
- Thuerauf N, Kaegler M, Renner B, Barocka A, Kobal G** (2000) Specific sensory detection, discrimination, and hedonic estimation of nicotine enantiomers in smokers and nonsmokers: are there limitations in replacing the sensory components of nicotine? *Journal of clinical psychopharmacology* **20**: 472–8

- Tso TC, Jeffrey RN** (1953) Paper chromatography of alkaloids and their transformation products in Maryland tobacco. *Archives of Biochemistry and Biophysics* **43**: 269–285
- Wada E, Kisaki T, Ihida M** (1959) The tobacco alkaloids in the root and sap of some *Nicotiana* plants. *Archives of Biochemistry and Biophysics* **80**: 258–267
- Wade RC, Winn PJ, Schlichting I, Sudarko** (2004) A survey of active site access channels in cytochromes P450. *Journal of inorganic biochemistry* **98**: 1175–82
- Wang HH, Yin B, Peng XX, Wang JY, Xie ZH, Gao J, Tang XK** (2012) Biodegradation of nicotine by newly isolated *Pseudomonas* sp. CS3 and its metabolites. *Journal of applied microbiology* **112**: 258–68
- Wang S, Yang S, An B, Wang S, Yin Y, Lu Y, Xu Y, Hao D** (2011) Molecular Dynamics Analysis Reveals Structural Insights into Mechanism of Nicotine N-Demethylation Catalyzed by Tobacco Cytochrome P450 Mono-Oxygenase. *PLoS ONE* **6**: e23342
- Warfield AH, Galloway WD, Kallianos AG** (1972) Some new alkaloids from burley tobacco. *Phytochemistry* **11**: 3371–3375
- Wei X, Sumithran SP, Deaciuc a G, Burton HR, Bush LP, Dwoskin LP, Crooks P a** (2005) Identification and synthesis of novel alkaloids from the root system of *Nicotiana tabacum*: affinity for neuronal nicotinic acetylcholine receptors. *Life sciences* **78**: 495–505
- Werck-Reichhart D, Hehn A, Didierjean L** (2000) Cytochromes P450 for engineering herbicide tolerance. *Trends in plant science* **5**: 116–23
- Wernsman EA, Matzinger DF** (1968) Time and site of nicotine conversion in tobacco. *tobacco science* **167**: 58–60
- Xu D, Shen Y, Chappell J, Cui M, Nielsen M** (2007a) Biochemical and molecular characterizations of nicotine demethylase in tobacco. *Physiologia Plantarum* **129**: 307–319
- Xu D, Shen Y, Nielsen M** (2007b) Development of lower nornicotine tobacco lines through genetic engineering and mutagenesis. 61ST Tobacco Science Research Conference. Charlotte, North Carolina USA, p 33
- Yamanaka H, Nakajima M, Fukami T, Sakai H, Nakamura A, Katoh M, Takamiya M, Aoki Y, Yokoi T** (2005) CYP2A6 and CYP2B6 are involved in nornicotine formation from nicotine in humans: interindividual differences in these contributions. Drug metabolism and disposition: the biological fate of chemicals **33**: 1811–8

Yildiz D, Ercal N, Armstrong DW (1998) Nicotine enantiomers and oxidative stress. *Toxicology* **130**: 155–165

Ziegler J, Facchini PJ (2008) Alkaloid biosynthesis: metabolism and trafficking. *Annual Review of Plant Biology* **59**: 735–769

Vita

1) Born in Jiaozuo, Henan (China) on July 10, 1982

2) Master of Science in Food Science at Zhengzhou Tobacco Research Institute (China), Jul. 2007

Bachelor of Science in Engineering/Tobacco Engineering at Henan Agriculture University (China), Jul. 2004

3) No professional positions held.

4) Philip Morris Graduate Fellowship, 2008 – 2012

TSRC Scholarship, 2011

Study Grant of CORESTA Congress, 2008

5) Publications:

Bin Cai, Balazs Siminszky, Joseph Chappell, Ralph Dewy and Lowell Bush. Enantioselective demethylation of nicotine as a mechanism of variable nornicotine composition in tobacco leaf. (In preparation)

Bin Cai, Anne Jack, Ramsey S. Lewis, Ralph Dewey and Lowell Bush. (R)-nicotine biosynthesis, metabolism and translocation as determined in nicotine demethylase mutants. (In preparation)

Bin Cai, Q. Yin and J. Yang. (2007) Validity of advance nicotine conversion induced by 2-chloroethyl phosphonic acid in burley. Tobacco science & technology.

Jun Yang, B. Cai, J. Xi, H. Zhou, J. Song and Q. Yin. (2007) Tobacco resistance against tobacco black shank induced by chitoooligosaccharides from housefly larvae. Tobacco science & technology.

6) Bin Cai